Stony Brook University

Tissue Plasminogen Activator & Plasminogen System in Chondroitinase-mediated Axonal Plasticity

A Dissertation Presented

by

Noreen Bukhari

to

The Graduate School

in Partial Fulfillment of the

Requirements

for the Degree of

Doctor of Philosophy

in

Neuroscience

Stony Brook University

August 2010

Stony Brook University
The Graduate School

Noreen Bukhari

We, the dissertation committee for the above candidate for the
Doctor of Philosophy degree, hereby recommend
acceptance of this dissertation.

Styliani-Anna E. Tsirka, Ph.D. – Dissertation Advisor
Professor, Department of Pharmacological Sciences

David Talmage, Ph.D. – Chairperson of Defense
Associate Professor, Department of Pharmacological Sciences

Holly Colognato, Ph.D.
Assistant Professor, Department of Pharmacological Sciences

Victor L. Arvanian, Ph.D.
Assistant Professor, Department of Neurobiology & Behavior

Mirjana Maletic-Savatic, M.D. Ph.D.
Assistant Professor, Department of Pediatric Neurology & Developmental Neuroscience, Baylor College of Medicine

This dissertation is accepted by the Graduate School

Lawrence Martin
Dean of the Graduate School

Abstract of the Dissertation

Tissue Plasminogen Activator & Plasminogen System in

Chondroitinase-mediated Axonal Plasticity

By

Noreen Bukhari

in

Neuroscience

Stony Brook University

2010

Following Spinal Cord Injury (SCI) the injured neurons are unable to regenerate as they face an inhibitory external environment and the lack of guidance cues for direct regrowth of severed axons. A component of the inhibitory extracellular environment is the glial scar. Chondroitinase ABC (ChABC) is an enzyme able to degrade the sugar chains of chondroitin sulfate proteoglycans (CSPGs), a major constituent of the glial scar, and thus allow for improvements in SCI functional repair. The mechanism underlying this repair remains unclear. Our group has previously reported that ChABC enhances the interaction of the extracellular serine protease, tissue plasminogen activator (tPA) and its downstream product, plasmin, with the extracellular matrix molecules of the glial scar in *in vitro* and *ex vivo* models of SCI.

In my Dissertation, I tested the contribution of tPA/plasmin to ChABC promoted axonal repair using mice deficient in tPA (tPA KO), hypothesizing that tPA acts downstream of ChABC to promote axonal plasticity after SCI. I found that tPA is upregulated after a moderate contusion in wildtype (WT) mice, and that in the absence of

the tPA/plasmin system, CSPG (NG2, Neurocan, and Phosphacan) degradation is reduced after ChABC treatment. In contrast to their genotypic equivalent WT cultures, tPA KO primary cortical neurons grown on *ex vivo* SCI homogenates show attenuated neurite outgrowth after ChABC treatment. Co-administration of ChABC and plasmin can rescue this phenotype. To test the hypothesis *in vivo*, I performed motor behavior assay and sensory anatomical tracings. A single high-dose bolus injection of ChABC allowed for significant sensory axon outgrowth and motor recovery in WT SCI mice but attenuated recovery in tPA KO mice. Furthermore, therapeutic co-administration of plasmin with ChABC enhanced the behavioral and axonal recovery in WT SCI mice over recovery due to the enzyme alone. Collectively, these findings suggest that after SCI, the tPA/plasmin system plays an important role in ChABC-mediated axonal plasticity and may provide new opportunities to enhance the enzyme's treatment efficacy.

Dedicated to my mother, Ms. Najma Bukhari,
for showing me, by example, the value of hard work

Table of Contents

List of Abbreviations

CNS:	Central Nervous System
SCI:	Spinal Cord Injury
CSPGs:	Chondroitin sulfate proteoglycans
ChABC:	Chondroitinase ABC
Pen:	Penicillinase
GAG:	Glycosaminoglycan
ECM:	Extracellular matrix
GFAP:	Glial fibrillary acidic protein
CST:	Corticospinal tract
PSN:	Propiospinal neurons
OPC:	Oligodendrocyte precursor cells
MAG:	Myelin-associate glycoprotein
RPTPβ:	Receptor protein tyrosine phosphatase β
PTPσ:	Protein tyrosine phosphatases σ
tPA	Tissue plasminogen activator
uPA	Urokinase
C4S	Chondroitin-4-sulfate
BDA	Biotinylated dextran amine
CTB	Cholera toxin B subunit
HRP	horseradish peroxidase
DAB	DiAminoBenzidine
in vitro	in a controlled environment such as test tubes

in vivo	in a living organism
ex vivo	samples isolated from a living organism and placed in a controlled environment

List of Figures

Figures

List of Tables

Acknowledgements

I would like to thank the members of my thesis committee, Dr. David Talmage, Dr. Holly Colognato, Dr. Victor Arvanian and Dr. Mirjana-Maletic Savatic. Their questions and perspective on my work at each meeting always led me to more critically analyze my work and ultimately, pushed me to develop a deeper understanding of my scientific research. I believe their suggestions and insights allowed me to progress my work at a faster pace and I greatly appreciate their time and sound advice during this process.

I would also like to thank Dr. John Robinson for his help and collaboration with the behavior experiment. What initially began as a one month experiment ended up lasting for 8 months during which time, Dr. Robinson allowed me to use his lab space, instruments, and offered useful advice and encouragement on the experiment. Without his guidance, the behavior experiment would not have been possible.

The Tsirka lab has always cultivated an amiable learning environment where the lab members are constantly teaching each other. As a result, I had the fortune of learning something from every former and current student that I interacted with in the lab. Dr. Westley Nolin, who along with Jaime Emmetsberger, had the great patience to teach me spinal cord injury and answered my unendless list of technical questions as a new member of the Tsirka lab. As the only other student in the lab who studied SCI, Jaime also taught me CTB injections and provided insights on other SCI techniques or research based on her work in the field. Haiyan Zhai had the strong forbearance to work with me on and off for a year to try to get the neurite outgrowth assay to work. Dr. Kyungmin Ji organized all the antibodies and primers in the lab and as a result, made all of our work

more productive. Yao Yao, a co-aisle lab member kept me entertained during the long weeknights in the lab, Zhen Gao for understanding the trials and tribulations of PiN and Ariel Abraham for being able to empathize with the constant anxieties of the dual doctorate track. Finally, I especially need to thank Jillian Cypser (aka Junior Stud!) for literally getting down on her hands and knees and helping me catch mice during the motor coordination experiment, for helping me transport the behavior apparatus between the HSC and Psychology dept as well as for teaching me to be a better mentor and friend. I would also like to thank Dr. Iordanis Gravanis, Dr. Martine Mirrione, Dr. Muzhou Wu, Chun Zhou, Dorothy, and George (all former members of the Tsirka lab) for keeping the lab an enjoyable place to work. Thank you all for your help and support; your presence made the Tsirka lab experience all the more special and I will cherish these memories.

Special thanks to Dr. Joel Levine for giving us free NG2 protein and antibody. Also, thank you to his current lab member, Justin Rodriguez, who worked with me multiple times to optimize SCI techniques, and especially in the last month of my experiments, helped me a great deal with the ever-finicky Neurolucida microscope and softwares.

Deep gratitude to the members of Colognato lab (Iva, Chris, Tom, Jenne, Cindy, Freyja and Dan) who all have aided me at some point during my graduate training with either a technique or scientific knowledge in addition to being lab neighbors and weekend meal buddies.

Finally and most importantly, I would like to thank my current and hopefully life-long academic mentors beginning with my advisor, Dr. Stella Tsirka. It's truly been an honor working with and for such a well rounded and great scientist like her.

Academically, she gave me the freedom to pursue risky ventures and make mistakes and at the same time, was available to provide guidance and direction when I was flailing. Personally, she has a statistically significant ($p<0.00001$) amount of patience and forbearance to help me deal with the stress when I felt overwhelmed and help me realize my mistakes when I couldn't see them myself. Throughout my graduate training, she has not only taught me scientific skills but also directly and indirectly, the important attributes of a successful scientist. Overtime, Stella has become both a mentor and a great role model for me to learn from and emulate.

I would also like to thank Dr. Michael Frohman who has been an academic mentor to me throughout my dual doctorate training. He has stepped in at critical junctures during my MD/PhD training to help me progress whether it was for the MSTP grant, NRSA fellowship, choosing a lab or editing my manuscript. I had an especially difficult time deciding on the scientific field and lab for my PhD and if it wasn't for Dr. Frohman's foresight and guidance, I would not have known about the Tsirka lab or realized that I really enjoyed Neuroscience research. I am also grateful for his openness and receptivity to the new (now old) initiatives for the MSTP program. Not many MSTP directors can be so directly involved in their students' academic training and I am grateful for his continued mentorship in my education.

Dr. Joseph Neale, was my first academic mentor and advisor, whom I worked under for all four years of my undergraduate research. Although I was quiet excited and eager to do basic science research, my initial impatience with the details of the procedures resulted in many failed experiments. It was, during this low point in my work, that Dr. Neale taught me the importance of a systematic and organized approach to

conducting scientific research that has become the hallmark of every new experiment or technique I learn. He also stepped in at critical times during my undergraduate education to provide pivotal academic and career advice. I probably would not have made it to a dual doctorate program without his sound judgment and guidance.

Last but by no means least, I would like to thank my sisters and Mom. My sisters, Ambreen, Sumera and Tayyaba, thank you for always being there for me, loving me with all of my oddities and helping me to stay connected to the outside world. I could not have retained my sanity throughout the last 6 years without your constant interference into my life. Mom, I know it hasn't been easy for you raising four girls on your own. We have been through some difficult times but you have always been there for me, making sacrifices, prioritizing my education and believing in me even when I didn't believe in myself. I could not have done this without you. I only hope that my achievements can someday make all of your hard work worthwhile.

Chapter I- Introduction

Epidemiology

The National Spinal Cord Injury Database estimates that 13% of new cases of spinal cord injury (SCI) occur in the United States each year with a national prevalence of 300,000 (Center) and international prevalence of 2.5 million (Schwab et al., 2006). In the United States, motor vehicle crashes account for 42% of cases followed by a small proportion due to falls and acts of violence such as gunshot wounds. Of these injured patients, 44% suffer from paraplegia and 51% from quadriplegia (Center). A review of published reports also reveals that most traumatic SCI are the result of contusive, compressive or stretch injury (Onose et al., 2009). Although majority of patients are able to return to a largely independent life, they retain a lifelong handicap and significantly reduced life expectancy especially in the first year after injury (Center).

Pathophysiology

SCI is clinically defined by the loss of sensory and motor function below the point of injury. Upon injury, the spinal cord undergoes primary and secondary damage. Primary damage consists of a vertebral fracture that causes local, segmental-limited damage of the spinal cord that results in rupture or contusion of axons and ensuing hemorrhage, ischemia, and edema (Schwab et al., 2006). Using *in vivo* imaging, this primary damage or lesion core has been correlated with proximal axon retraction, and distal axon degradation that is similar in mechanism to the delayed Wallerian degeneration but occurs during the first 24 hours after injury (Kerschensteiner et al., 2005). Secondary damage occurs during the first few weeks after the initial trauma when the lesion expands into the neighboring tissue and forms a region called the lesion

penumbra. During this critical time, the proximal axons retract and form retraction-bulbs and the distal axons degrade (Wallerian degeneration). A fluid-filled cavity called a pseudocyst and a fibrous scar form in humans and rats, while only a fibrous scar forms in mice. The fibrous scar consists of cells, reactive astrocytes, macrophages/microglia, oligodendrocyte precursor cells and fibroblasts, that are recruited to the site of injury. Extracellular matrix molecules such as chondroitin sulfate proteoglycans (CSPGs), myelin associated inhibitors, and axon guidance molecules also accumulate in the scar tissue (Fawcett and Asher, 1999; Grimpe and Silver, 2002; Stichel et al., 1999). The recruited cells release inflammatory cytokines such TNF-α and IL-1β, nitric oxide and chemoattractants which further recruit monocytes and leukocytes to the site of injury (Schwab and Bartholdi, 1996). In addition, systemic effects such as blood-brain barrier dysfunction, and energy depletion indirectly propagate other processes such as an imbalance of excitatory amino acids, ions, reactive oxygen species, free radicals and release of apoptotic signals and neurotoxic factors in the injured region (Onose et al., 2009). Collectively, these cells and inhibitory molecules form a region characterized by reactive gliosis and called glial scar which functions as a hostile physical and biochemical environment against axon repair.

Endogenous mechanism of repair

From an evolutionary perspective, the formation of a glial scar that inhibits axon regrowth would seem a counterintuitive CNS response. In an effort to resolve this discrepancy, two groups have suggested that the glial scar initially plays a beneficial role in response to tissue injury and the detrimental effects occur due to insufficient resolution

or excessive scar formation over time rather than its mere presence (Renault-Mihara et al., 2008; Rolls et al., 2009). As previously described, after SCI occurs, there is an increase in inflammatory molecules, neurotoxic factors and an imbalance of excitatory amino acids, ions, and free radicals among others in the tissue microenvironment. To reduce the further spread of injury, both groups reasoned that the lesion site must be sealed off and protective responses upregulated. To achieve these ends, they cited studies showing that astrocytes are upregulated after SCI, demarcate the lesion area and separate it from the healthy tissue (Okada et al., 2006; Reier and Houle, 1988). Astrocytes also serve as scavengers, clearing excessive glutamate, ions, and nitric oxide from the microenvironment (Chen et al., 2001; Cui et al., 2001; Roitbak and Sykova, 1999; Vorisek et al., 2002) and providing trophic support in the form of nerve growth factors, brain derived neurotrophic factors and neurotrophin 3 after CNS injury (do Carmo Cunha et al., 2007; Schwartz and Nishiyama, 1994; White et al., 2008; Wu et al., 1998). Furthermore, removal of astrocytes from the spinal cord injury site results in larger lesions, local tissue disruption, severe demyelination, and neuron and oligodendrocyte death (Bush et al., 1999; Faulkner et al., 2004). It was also shown that the timing of astrocytic clearance and degradation of secreted-by-astrocytes extracellular matrix molecules, chondroitin sulfate proteoglycans' (CSPGs), is crucial in determining the final effect on the injury. Overall, the two groups concluded that the glial scar is required during the acute phase to seal off the injury and restore homeostasis, but in the chronic phase it becomes inhibitory (Okada et al., 2006; Rolls et al., 2008; Rolls et al., 2009).

In conjunction with this dualistic perspective of glial scar in CNS repair, two groups have also investigated the endogenous CNS axon repair after injury. They found

that after dorsal hemisection, transected hindlimb corticospinal tract (CST) axons sprouted into the cervical gray matter to contact short and long propiospinal neurons (PSNs) as early as 3 weeks after injury (Bareyre et al., 2004; Courtine et al., 2008). Therefore, the astrocytic demarcation of lesion and release of tropic factors and extracellular matrix molecules into the microenvironment may also allow severed axons to navigate to neighboring healthy tissue and form collateral connections. The two groups also showed that connections with long PSNs that bridged the lesion were maintained after 12 weeks while contacts with short PSNs that did not bridge the lesion were lost (Figure 1) (Bareyre et al., 2004; Courtine et al., 2008). Long PSNs in turn connected to lumbar motor neurons and the rodents were able to regain minimal but not complete motor function as measured by behavior and electrophysiological recordings. These findings, therefore, demonstrate that endogenous mechanisms are active but insufficient for CNS repair. Moreover, these studies suggest that unlike peripheral nerve regeneration where axons reach their targets through long distance outgrowth along preexisting pathways (Nguyen et al., 2002), spinal cord regeneration occurs through a detour pathway.

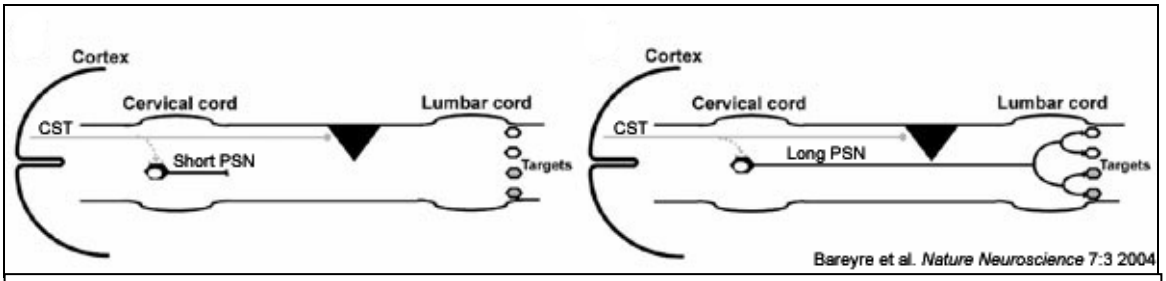

Figure 1: Connections with long PSNs that bridge the lesion but not short PSNs are maintained.

This axon repair strategy may be due to two distinguishing features of the CNS: 1) a nonpermissive chronic microenvironment for long-distance outgrowth and 2)

availability of numerous parallel pathways and interneuronal connections. Therapies for spinal cord injury should, therefore, focus on neuroprotection and stabilization of the injury during the acute-subacute phase and neuroregeneration (through combination of extrinsic degradation of the glial scar and intrinsic induction of neuronal activity) during the chronic phase of SCI. Therapies that build on CNS endogenous repair pathways could also enhance efficacy. Collectively, these insights can help us develop better repair strategies.

Therapeutic Approaches

In North America, a high-dose methylprednisolone administered within 8 hours after a non-penetrating spinal cord injury is the standard of medical care (Schreiber, 2009). This treatment, unfortunately, is not accepted worldwide and no repair therapies are currently available for chronic SCI patients. As a beacon of hope for translational research, it should be noted that clinical trials are currently underway in the US for a few pharmacological compounds identified in basic science research (Table 1) (Medicine, 2008; Onose et al., 2009).

Table 1: A list of pharmacological compounds under clinical trial for chronic SCI treatments

Lead Compound	Mechanism of Action	FDA phase	Reference
Lithium	Reduces host immune response	I	(Young, 2008)
Anti-Nogo antibodies	Inhibits myelin protein, Nogo-A	I	(Fouad et al., 2004; Freund et al., 2007)
MAG antagonist	Block myelin associated glycoproteins	I	(Vyas et al., 2005)
Nerisperidine	Blocks Voltage gated Sodium Channels	II	(Tarnawa et al., 2007)

However, many repair strategies still remain in the basic science and preclinical phases of development. One such repair strategy involves targeting extracellular components of the glial scar (axon guidance molecules, myelin inhibitors, and CSPGs) to reduce the extrinsic barrier and thereby, create a more permissive environment for axon repair. Although myelin inhibitor molecules have been successfully identified as lead compounds in this repair strategy (Table 1), blockade of the other two extracellular matrix molecules (axon guidance and CSPGs) in the SCI literature also offers promising lead compounds for therapy. The focus of this dissertation is on the therapeutic potential of CSPG degradation in the glial scar region after chronic SCI.

Chondroitinase ABC is a leading preclinical therapy against axon repair

CSPGs are a family of primarily six core proteins covalently linked to various levels of glycosaminoglycan (GAG) chains (Figure 2) and divided into three groups based on structural homology (Morgenstern et al., 2002). Neurocan, brevican, versican, and aggrecan are secreted by reactive astrocytes *in vivo* and collectively characterized as lecticans due to their similar hyaluranon and lectin domains (Jones et al., 2003a). NG2 and phosphacan are both unique CSPGs with no significant homology to other proteins. NG2 is the secreted form of a transmembrane protein found on the

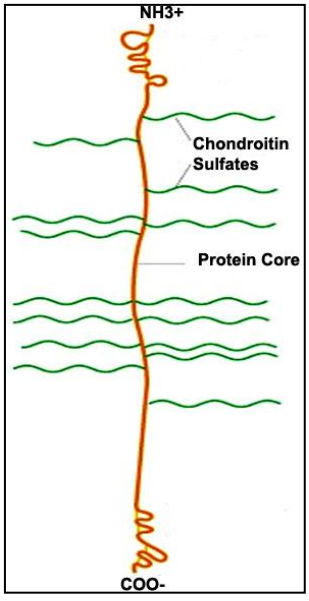

Figure 2: Representative CSPG molecule

surface of oligodendrocyte precursor cells, and macrophages (Jones et al., 2002; Nishiyama et al., 1991). Phosphacan corresponds to the extracellular domain of the receptor protein tyrosine phosphatase β (RPTPβ) (Dobbertin et al., 2003; Tang et al., 2003). The receptor for CSPG proteins that inhibits neurite outgrowth after CNS injury was recently identified to be the transmembrane protein tyrosine phosphatases σ (PTPσ) and knockouts of the protein exhibit corticospinal tract regeneration in both dorsal hemisection and contusion injury models of spinal cord injury (Fry et al.; Shen et al., 2009).

As the most abundant extracellular matrix protein group in the CNS, CSPGs are known to play a role in closing the anatomical plasticity of neural circuits (critical periods) during early development (Galtrey and Fawcett, 2007). Therefore, one may speculate, that degrading CSPGs after adult CNS injury may allow for a rearrangement of the neural circuitry and thereby augment the endogenously formed detour circuits. Indeed, studies show that upregulation of CSPGs prevents axon growth in the rat CNS (Davies et al., 1997) while degradation using Chondroitinase ABC (ChABC), a bacterial enzyme, enhances axon repair and allows for some functional recovery (Bradbury et al., 2002; Moon et al., 2001). Jones and colleagues investigated the role of different CSPGs in a rodent SCI model and found significantly higher levels of NG2 CSPG at the lesion site (Jones et al., 2003b). Although inhibitors of NG2 shows limited regeneration in a similar rodent injury model, when combined with intrinsic neuronal induction through a peripheral conditioning lesion, show sensory axon regeneration and correct anatomical growth of CST axons into the lesion site (Tan et al., 2006). Ectopic expression of ChABC in astrocytes resulted in similar limited morphological regeneration, but when

combined with an intrinsic neuronal induction, such as dorsal rhizotomy, it resulted in sensory axon regeneration and CST axon growth into the lesion (Cafferty et al., 2007). These studies suggest that degradation of CSPG molecules removes a critical extrinsic barrier to axon repair and when combined with an inducer of neuronal growth may allow for functionally significant levels of spinal repair.

Degradation of CSPGs by ChABC creates a permissive environment for axon regrowth in multiple models of SCI (Bradbury et al., 2002; Cafferty et al., 2008; Houle et al., 2006; Moon et al., 2001; Yick et al., 2000). ChABC, therefore, serves as a promising potential treatment and is currently under preclinical development for SCI patients (Caggiano et al., 2005; Fulmer, 2009). The downstream effects of ChABC action that allow for improvements in functional repair remain unclear. It is known that ChABC cleaves the GAG chains of the CSPG molecules (Bradbury et al., 2002). *In vitro* studies have shown that the GAG chains serve as neuronal guidance cues and mediate axonal growth inhibition (Laabs et al., 2007; Wang et al., 2008). However, *in vitro* studies of CSPGs also found the core protein to be inhibitory for neurite outgrowth (Dou and Levine, 1994; Oohira et al., 1991). To the best of our knowledge, no studies have looked at the effect of the core protein downstream of ChABC cleavage *in vivo*. The connection between degradation of core CSPG proteins after ChABC cleavage of the GAG chains and improvements in functional repair is the focus of this work.

Tissue plasminogen activator can degrade CSPGs and induce axon repair

Tissue plasminogen activator (tPA) is an extracellular serine protease initially described for its ability to cleave and activate plasminogen to plasmin, an event that

subsequently leads to the breakdown of blood clots (Collen, 1999). tPA, however, has also been shown to play a role in neurodevelopment (Carroll et al., 1994; Sumi et al., 1992), neurotoxicity (Tsirka et al., 1995; Tsirka et al., 1997b), tissue remodeling (Lee et al., 2001; Seeds et al., 1999; Zhang et al., 2005) and synaptic plasticity (Pang et al., 2004; Seeds et al., 1995). During neurodevelopment, the highest tPA expression is confined to the floor plate cells of the ventral spinal cord from embryonic day 10.5 to 17 (Sumi et al., 1992), while moderate levels are also found in the dorsal horn and intermediate neurons of the spinal cord (Carroll et al., 1994). Since floor plate cells act as guide posts for growing commissural fibers in the spinal cord, the highest tPA expression in these cells suggests a role for the serine protease in axon guidance. Indeed, these neurodevelopment studies confirmed a decade earlier discovery of tPA at the tips of neuronal growth cones (Krystosek and Seeds, 1981) and later findings that mice lacking the tPA gene show retarded neuronal migration (Seeds et al., 1999). Collectively, these findings suggest that tPA can act as an inducer of neurite outgrowth and opened up a whole array of investigations on the role of tPA in neurodegenerative diseases.

Since then, tPA has been found to play a role in brain neuronal degeneration and peripheral nerve regeneration. Specifically, it has been shown that hippocampal neurons of tPA –deficient mice are resistant to excitotoxic death after kainate injection (Tsirka et al., 1995). An imbalance of tPA (both too high and too low) in mouse cerebellum also leads to motor impairments (Li et al., 2006; Seeds et al., 2003). After seizures, however, tPA appears to regulate hippocampal mossy fiber outgrowth (Wu et al., 2000). In peripheral nerve crush injuries, tPA knockout mice also show delayed functional regeneration, and exogenous tPA enhances functional recovery (Siconolfi and Seeds,

2001; Zou et al., 2006), suggesting a neuroprotective role for this protease in seizures and peripheral axon regeneration.

To better understand the dichotomous role of tPA/plasmin cascade in the various neurodegenerative diseases, it is important to know the downstream effectors and pathway it targets. In excitotoxic death, it is the plasmin-catalyzed degradation of laminin that in part promotes neuronal degeneration in the hippocampus (Chen and Strickland, 1997; Tsirka et al., 1997a). During seizures, it is the plasmin catalyzed degradation of CSPGs, neurocan and phosphacan, in the brain's extracellular matrix which promotes neurite reorganization (Wu et al., 2000). In peripheral regeneration, it is the plasmin mediated degradation of fibrinogen that results in axonal regeneration under inflammatory conditions (Akassoglou et al., 2000). Furthermore, tPA's excitotoxic effect also appears to be mediated by activation of microglia and this activation is independent of its proteolytic activity (Rogove and Tsirka, 1998; Siao and Tsirka, 2002).

Studies exploring the role of tPA in SCI suggest that both proteolytic and non-proteolytic pathways are at play but interacting in different contexts. An early study demonstrated that tPA knockout mice display decreased neural damage after SCI due to reduced recruitment of microglia to the white matter and consequent demyelination of axons (Abe et al., 2003). A recent study confirmed these findings and showed that the peak of tPA activity occurred around day 21 after SCI in rats and corresponded with minimal myelin basic protein expression (Veeravalli et al., 2009). Interestingly, *in vitro* studies on purified myelin proteins suggest that tPA also plays a role in the conditioning-injury induced axonal regeneration and the mechanism of action, although still unclear, was shown to be plasminogen-independent (Minor et al., 2009; Steinmetz et al., 2005;

Tan et al., 2006). In contrast to tPA's non-proteolytic role, only few studies have looked at its proteolytic pathway in SCI. tPA has a partner, urokinase (uPA), that is secreted by certain classes of neurons in CNS and PNS and also functions by cleaving plasminogen to plasmin (Sumi et al., 1992). Both plasminogen activators (uPA and tPA), albeit more so uPA, were recently shown to play a role in the crossed phrenic phenomenon recovery of respiratory function following SCI, a dramatic example of synaptic plasticity and tissue remodeling (Minor and Seeds, 2008; Seeds et al., 2009). tPA's substrate, plasminogen, and its product, plasmin, have also been implicated in the decorin mediated degradation of neurocan, brevican, phosphacan, and in NG2 expression in a rat SCI model (Davies et al., 2006; Davies et al., 2004).

Our group has previously shown that after seizure, tPA/plasmin pathway catalyzes degradation of two CSPGs, neurocan and phosphacan, in the brain's extracellular matrix and this degradation promotes neurite reorganization (Wu et al., 2000). We also recently demonstrated that tPA and plasminogen both interact with NG2 *in vitro* and this interaction results in degradation of NG2 in *in vivo* and *ex vivo* SCI. Furthermore, we showed that ChABC degradation of GAG chains on NG2 protein enhances the CSPG protein's interaction with tPA and plasmin, suggesting that CSPG core proteins may function as a scaffold for tPA binding and conversion of plasminogen to plasmin. Plasmin, in turn, can degrade the CSPG core protein (Nolin et al., 2008). Based on these previous findings, I assessed the contribution of tPA/plasmin to ChABC promoted axonal repair. Using mice deficient in tPA (tPA KO), **I hypothesized that tPA acts downstream of ChABC to promote axonal plasticity after SCI**. To investigate this hypothesis, I asked the following specific questions:

1: Does the tPA/plasmin system act on CSPGs after ChABC cleavage in a mouse spinal cord injury model?

2: Does tPA/plasmin system contribute to ChABC mediated axonal plasticity after spinal cord injury?

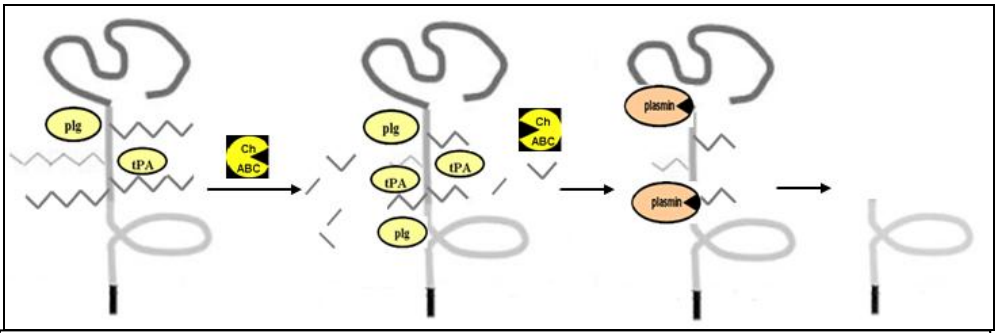

Figure 3: tPA acts downstream of ChABC cleavage of GAG chains. An illustration showing the interaction of tPA and plasminogen with CSPG proteins. A representative CSPG image is shown in gray in the above diagram with GAG chains represented by zig-zag lines. tPA and plasminogen bind in this GAG region of CSPG proteins. After ChABC cleavage of GAG chains, more tPA and plasminogen can bind and form more plasmin. Plasmin, in turn, can degrade the core protein and allow for its clearance.

A confirmation of tPA/plasmin pathway's role in axon regeneration will be medically significant on two levels: Chondroitinase ABC (ChABC) has consistently been shown to reduce the glial scar and facilitate spinal repair (Barritt et al., 2006; Bradbury et al., 2002). Knowledge of the enzyme's mechanism of action will allow for enhanced efficacy. Although suppressing the host's immune response and injecting the bacterial enzyme can serve as a potential therapy for human spinal cord injury, a more beneficial approach may be to identify the enzyme's mechanism of action, and create other synthetic targets to upregulate the downstream endogenous effectors of the pathway. Our lab's previous data suggest that the tPA/plasmin pathway may be a downstream

effector of ChABC action. Exploring the role of the tPA/plasmin in axon repair, therefore serves as an evaluation of this enzyme's mechanism of action and can open up a new therapeutic opportunity for ChABC mediated axon repair.

Chapter II- tPA/plasmin system act on CSPGs after ChABC cleavage *in vivo* in a mouse SCI model

Materials & Methods

Animals and Surgery: All experiments conform to the NIH guidelines and were approved by the Department of Laboratory Animal Research at Stony Brook University. tPA knockout (KO) have been backcrossed for 12 generations to the C57Bl/6 background. Age and gender-matched adult C57BL/6 (WT) and tPA KO mice weighing 25-30g were anesthetized with isoflurane and placed in a stereotaxic apparatus. A dorsal laminectomy was performed between thoracic levels 8-10 and spinal cord stabilized with fine forceps. Animals were then transferred to an Infinite Horizon Impactor (Precision Systems and Instrumentation) and a 50kdyne impactor tip with 1.25mm tip diameter was dropped from a height of 2cm on the central canal between T8-T10. The overlying muscle and skin were sutured. Sham-operated groups underwent laminectomy without contusion. Postoperatively, mice were injected with buprenorphine (0.03 mg/kg) subcutaneously to reduce pain and placed on a heating pad for 24hrs to recover. Mice were then transferred to 27°C temperature controlled room, and food pellets and liquid solution (napa) were placed at the bottom of their cages. Daily weight measurements were performed. Bladders were expressed twice daily, and 0.6-0.8cc 5% dextrose/saline injected subcutaneously for underweight animals (<25g) until end of experiment.

Tissue Processing: Spinal cord tissue was processed in one of two ways. To prepare spinal cord homogenates, mice were terminally anesthetized with 2.5% avertin and transcardially perfused with PBS. Using the injury epicenter as the origin, 2mm each in the rostral and caudal direction of the spinal cord were isolated and suspended in Tris-buffer saline pH 7.0. Isolated spinal cord was manually homogenized and centrifuged at

20,800g for 30minutes at 4°C. Supernatant was collected and total protein content measured using Bio-Rad Bradford protein assay (Hercules, CA). To prepare spinal cord sections, mice were transcardially perfused and postfixed with 4% PFA pH 7.4, cryoprotected with 30% sucrose overnight at 4°C, and frozen in OCT (Triangle Biomedical Sciences, Durham, NC). 18µm sagittal sections through the thoracic spinal cord were prepared. All spinal cord samples were stored at -80°C until further use.

Amidolytic: For the direct amidolytic assay, 5day SCI homogenates from WT and tPA KO mice (15µg protein/sample) were incubated in 1M Tris buffer pH 8.1 with 0.1% Tween-80, 1mM amiloride (to block uPA activity in the samples) and 0.3mM chromogenic substrate-2288 for 2.5hrs in the dark at room temperature. Binding of the substrate to tPA generated a color change that was quantified at 405nm. For the indirect amidolytic assay, SCI homogenates from WT and tPA KO mice (10µg protein/sample) were incubated with 0.68µM plasminogen in a 50mM Tris buffer pH 8.1 with 2% BSA and 0.3mM chromogenic substrate-2251 (Chromogenix) overnight in the dark at room temperature. Cleavage of the chromogenic substrate S-2251 by serine protease-generated plasmin and the subsequent color change was quantified at 405nm. In both cases, a dose response for pure recombinant tPA activity was simultaneously run alongside the test samples and the time point when the R^2 value for the dose response was closest to 1 was used to measure the concentration of serine protease in the samples. All samples were run in triplicates. 1mM amiloride was also used in the indirect assay to block uPA and measure specific tPA activity in the samples.

Zymography: 14day SCI homogenates from WT and tPA KO mice (20µg protein/sample) were analyzed on 10% SDS-PAGE copolymerized with plasminogen (13mg/ml) and casein (3mg/ml). After electrophoresis, SDS was removed by incubating the gel with 2.5% Triton X-100 for an hour. The gel was then incubated with 0.1M Tris pH 8.0 overnight at 37°C. Next day, gel was stained with coomassie blue for two hours and destained until clear zones of lysis became visible. Pure, recombinant tPA (300mU; Genentech) was used as positive control.

Immunoblot (Western Blot): WT and tPA KO Sham and SCI homogenates (50µg) were treated with ChABC (0.5U/ml ; Seikagaku, Japan) in 100mM Tris-Acetate pH 7.4 for 3hrs at 37°C on cover slips. Sample buffer containing 5% β-mercaptoethanol was then added and the protein mix denatured at 100°C for 10minutes. Samples were run on 6% SDS-PAGE containing tris-glycine and transferred onto a polyvinyldene fluoride membrane. Membranes were blocked in 5% milk in PBS for 1 hour and probed overnight with one of the following primary antibodies: NG2 (1/500, rabbit anti-NG2; gift from Dr. Joel Levine) or Neurocan (1/100; mouse-1F6; DSHB). The following day, membranes were washed with PBS-T and incubated with the species-appropriate peroxidase conjugated secondary antibody (1/2000-1/5000; Vector Labs) for 1 hour at room temperature. After multiple washes with PBS-T, antibody binding was visualized using chemiluminescence kit according to the manufacturer's protocol (Thermo Scientific). For pure protein experiments, 10ng of pure NG2 (gift from Joel Levine) or 2.5µg of CSPG mix (CC117; Chemicon) were incubated with plasminogen (0.68µM) and pure recombinant tPA or uPA (0.5Uml, 1U/ml 5U/ml) in addition to ChABC and Tris-Acetate

buffer as above. To confirm equal loading, membranes were stripped with 0.2M Tris-Glycine pH2.2 and 0.5M NaCl strip buffer overnight at room temperature. Samples were re-probed with α-tubulin antibody (1/2000; Sigma). Protein bands were quantified by densitometry in ImageJ (NIH) software and data normalized against α-tubulin protein bands.

***In Vivo* ChABC treatment:** 2 weeks after contusion injury, WT and tPA KO mice were re-anesthetized and placed in the stereotaxic apparatus. The injured region was re-exposed and 1µl of ChABC (50U/ml, Seikagaku, Japan) or Penicillinase (Sigma) was injected into the central canal (1mm depth, rate of 0.4µl/min) using a 28-gauge Hamilton syringe attached to an automated microinjector. The needle was withdrawn after an additional one minute to prevent reflux.

***In Vivo* Immunohistochemistry:** 7, 16 and 21 days after SCI, mice were terminally anesthetized, fixed with 4% PFA and sagittal spinal cord sections prepared as previously outlined. Sections were sequentially blocked with mouse blocking serum (Vector lab) and goat serum, and then briefly incubated in mouse diluent before probing with one of the following primary antibodies for 30 minutes at room temperature: CSPG (1/200, CS56; Sigma), NG2 (1/1000, rabbit anti-NG2; gift from Joel Levine), Neurocan (1/50, 1F6; DSHB), Phosphacan (1/100, mouse-3F8; DSHB), or Chondroitin-4-sulfate (mouse-MAB2030, 1:1000; Chemicon). Species appropriate-Alexa 488 antibody was then applied followed by overnight incubation with glial fibrillary acidic protein (GFAP 1/1000; DAKO) to outline the glial scar. Species-appropriate-Alexa 555 antibody was

then applied and sections were mounted with the nuclear labeling mounting medium. To quantify multiple images around the glial scar border (indicated by upregulated GFAP expression) in each section were captured at a digital resolution of 1024 x 1024 with a Zeiss confocal microscope using LSM 510 Meta software. 4 sagittal sections every 10 sections (180μm) apart were imaged per biological replicate. ImageJ (NIH) was used to quantify the total mean intensity/area for each biological replicate and each antibody staining. Representative images were oriented with dorsal side up in Adobe Photoshop 7.0.1.

Statistics: To analyze the amidolytic assay, One-Way Repeated Measures ANOVA was used to compare across time points. For the *in vivo* immunohistochemistry experiment, One-Way ANOVA was used for multiple group comparisons within each genotype. Holm Sidak test was used in all *post hoc* analyses. To compare the two genotypes within each treatment or time point, t-test was used. A minimum alpha value of 0.05, was accepted as statistically significant. Data are presented as mean $\pm$ SEM.

Results

tPA and uPA activities are significantly upregulated after 14 days of contusion injury

We previously reported an interaction between ChABC, the tPA/plasmin cascade and the CSPG molecule NG2 using biochemical techniques, and *ex vivo* techniques after SCI (Nolin et al., 2008). Here, I explored these interactions in more physiologically relevant conditions, such as tissue culture assays and *in vivo* models of SCI. As a first step, I measured tPA activity 5 days after SCI using a direct amidolytic assay (Figure 4). Significantly higher tPA activity was measured in WT group compared to tPA KO group. However, residual, instead of negligible, activity was found in the tPA KO group. Further research on the technique revealed that the chromogenic substrate 2288 used for the direct amidolytic assay has affinities of 1100, 430 and 170 times more for plasma kalikrein, factor XIa, and thrombin respectively while tPA has an affinity of 100. In contrast, the chromogenic substrate 2251 in the indirect amidolytic assay only shows 2, 2, 3, and 4 times affinity for single chain tPA, APC, factor XIa, and thombin respectively while plasmin shows an affinity of 100 (Diapharma). Based on these findings, the indirect amidolytic assay was chosen for further quantifications.

Since even the indirect chromogenic substrate could bind other clotting factors, I took a more systematic approach to specifically measure tPA activity. Overall serine protease activity at various time points after injury in both the WT and tPA KO groups were first measured. Serine protease activity was significantly upregulated beginning 4hrs after injury and lasted up to 14 days in WT mice compared to their respective sham control (Figure 5A). The urokinase blocker, amiloride, was then used to inhibit uPA and specifically measure tPA activity; a significant tPA upregulation was measured in WT

mice after 14 days of injury (Figure 5B). In contrast, overall serine protease activity was also significantly upregulated in spinal cord homogenates of tPA KO mice 14 days after SCI but this activity was eliminated by the uPA inhibitor. Zymography also confirmed the upregulation of specific tPA (68kd) and uPA activity (33kd) in WT mice 14 days after contusion, but only uPA activity in the respective tPA KO group (Figure 5C). These results suggests that the plasminogen activators, tPA and uPA, account for the total serine protease activity at chronic timepoints (7 and 14 days). Consequently, the 14 day timepoint after SCI was used in subsequent experiments. My results also paralleled previous findings that tPA expression and activity are chronically elevated in a rat contusion injury model. Their work, however, differed from my results in three ways: they used the direct amidolytic assay, did not distinguish between tPA and uPA activity and measured upregulation as early as 7 days with a peak at 21 days after rat SCI (Veeravalli et al., 2009).

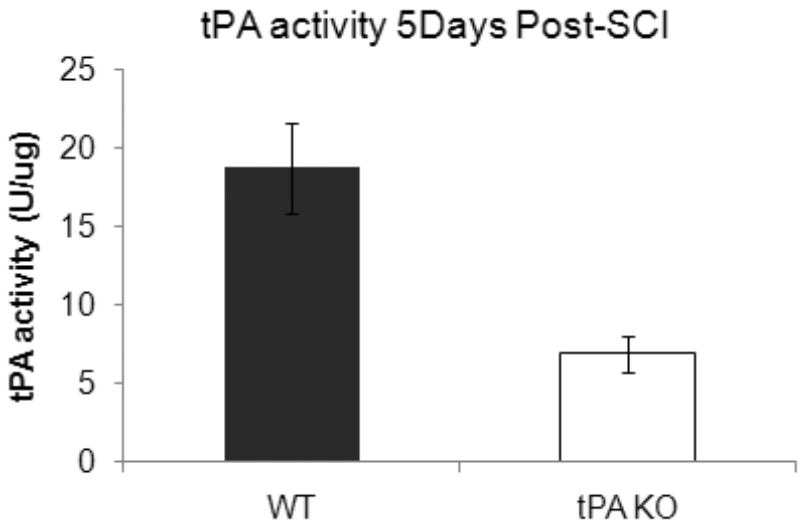

Figure 4: The tPA/Plasmin(ogen) system is significantly upregulated 5 days after SCI. tPA activity was quantified by direct amidolytic assay using SCI homogenates from WT and tPA KO mice 5 days after contusion injury (n=2).

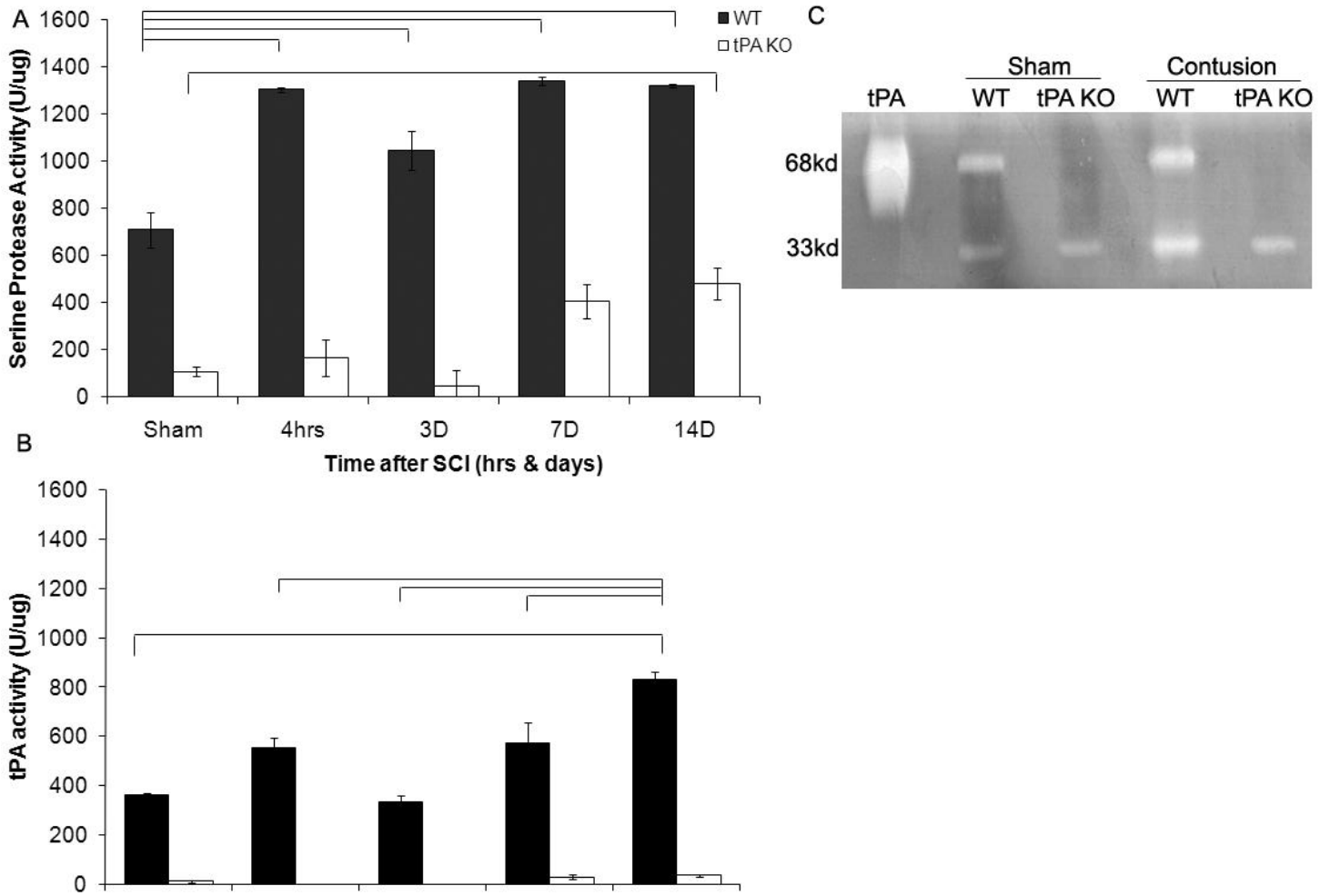
A
Serine Protease Activity (U/ug)
1600
1400
1200
1000
800
600
400
200
0
WT
tPA KO
Sham
4hrs
3D
7D
14D
Time after SCI (hrs & days)
B
tPA activity (U/ug)
1600
1400
1200
1000
800
600
400
200
0
C
Sham
Contusion
tPA
WT
tPA KO
WT
tPA KO
68kd
33kd

Figure 5: The tPA/Plasmin(ogen) system is significantly upregulated 14 days after SCI. A) Serine protease activity was quantified by amidolytic assay using SCI homogenates from WT and tPA KO sham and 0 (4hours), 3, 7 and 14 days after contusion injury. Amiloride, a specific uPA blocker, was used to allow the measurement of tPA activity only (B) (n=3). Repeated Measures ANOVA was used to compare across time points within each genotype. Significant ANOVA values were followed by *post hoc* Holm Sidak test. Significant *post hoc* differences at $p<0.05$ are indicated by brackets. C) Zymography assay with casein substrate was used to visualize serine protease activity in protein cell lysates obtained from WT and tPA KO sham and 14 days contusion-injured mice. The tPA band is seen at 68kd and uPA at 33kd. Pure recombinant tPA was used as positive control (n=4).

NG2, phosphacan and neurocan core proteins are degraded by the tPA/plasmin system after ChABC cleavage *in vivo*

To examine potential synergy between the tPA/plasmin system and ChABC-treated SCI, I first, characterized the CSPG protein expression before and after enzyme injection to technically verify the enzyme delivery mode and determine the optimal time for protein analysis after injection. WT and tPA KO mice underwent contusion injury and the spinal cords were isolated 7 days later. To localize protein expression to the glial scar region, the astrocytic protein marker, GFAP, was probed (Figure 6A). GFAP expression was negligible at the center of the injury ("a no cell's land") but highly upregulated around the border allowing for a clear demarcation of the injured region. Similarly, minimal CSPG protein expression was found at the center of the injury and modestly upregulated around the border (Figure 6B). One high dose of ChABC (1µl x 50U/ml) or control enzyme penicillinase (Pen) was then intraspinally injected on day 14 in another set of injured mice and spinal cord isolated one week later. On day 21 after injury, vehicle enzyme groups of both genotypes showed modest upregulation of CSPG protein around the injury border (Figure 7). However, CSPG protein expression was absent in the WT ChABC treated group confirming that a single high dose of injected enzyme was sufficient to hydrolyze the majority of the CSPG molecules in the glial scar region and may allow us to test our hypothesis *in vivo*. In contrast, the tPA KO ChABC treated group showed a retention of CSPG protein expression at the injury border suggesting that in the absence of tPA, ChABC enzyme activity is attenuated.

To explore the ChABC and tPA/plasmin interaction further, it was necessary to characterize the specific subtypes of CSPG proteins that were affected in the absence of tPA. Our previous work on CSPGs had demonstrated that the tPA/plasmin system

interacts with phosphacan and neurocan in the brain (Wu et al., 2000) and NG2 in the spinal cord (Nolin et al., 2008). As a result, I decided to characterize these three CSPG proteins after ChABC cleavage in WT and tPA KO mice. To investigate the interaction of the CSPG core proteins with the tPA/plasmin system, it was important to analyze their protein expression when the majority of these three proteins were stably upregulated and deglycanated by ChABC but not cleared away. A review of the literature revealed that NG2 protein expression peaks around 7 days, phosphacan at 2 months and neurocan at 14 days in a rat dorsal hemisection injury model (Jones et al., 2003a). Furthermore, most of the CSPG protein deglycanation occurs in the first day after ChABC infusion and progressively decreases, with no ChABC enzyme activity seen beyond 4 days. The effects of ChABC activity, however, persist for at least one week, but not more than 2 weeks after injection (Crespo et al., 2007; Garcia-Alias et al., 2008). Based on the upregulation of tPA and CSPG protein expression and ChABC enzyme efficacy, I chose to analyze protein expression 2 days after a single intraspinal ChABC injection.

As before, I performed contusion injury on WT and tPA KO mice and administered ChABC or Pen intraspinally 14 days after injury. Spinal cords were isolated 2 days later and assessed for the expression of CSPG protein. In sham-treated control WT and tPA KO mice, NG2 protein was minimally expressed in cells with stellate morphology, consistent with its known expression on OPCs (Jones et al., 2003a). In injured WT and tPA KO mice treated with Pen, NG2 protein expression was strongly upregulated (Figures 8 & 16). In contrast, administration of ChABC caused a 43% decrease in NG2 levels in WT mice compared to its respective Pen-treated group. However, a much more modest decrease in NG2 was observed in tPA KO SCI mice

injected with ChABC (16% compared to tPA KO Pen group), suggesting that tPA facilitates ChABC-mediated degradation of NG2. NG2 expression levels were also evaluated using immunoblotting, confirming that in the absence of tPA, ChABC-mediated clearance of NG2 is substantially attenuated (Figures 11 top and 12A, ; note - NG2 protein expression could not be evaluated after Pen treatment *in vitro* using western blotting, since the presence of GAG chains resulted in a non-distinct protein band, not shown). My findings revealed that uPA, despite being upregulated in SCI, cannot fully functionally assume the role performed by tPA. I, nonetheless, examined the possibility that uPA might partially compensate for the loss of tPA by testing *in vitro* the possibility that uPA can promote the degradation of the NG2 core protein by plasmin after ChABC cleavage of the GAG chains. However, in contrast to tPA, which can efficiently bind to the NG2 core protein (Nolin et al., 2008), uPA was unable to use NG2 as a scaffold for plasmin generation and subsequent degradation (Figure 13A). Thus, tPA functions as the only relevant serine protease in this model injury system that can bind to NG2 core protein and use it as a scaffold to target plasmin generation and subsequent degradation of this CSPG core protein.

Since we had previously reported an interaction between the tPA/plasmin system and phosphacan and neurocan proteins after seizure in mice (Wu et al., 2000), I also assessed the fate of these two CSPG proteins. Intact WT and tPA KO mice showed only negligible levels of phosphacan and neurocan protein expression (Figures 9-10). In contrast, Pen-injected WT and tPA KO SCI groups expressed significantly higher levels of both CPSG proteins. After ChABC cleavage in WT SCI mice, similar to NG2 protein, there was a 42% reduction in phosphacan and 58% in neurocan expression levels

compared to WT Pen groups respectively (Figures 9-10 and quantification in Figure 16). However, ChABC cleavage in tPA KO SCI mice resulted in only 14% clearance of phosphacan but 42% clearance of neurocan compared to tPA KO Pen group. No statistical differences were found in the processing of neurocan after ChABC cleavage in WT and tPA KO spinal cord homogenates using western blot analysis (Figures 11 middle, 12B). *In vitro* cleavage experiments revealed that pure neurocan protein could bind both uPA and tPA serine proteases and be targeted for degradation by plasmin after ChABC cleavage (Figure 13B). I was not able to evaluate phosphacan protein expression using western blot in either pure protein or *ex vivo* SCI homogenates. Collectively, these results suggest that the tPA-mediated plasmin preferentially binds and degrades phosphacan core protein, while both uPA and tPA-mediated plasmin pathways can bind and degrade the neurocan core protein after ChABC cleavage of the GAG chains.

I then analyzed the role of tPA/plasmin in total CSPG protein levels before and after ChABC cleavage *in vivo*. The epitope, CS56, is found at the ends of CSPG GAG chains and allows us to visualize the intact CSPG protein. After ChABC cleavage, this epitope is removed while the C4S antigen found within the GAG chains is exposed and confirms presence of the CSPG core protein after ChABC cleavage. Intact CSPG proteins were expressed at low levels in intact WT and tPA KO mice and significantly upregulated after injury in vehicle enzyme injected groups (Figure 14). After ChABC cleavage, CSPG protein level was significantly reduced in both WT (80%) and tPA KO SCI mice (68%) compared to the SCI+Pen group of the same genotype (Figures 14 & 16). Compared to intact CSPG protein, the stub protein C4S was found to be inversely expressed in these groups. In WT ChABC treated group, C4S protein expression

localized to the border of the glial scar, while when such staining was performed in the tPA KO animals, higher protein expression was observed that localized in both the border and the dead region of the glial scar (Figure 15). These results are consistent with our earlier findings that the tPA/plasmin system affects degradation of core protein after ChABC cleavage of intact CSPGs.

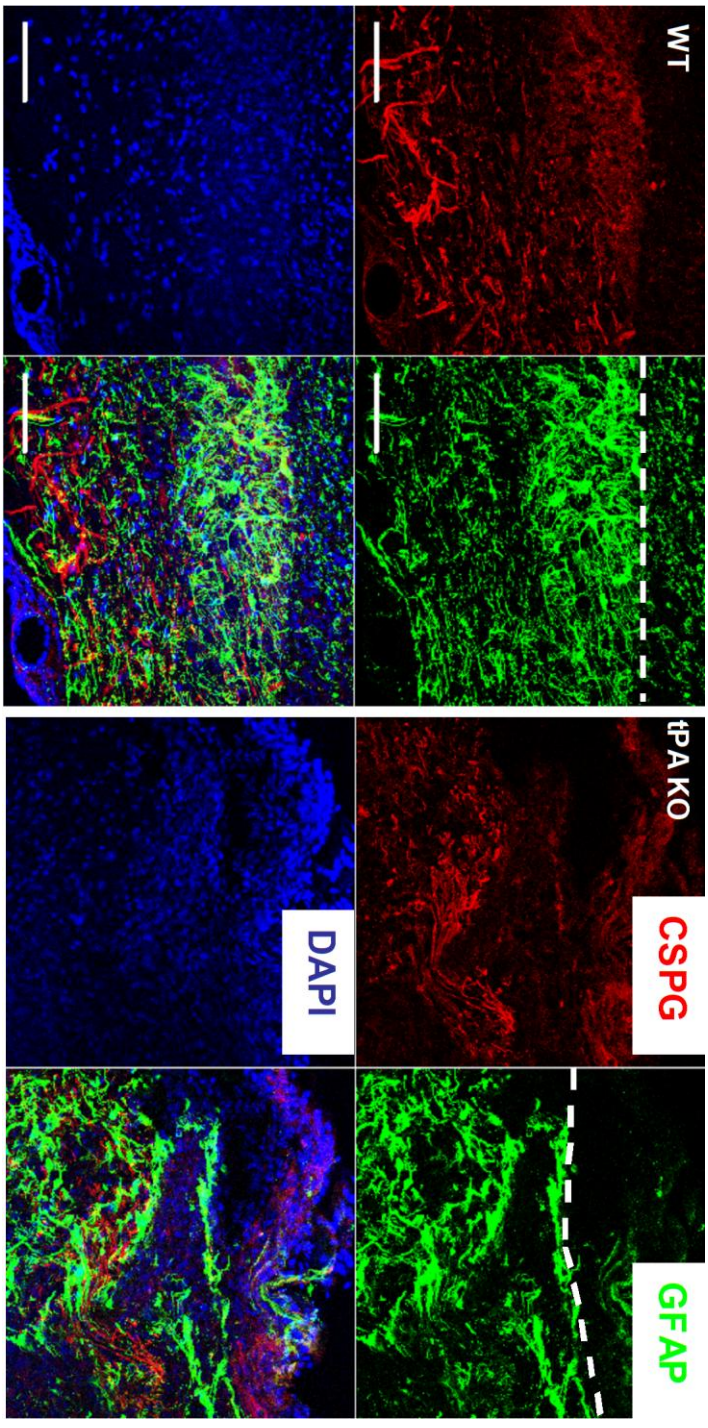
WT
tPA KO
CSPG
GFAP
DAPI

Figure 6: CSPG and GFAP protein expressions are modestly upregulated 7 days after contusion injury. Sagittal view of spinal cord from 7 days post contusion injured WT and tPA KO mice were isolated and perfused with PFA. 18μm sagittal sections were prepared and triple-stained for CSPG (red, Sigma), GFAP (green) and 4'-6-Diamidino-2-phenylindole (DAPI, blue, nuclear marker). The glial scar region was visualized with a Zeiss confocal microscope using LSM 510 Meta Software. Images are representative of 3-4 biological replicates per group. Dashed lines indicate border of injury region. Scale bar = 100μm.

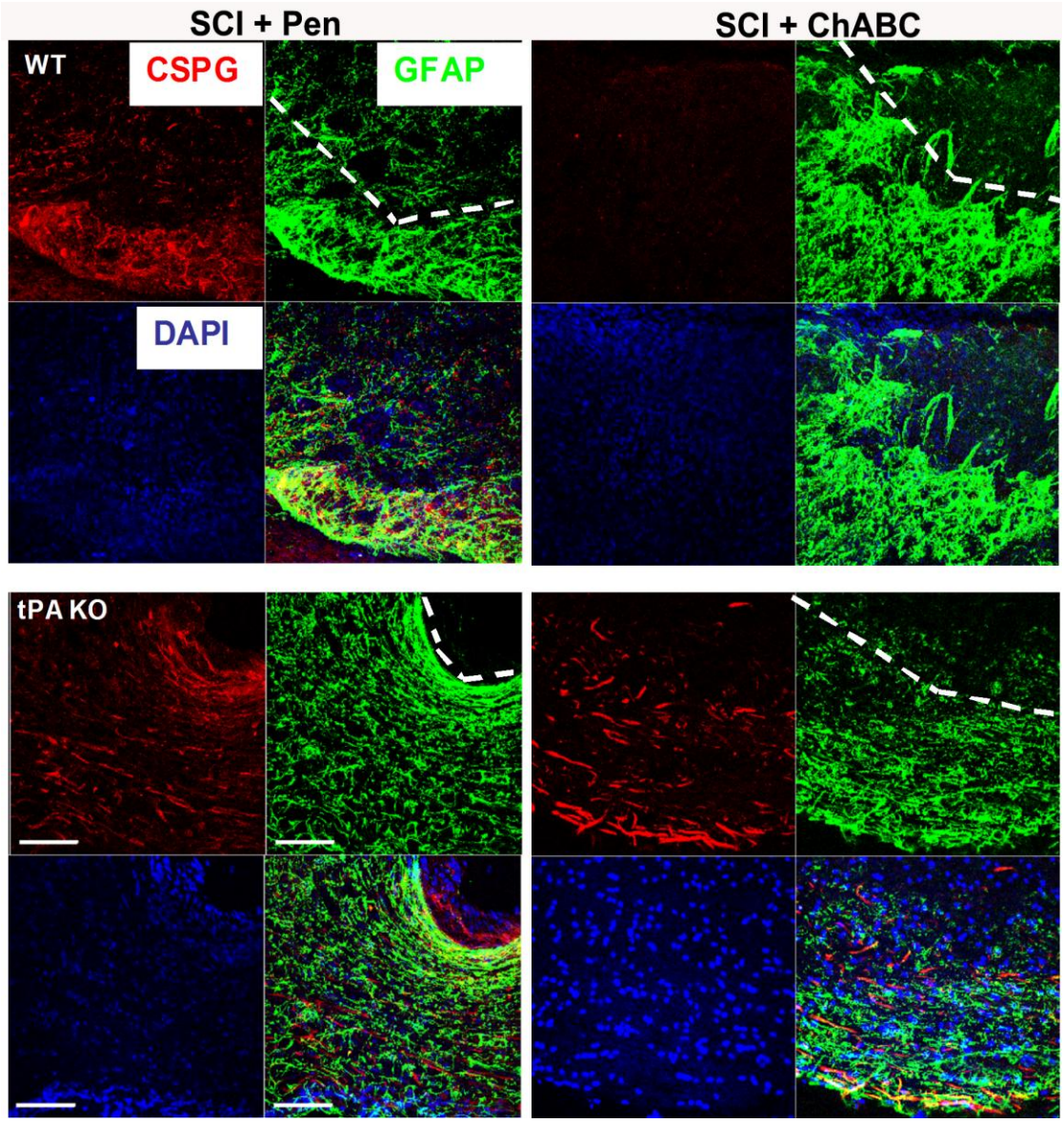

Figure 7: ChABC activity is attenuated in the absence of tPA. 14 days contusion injured WT and tPA KO mice received Pen or ChABC injection (50U/ml x 1µl). One week later, spinal cords were isolated and perfused with PFA. 18µm sagittal sections were prepared and triple-stained for CSPG (red), GFAP (green) and DAPI (blue). Images are representative of 3-4 biological replicates per group. Dashed lines indicate border of injury region. Scale bar = 100µm.

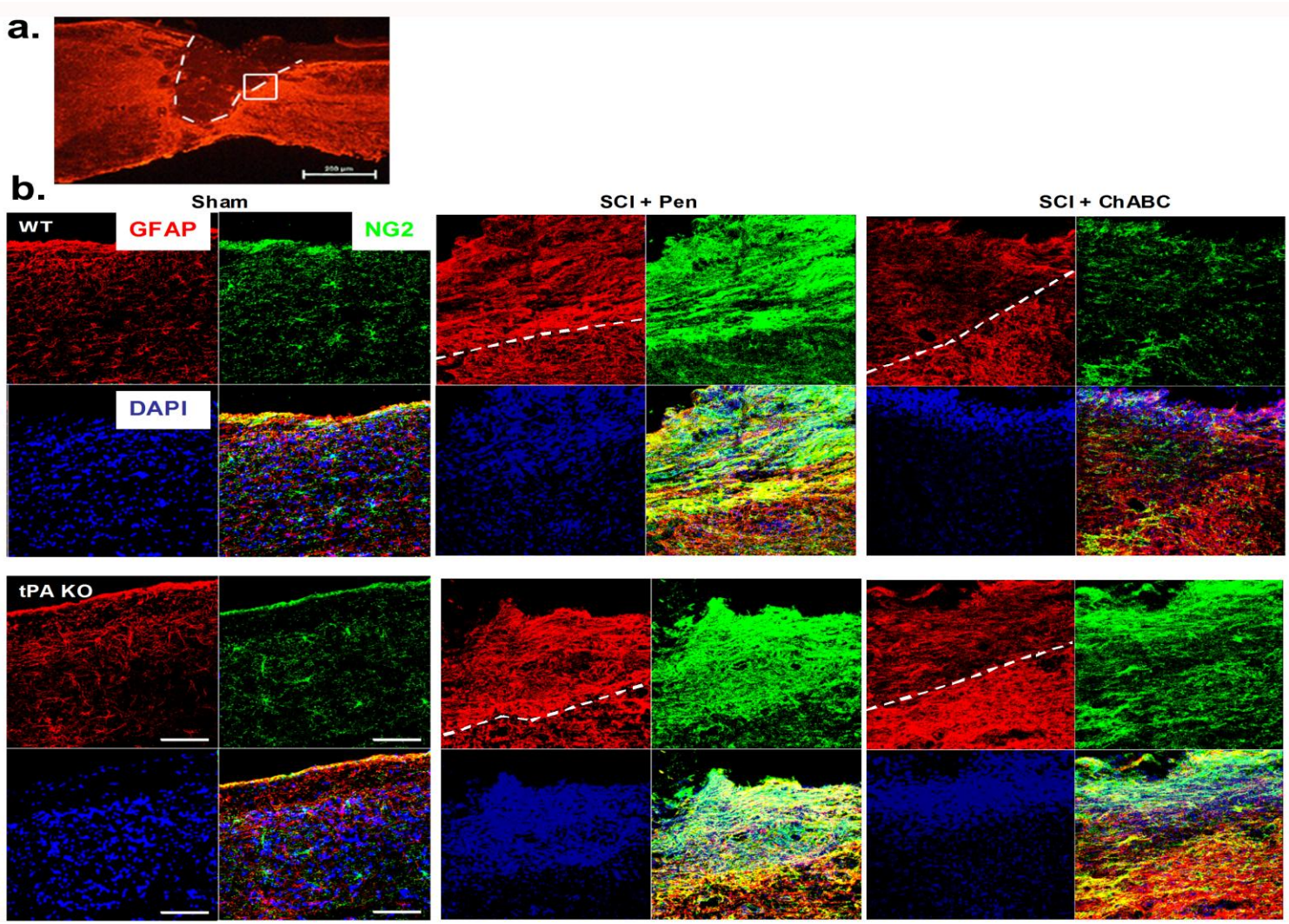
a.
b.
Sham
SCI + Pen
SCI + ChABC
WT
GFAP
NG2
DAPI
tPA KO

Figure 8: The tPA/plasmin system degrades NG2 protein after ChABC cleavage *in vivo.* 14 days contusion injured WT and tPA KO mice received Pen or ChABC injection (50U/ml x 1µl). Two days later spinal cords were isolated, perfused with PFA and 18µm sagittal sections prepared. **a**) A 14 day contusion injured WT mouse spinal cord section stained with GFAP (red, DAKO) & showing the injury region (dashed lines) with the dorsal side up. Higher magnification images were captured in (**b**) along the border of glial scar region as indicated by boxed area. Scale bar = 200µm. **b**) Spinal cord sections were triple-stained for NG2 (green, Chemicon), GFAP (red) and 4'-6-Diamidino-2-phenylindole (DAPI, blue, nuclear marker) and images captured with a Zeiss confocal microscope using LSM 510 Meta Software. Dashed line indicates border of injury region. Images are representative of 3-4 biological replicates per group. Scale bar = 100µm.

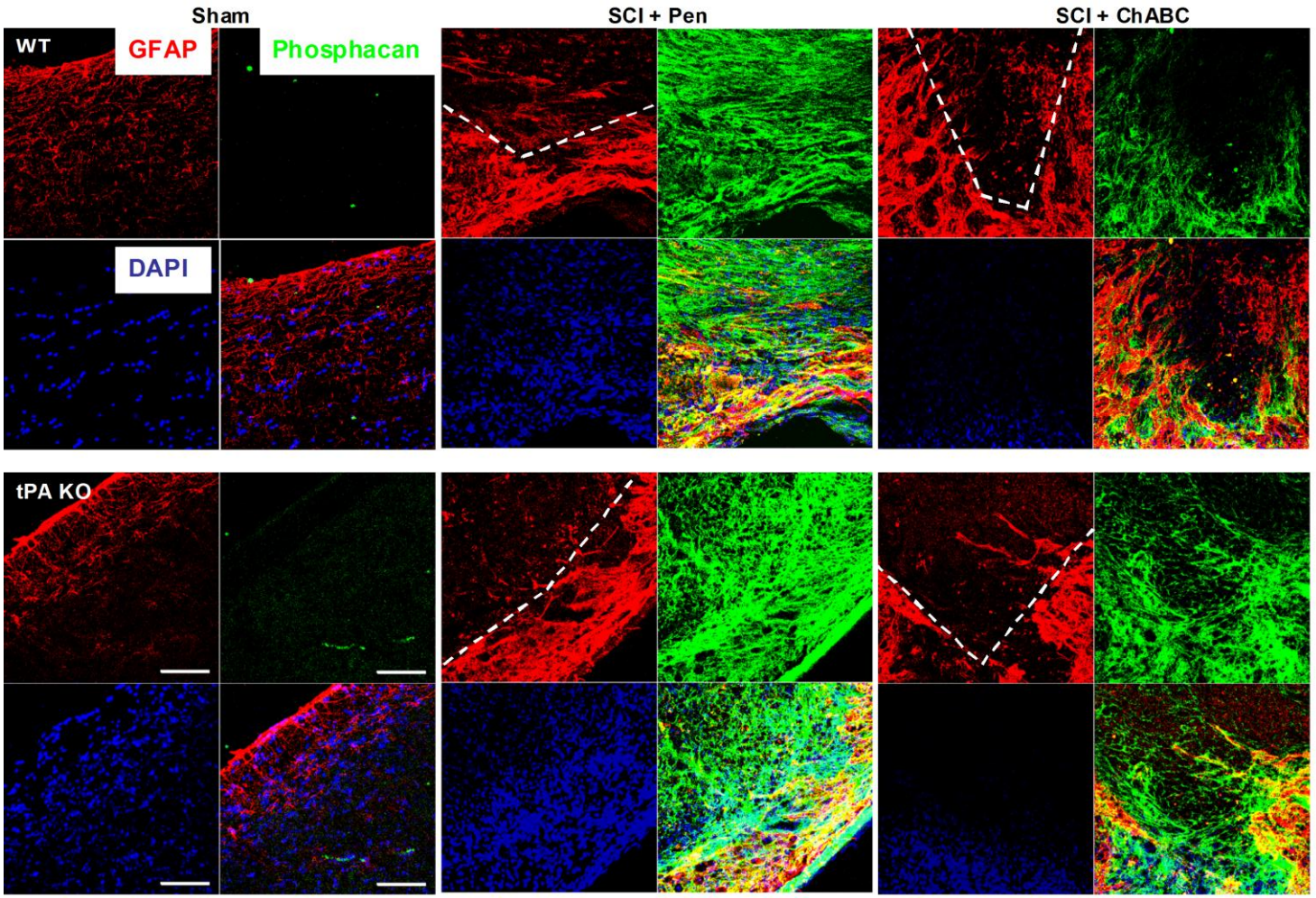
Sham
SCI + Pen
SCI + ChABC
WT
GFAP
Phosphacan
DAPI
tPA KO

Figure 9: The tPA/plasmin system degrades phosphacan protein after ChABC cleavage *in vivo.* 14 days contusion injured WT and tPA KO mice received Pen or ChABC injection and spinal cords were processed as described. Spinal cord sagittal sections were triple-stained for phosphacan (green; 3F8; DSHB), GFAP (red) and DAPI (blue). Images are representative of 3-4 biological replicates per group. Dashed lines indicate border of injury region. Scale bar = 100μm.

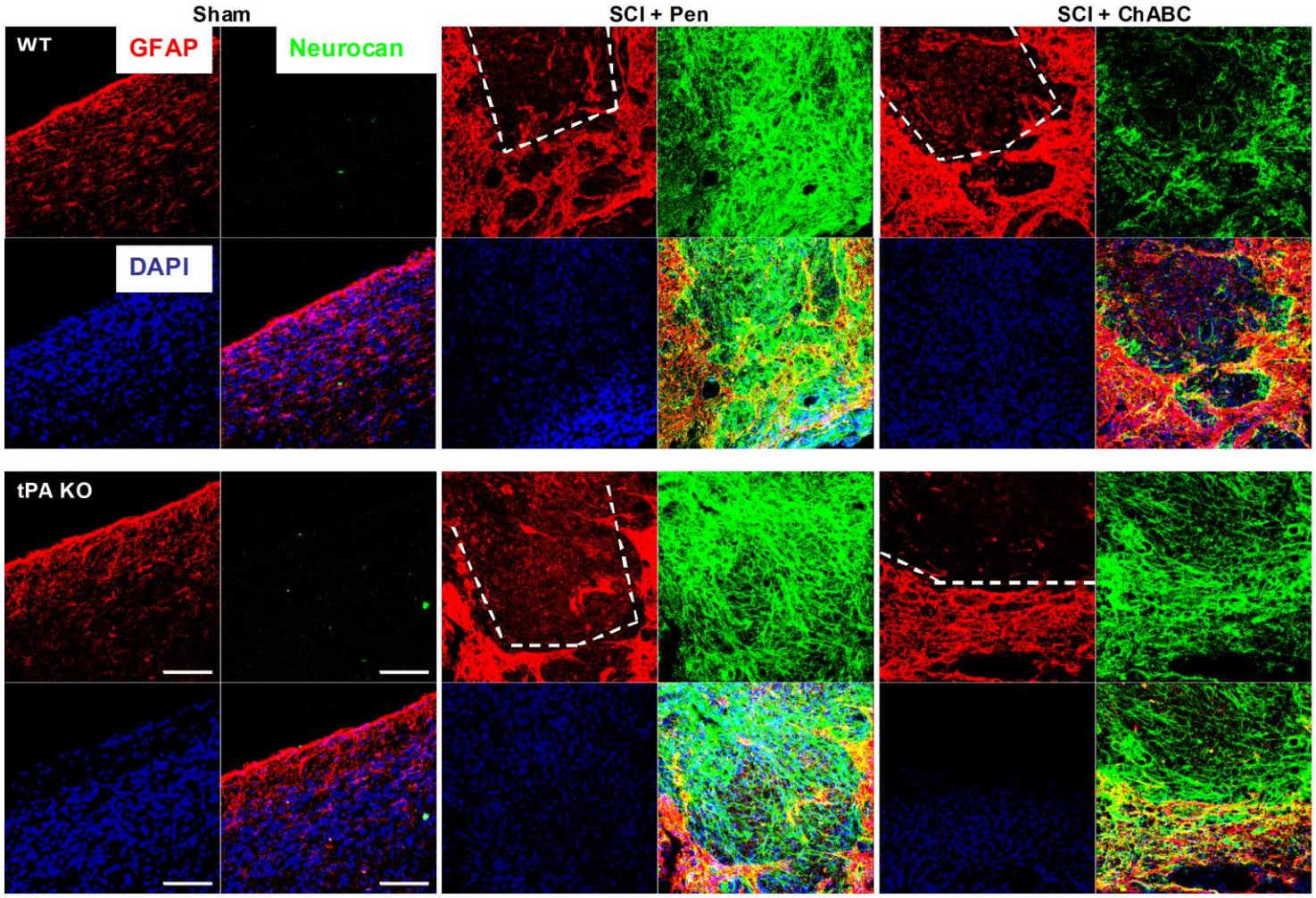
Sham
SCI + Pen
SCI + ChABC
WT
GFAP
Neurocan
DAPI
tPA KO

Figure 10: The tPA/plasmin system degrades neurocan protein after ChABC cleavage *in vivo*. 14 days contusion injured WT and tPA KO mice received Pen or ChABC injection and spinal cords were processed as described. Spinal cord sagittal sections were triple-stained for neurocan (green; 1F6; DSHB), GFAP (red) and DAPI (blue). Images are representative of 3-4 biological replicates per group. Dashed lines indicate border of injury region. Scale bar = 100µm.

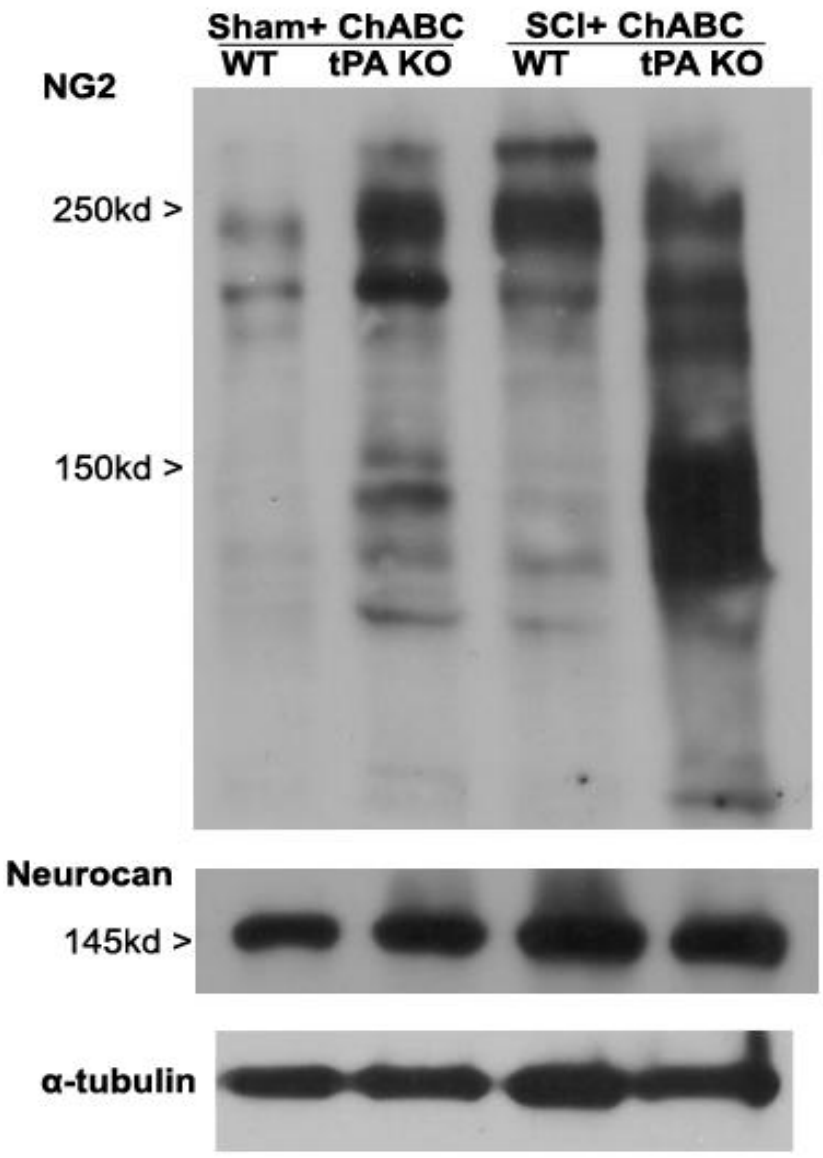

Figure 11: In the absence of tPA, NG2 but not neurocan protein degradation is attenuated after ChABC cleavage *in vitro*. Representative immunoblot of NG2 (top) and neurocan (middle) proteins in WT and tPA KO sham and 14day SCI homogenates incubated with ChABC for 3hrs at 37°C and probed with rabbit anti-NG2 and 1F6 antibodies. Protein bands were quantified by densitometry in Image J and data normalized against α-tubulin (bottom) loading control and total protein levels. Immunoblot representative of three biological replicates.

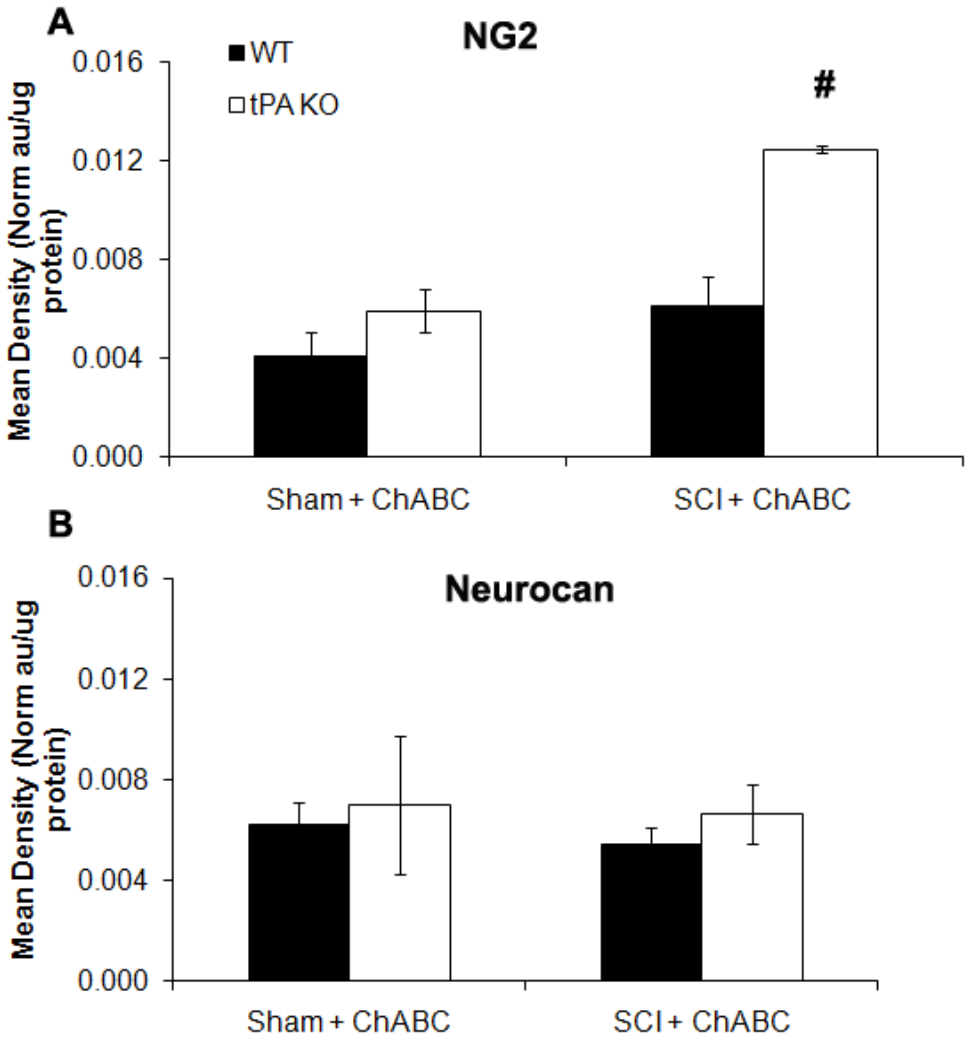

Figure 12**: In the absence of tPA, NG2 but not neurocan protein was significantly retained after ChABC cleavage *in vitro*.** Quantification of NG2 (A) and neurocan (B) protein in WT and tPA KO sham and 14day SCI homogenates incubated with ChABC for 3hrs at 37°C and probed with rabbit anti-NG2 and 1F6 antibodies. Protein bands were quantified by densitometry in Image J and data normalized against α-tubulin loading control and total protein levels. One Way ANOVA was used to compare all groups. Significant ANOVA was followed by *post hoc* Holm Sidak test. # indicates significant *post hoc* differences at $p<0.001$ (n=3).

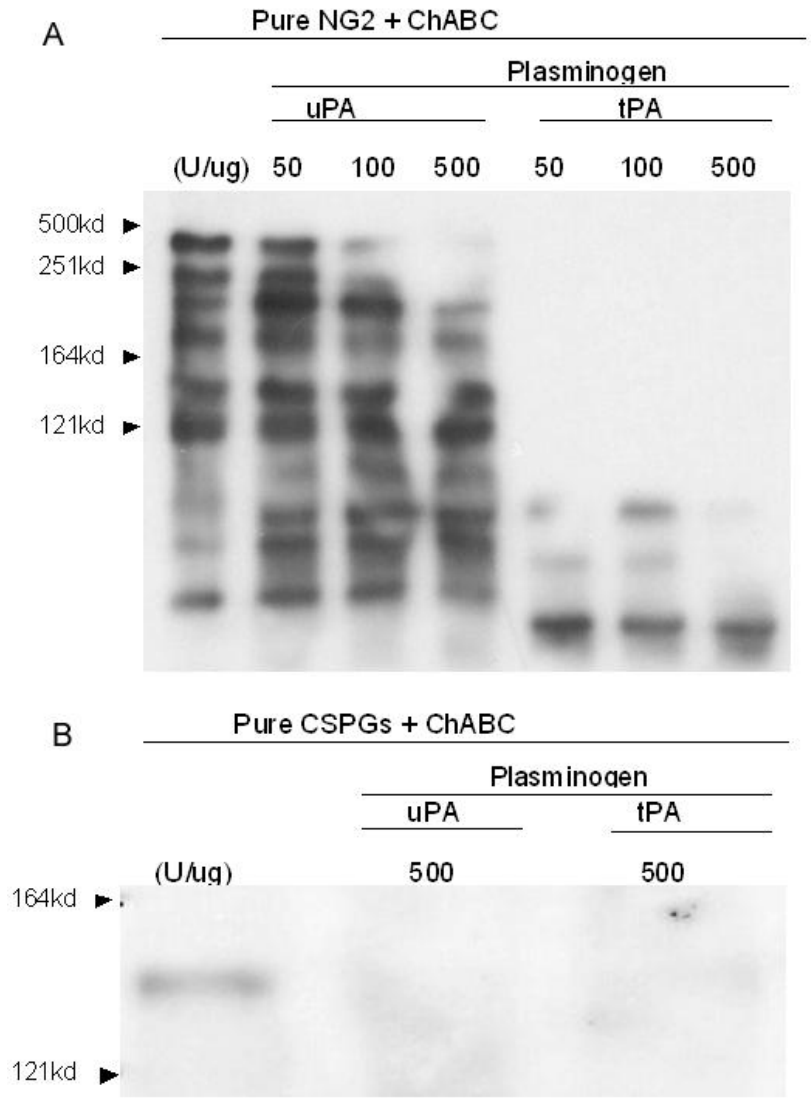

Figure 13: tPA/plasminogen system cleaves both pure NG2 and neurocan proteins while uPA/plasmin system cleaves only neurocan protein. A) Western blot of pure NG2 protein (gift from Dr. Joel Levine) incubated with ChABC and pure plasminogen and pure recombinant uPA and tPA for 3hrs at 37°C followed by probe with rabbit anti-NG2 antibody. B) Western blot of pure CSPG protein (CC117; Chemicon) incubated with ChABC, pure plasminogen, uPA and tPA as above and probed for neurocan protein (1F6).

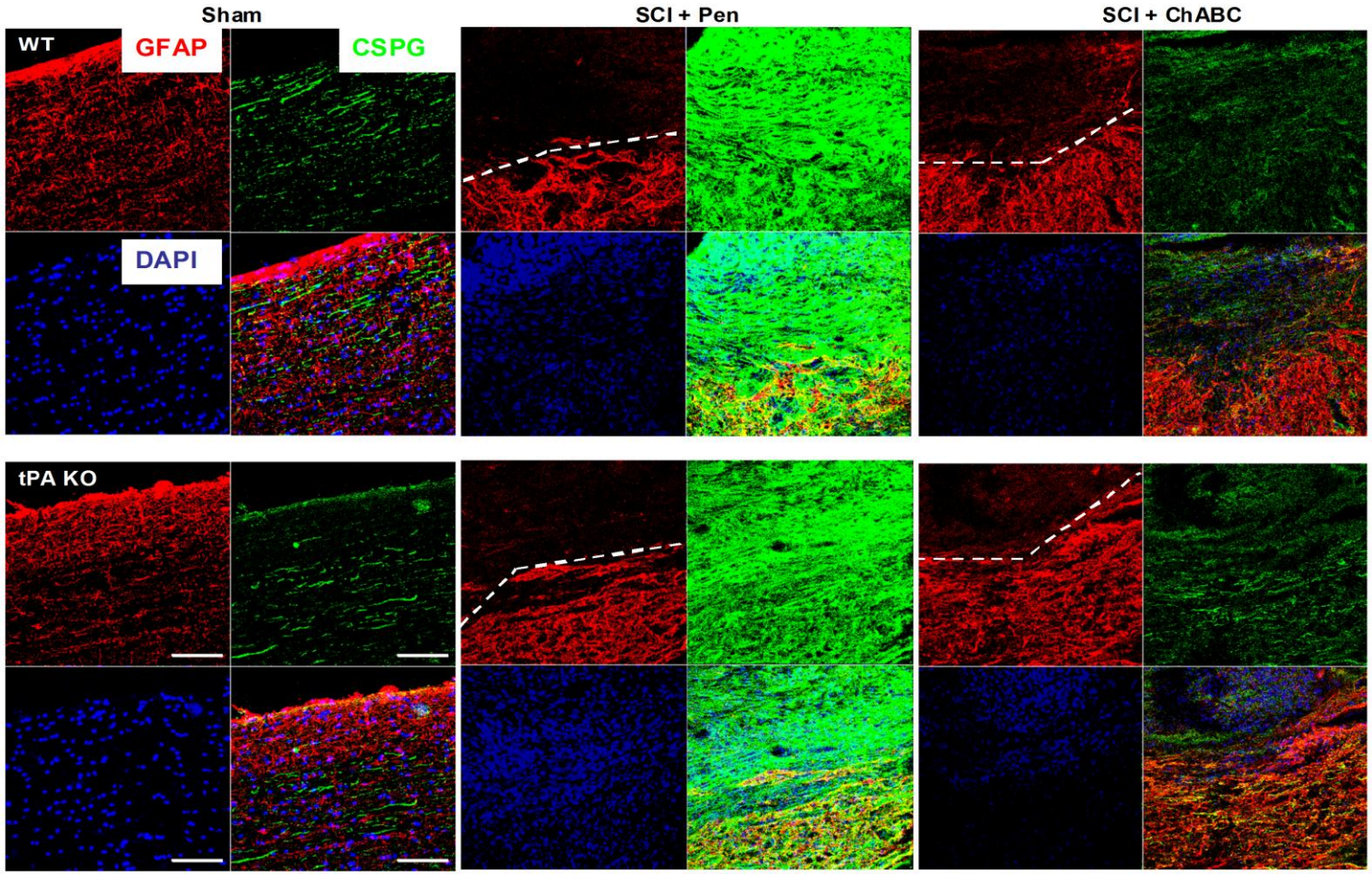
Sham
SCI + Pen
SCI + ChABC
WT
GFAP
CSPG
DAPI
tPA KO

Figure 14: CSPG protein expression reduced in both WT and tPA KO SCI mice after ChABC cleavage *in vivo.* 14 days contusion injured WT and tPA KO mice received Pen or ChABC injection and spinal cords were processed as previously described. Spinal cord sagittal sections were triple-stained for CSPG (green), GFAP (red) and DAPI (blue). Images are representative of 3-4 biological replicates per group. Dashed lines indicate border of injury region. Scale bar = 100µm.

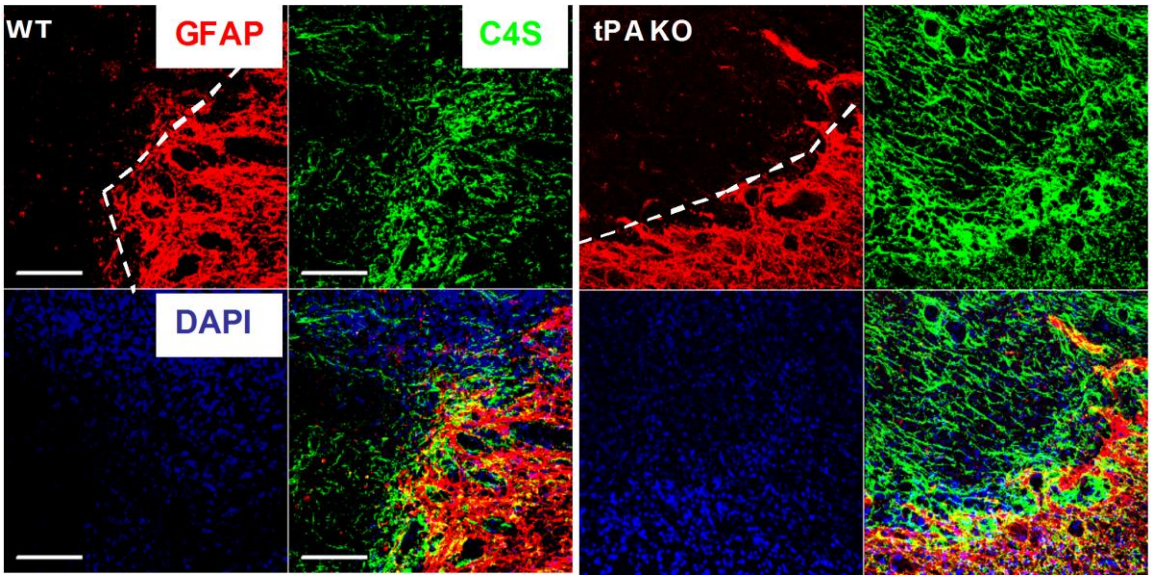

Figure 15: In the absence of tPA, C4S protein expression was retained after ChABC cleavage *in vivo.* 14 days contusion injured WT and tPA KO mice received Pen or ChABC injection and spinal cords were processed as previously described. Spinal cord sagittal sections were triple-stained for Chondroitin-4-Sulfate (green; MAB2030; Chemicon), GFAP (red) and DAPI (blue). Images are representative of 2 biological replicates per group. Dashed lines indicate border of injury region. Scale bar = 100µm.

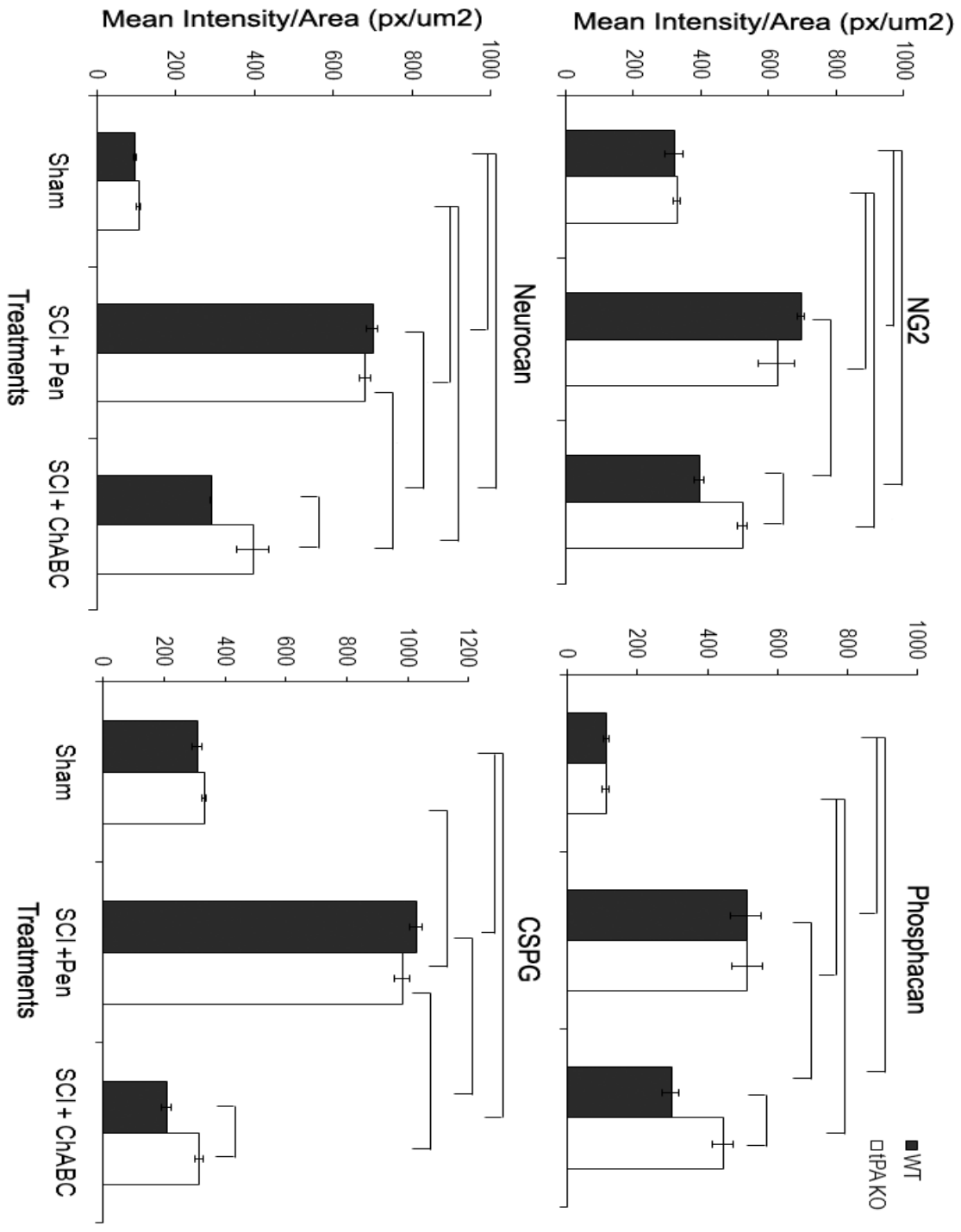
Mean Intensity/Area (px/um2)
NG2
Phosphacan
Neurocan
CSPG
WT
tPA KO
Sham
SCI + Pen
SCI + ChABC
SCI +Pen
Treatments

Figure 16: In the absence of tPA/plasmin system, NG2, phosphacan, and neurocan protein expression were significantly retained after ChABC cleavage *in vivo*. Multiple images of NG2, phosphacan, neurocan, and intact CSPG protein expression around the glial scar region (identified by upregulated GFAP expression) were captured. ImageJ software (NIH) was used to prepare stacks of glial scar images for each biological replicate and protein staining. Mean intensity/area was calculated (n=3-4). t-test was used to compare within each treatment and one-way ANOVA to compare within genotype. Significant ANOVA values were followed by *post hoc* Holm Sidak. Brackets indicate significance due to t-test or *post hoc* analyses with a minimum of $p<0.05$.

Chapter III- tPA/plasmin system contribute to ChABC mediated axonal plasticity after SCI

Materials & Methods

Zymographic assay for plasminogen activator activity: Embryonic day 15 cortical neurons from WT and tPA KO mice (20µg protein/sample) were analyzed on 10% SDS-PAGE copolymerized with plasminogen (13mg/ml) and casein (3mg/ml). After electrophoresis, SDS was removed by incubating the gel with 2.5% Triton X-100 for an hour. The gel was then incubated with 0.1M Tris pH 8.0 overnight at 37°C. Next day, gel was stained with coomassie blue for two hours and destained until clear zones of lysis became visible. Pure, recombinant tPA (300mU; Genentech) was used as positive control.

Amidolytic assay for quantification of plasminogen activator activity: Embryonic day 15 cortical neuron cell lystes and media from WT and tPA KO mice (10µg protein/sample) were incubated with 0.68µM plasminogen in a 50mM Tris buffer pH 8.1 with 2% BSA and 0.3mM chromogenic substrate-2251 overnight in the dark at room temperature. Cleavage of S-2251 by serine protease-generated plasmin and the subsequent color change was quantified at 405nm. A dose response for pure recombinant tPA activity was simultaneously run alongside the test samples and the time point when the R^2 value for the dose response was closest to 1 was used to measure the concentration of serine protease in the samples. All samples were run in triplicates. 1mM amiloride was used to block uPA in the samples.

Neurite Outgrowth Assay: 25mm coverslips were UV-irradiated and coated overnight with poly-d-lysine (25µg/ml) and laminin (10µg/ml) at 37°C. Next day, embryonic day 15 cortices were isolated from WT and tPA KO mice and manually dissociated in

Neurobasal Media with B27 supplement (Invitrogen), L-glutamine, gentamicin, and Penicillin/streptomycin. Cells were plated at a density of 100,000 cells/coverslip on WT or tPA KO Sham and SCI homogenates previously treated with ChABC or Pen (0.5U/ml) *in vitro* for 3 hrs at 37°C as detailed in western blot procedure. For the rescue experiment, tPA KO SCI homogenates were co-treated with pen and plasmin (0.06U/ml; List Labs) or ChABC and plasmin *in vitro* for 3 hrs at 37°C. After 2 days in culture, cells were fixed with 4% PFA for 1 hour, blocked with 2% goat serum and incubated overnight with CSPG (1/200 CS56; Sigma). The following day, the cells were washed in PBS and incubated with goat anti-mouse-Alexa 555 secondary antibody (1/1000; Invitrogen) for 1 hour followed by a second overnight incubation with β-tubulin III antibody (1/2000; Covance). On the last day, cells were washed again in PBS and incubated with goat anti-rabbit Alexa 488 antibody (1/2000; Invitrogen) and slides prepared with aqueous mounting media (Fluoromount).

Images with digital resolution of 1024 x 1024 were captured with a Zeiss confocal microscope using LSM 510 Meta software. A grid format was used with CSPG-rich regions in each grid first identified and images of neurons on the CSPG-rich region then captured. 25 different regions were sampled per biological replicate. Data were calculated as a ratio of the total neurite length/neuron for each biological replicate. Total neurite length in each image panel was quantified using Neurite Tracer plugin in Image J (Pool et al., 2008) while total neurons were manually counted in each image panel. Data was normalized against cortical neurons only images of the same genotype and plotted as a percentage of neurite length/neuron. Approximately 400-600 neurons were quantified per biological replicate.

***In Vivo* ChABC and Plasmin treatments:** 2 weeks after contusion injury, WT and tPA KO mice were re-anesthetized and placed in the stereotaxic apparatus. The injured region was re-exposed and 1ul of ChABC (50U/ml) or Pen was injected into the central canal (1mm depth, rate of 0.4µl/min) using a 28-gauge Hamilton syringe attached to an automated microinjector. For the therapeutic experiment, 2µl of ChABC and plasmin (50U/ml & 0.1U/ml respectively) mix or Pen and plasmin mix were injected into WT SCI mice. The needle was withdrawn after an additional one minute to prevent reflux.

Motor Axon Injection & Staining: Intact mice and 16 days post-SCI WT and tPA KO mice were re-anesthetized and their head secured to a stereotaxic device. Mouse's cortex was then exposed and 0.5µl of 10% biotinylated dextran amine (BDA; Sigma) was injected at 4 sites (coordinates: 1.0mm medial-lateral, & 0.5mm anterior or 1mm posterior to bregma) at a depth of 0.5mm to the cortical surface with a 30 gauge Hamilton syringe connected to an automated microinjector (0.5µl/min). The needle was withdrawn after an additional minute to prevent reflux. Overlying muscle and skin was sutured and mice were injected with buprenorphine (0.03 mg/kg) subcutaneously to reduce pain and placed on a heating pad to recover. Spinal cords were isolated 14 days later as previously outlined.

To visualize BDA labeled axons, sections were first incubated with 3% hydrogen peroxide to quench endogenous peroxidase activity. Sections were then stained with avidin and biotinylated horseradish peroxidase (HRP; Vectastain ABC Kit) for 2 hrs followed by a second incubation with DiAminoBenzidine (DAB)/H_2O_2 mix for 15

minutes at room temperature and allowed to dry overnight. DAB stainings were then intensified by sequential incubation at room temperature with 1% silver nitrate in the dark for 50 minutes followed by a second incubation in 0.2% gold chloride in the dark for 15 minutes and 5% sodium thiosulfate for 15 minutes. Sections were successively dehydrated in ethanol for 10 minutes and xylene for 20 minutes and coverslipped with Permount (Fisher) mounting media.

Motor Axon Quantification: Images of stained sections were captured with Nikon E600 microscope using Nis-Elements software at a digital resolution of 1280 x 1960. Using the injury region as the center of the 40x visual field, images were captured at the injured region (0µm), 200, 400 and 600µm in the rostral and caudal directions per serial sagittal section. Images were captured for all the sections in one spinal cord. ImageJ (NIH) software was then used to create biological stacks for each region of the spinal cord. The hessian filter in plugin FeatureJ in ImageJ software was then used to create binary traces of axons in the biological stacks as outlined by another group (Grider et al., 2006). These binary traces were then thresholded and total pixel intensity and section area per biological stack (one for each region of the spinal cord) measured. Data were exported to Excel and total pixel intensity/area calculated. Data were normalized and presented as a percentage of the region with the highest axon density (600µm rostral region).

Sensory Axon Injection & Staining: On day 22, intact and injured WT and tPA KO mice were re-anesthetized and the right sciatic nerve exposed. 2.5µl of 1.5% cholera

toxin B subunit (CTB, List Biological Laboratories) was injected into the nerve with a 32 gauge Hamilton syringe connected to an automated microinjector (0.4µl/min). The needle was withdrawn after an additional minute to prevent reflux. Overlying muscle and skin was sutured and mice were left on heating pad to recover. Spinal cords were isolated 4 days later.

To determine the optimal glial scar and CTB co-labeling reaction, three different sets of staining were tested. For the double immunofluorescent reaction, serial sagittal sections were labeled at an interval of 10 sections with goat anti-CTB antibody (1/5000; List Biological Laboratories) followed by a secondary donkey anti-goat-Alexa 594 antibody (1/2000; Invitrogen) for 1 hr at room temperature followed by an overnight incubation at 4°C with glial fibrillary acidic protein (GFAP 1/1000; DAKO) to outline the glial scar. Species-appropriate-Alexa 488 antibody was then applied for 1 hr at room temperature and sections were coverslipped with aqueous mounting media. For the DAB-immunofluorescent reaction, sections were labeled with goat anti-CTB antibody followed by a second probe with biotinylated rabbit anti-goat IgG (Vector labs). Sections were then sequentially incubated with avidin-biotinylated HRP and DAB to visualize the axons followed by an overnight incubation at 4°C with GFAP (1/1000) to outline the glial scar. Species-appropriate-Alexa 488 antibody was then applied for 1 hr at room temperature and sections were coverslipped with aqueous mounting medium. For the single DAB reaction, sections were labeled with goat anti-CTB antibody followed by a second probe with biotinylated rabbit anti-goat IgG. Sections were then sequentially incubated with avidin-biotinylated HRP and DAB as before. Silver-gold reaction was used to intensify axon staining. For all staining reactions, Nikon E600 microscope using

Nis-Elements software was used to capture images of co-labeled injured regions with a digital resolution of 1280 x 1960. Representative images were oriented with dorsal side up in Adobe Photoshop 7.0.1.

Sensory Axon Quantification: To measure axon density, two different softwares were tested. Using live image projection onto a computer monitor, Neurolucida software was used to outline whole sections, and the injured region within each section, at an interval of 10 sections per spinal cord. All the axons in the injured region and whole section were traced. Using reference points in each section, all the traced sections for a biological replicate were aligned and the tracings exported to Neurolucida Explorer. The 3D contour summary for the injured region and whole spinal cord was then measured. Due to the labor intensive approach of this technique, Stereoinvestigator software (MicroBrightField Colchester, VT) was then tested and ultimately used for sensory axon density quantification. Space Balls probe in Stereoinvestigator software was used to outline the injured region and measure the total axon length and injury volume per spinal cord. The probe divides the injured region into 500x500µm grid system in the x-y axis and uses a sphere to sequentially and randomly sample a small tissue volume within every grid block. Axons that intersect the sphere across the z-axis are marked by an observer. The probe then measures the total axonal length of all the marked axons in each spinal cord to provide a value of total axonal length and injured tissue volume. Data from both softwares were exported to Excel and the total axonal length was divided by the injured tissue volume to calculate axonal density per spinal cord.

Statistics: For axon tracing experiments, all surgeries and measurements were performed with an observer blinded to the genotype of the mice. To analyze the sensory axon density, One-Way ANOVA was used to compare differences due to treatment within the WT mice. Significant ANOVA results were followed by *post hoc* Holm Sidak test. t-test was used to compare differences within each treatment group and within the tPA KO mice (since there were only two groups with this genotype). A minimum alpha value of 0.05 was accepted as statistically significant. Data are presented as mean $\pm$ SEM.

Results

In the absence of tPA/plasmin system, cortical neurite outgrowth is attenuated after ChABC cleavage of *ex vivo* glial scar

ChABC cleavage of the GAG chains on CSPGs is known to enhance axonal plasticity after SCI (Bradbury et al., 2002; Moon et al., 2001). Our previous work has also demonstrated that tPA/plasmin cleavage of NG2, phosphacan and neurocan can mediate neurite outgrowth in *in vitro* and *ex vivo* assays (Nolin et al., 2008; Wu et al., 2000). I, therefore, investigated if the tPA/plasmin-facilitated degradation of three CSPG proteins may also affect CNS neurite outgrowth response after ChABC cleavage. Amidolytic assays were used to first confirm the presence and absence of serine protease and specific tPA activity in gestational day 15 cortical neurons from WT and tPA KO mice (note: mice were left to mate overnight and day after coitus was designated as gestational day 0). tPA activity was present in WT cortical neuron cell lysates and media but significantly downregulated in samples from tPA KO group (Figure 17B). Serine protease and tPA activity graphs significantly overlapped in both the relative trends and total activity levels of each group measured suggesting that tPA accounted for all of the serine protease activity in the cortical neuron culture system (Figure 17 A & B). Zymography assay of the same cortical neuron samples also confirmed these findings (Figure 17C).

Sham and SCI homogenates from WT and tPA KO mice were next plated on coverslips and incubated in culture for 3 hrs at 37°C and stained for CSPG and DAPI to determine if CSPG molecules in these samples could be maintained in a controlled *in vitro* environment. WT and tPA KO sham spinal cord homogenates stained for minimal CSPGs while SCI samples were composed of densely packed CSPG molecules (Figure

18). These results are consistent with the *in vivo* data that CSPG molecules are significantly upregulated after SCI and demonstrate that the *ex vivo* glial scar system can be used as a reliable representation of the *in vivo* CSPG environment. An *ex vivo* glial scar system was then used to test the neurite outgrowth response to ChABC cleavage in a more controlled environment.

Cortical neurons from WT and tPA KO mice were grown on their genotypic equivalent sham and 14day-SCI homogenates previously treated with Pen or ChABC *in vitro*. After 2 days in culture, cells were fixed and triple-stained for CSPG, β-tubulin III and DAPI to visualize neurite outgrowth on CSPG proteins. I quantified 400-600 neurons for each spinal cord homogenate sample and condition. Our results show that cortical neurons grew extensive processes on CSPG proteins from intact WT and tPA KO spinal cord homogenates, equivalent to cortical neurons grown in the absence of any substrate. After *in vitro* Pen-treatment in 14days SCI homogenates, neurite outgrowth was significantly reduced in both genotypic cultures. But after *in vitro* ChABC treatment, significant neurite outgrowth is seen in the WT cultures while the tPA KO cultures showed significantly lower levels of neurite outgrowth, albeit more than their corresponding Pen-treated group (Figure 19 & 21). When the downstream effector of the tPA/plg pathway, plasmin, was added in the culture with ChABC, neurite outgrowth in the tPA KO SCI group was rescued and was comparable to that of the WT ChABC-treated cultures. In comparison, minimal levels of neurite outgrowth were seen in the Pen plasmin co-treated tPA KO cultures (Figure 20 & 21). Collectively, these results suggest that in the absence of the tPA/plasmin pathway, CNS neurite outgrowth is significantly attenuated after ChABC cleavage of CSPGs in *ex vivo* glial scar.

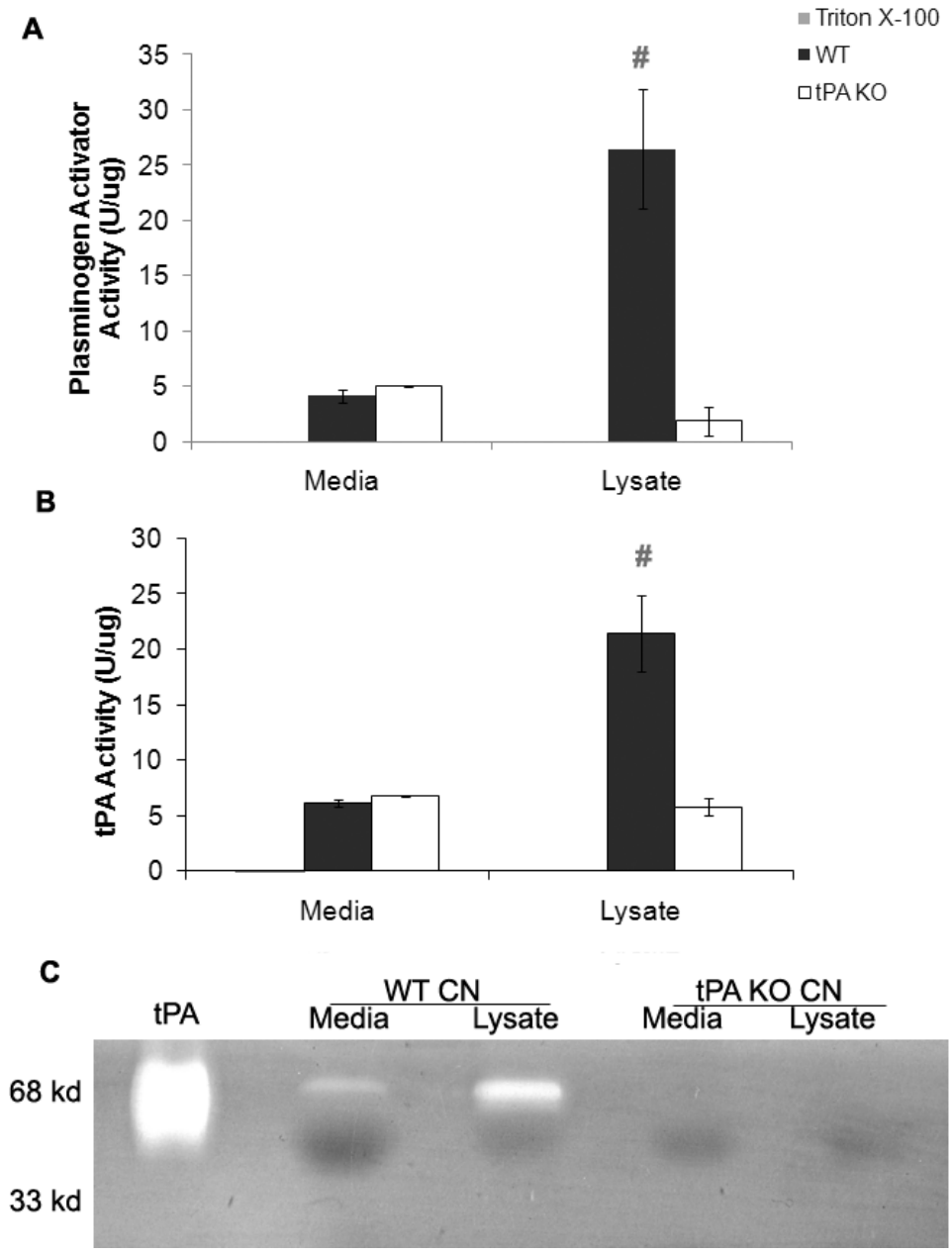
A
Triton X-100
WT
tPA KO
Plasminogen Activator Activity (U/ug)
35
30
25
20
15
10
5
0
#
Media
Lysate
B
tPA Activity (U/ug)
30
25
20
15
10
5
0
#
Media
Lysate
C
tPA
WT CN
Media
Lysate
tPA KO CN
Media
Lysate
68 kd
33 kd

Figure 17: tPA activity is present in cortical neurons from WT but not tPA KO mice. Amidolytic assay was used to quantify serine protease activity (A) and specific tPA activity (B) in media and cell lysates from WT and tPA KO cortical neurons and showed significantly higher levels in WT cell lysates compared to all other groups (n=3). One Way ANOVA was used to compare all groups. Significant ANOVA was followed by *post hoc* Holm Sidak test. # indicates significant *post hoc* differences at $p<0.001$. C) Zymography was then used to visualize tPA activity in the same samples. Pure recombinant tPA was used as positive control (n=2).

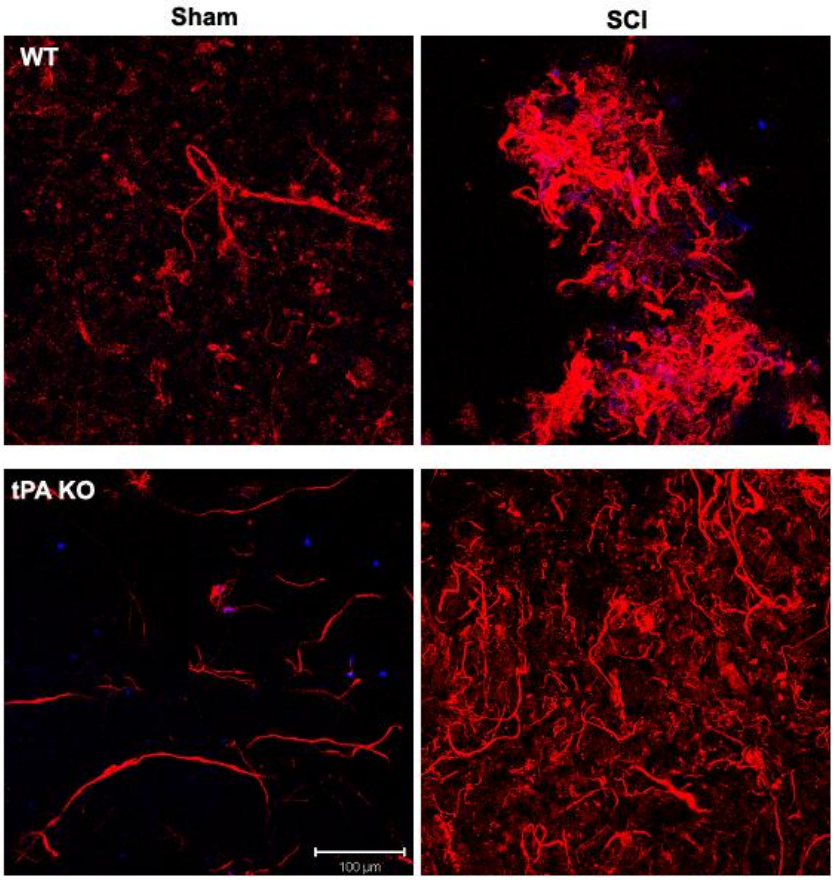

Figure 18: CSPG protein expression is upregulated in homogenized SCI tissue. Sham and 14 days contusion injured spinal cord from WT and tPA KO mice were isolated and manually homogenized in Tris-buffer saline. Spinal cord homogenates were plated on a coverslip and incubated for 3 hrs at 37°C. Spinal cords were then fixed with PFA and stained with CSPG (red) and DAPI (blue). Images are representative of 3 biological replicates per group. Scale bar = 100µm**.**

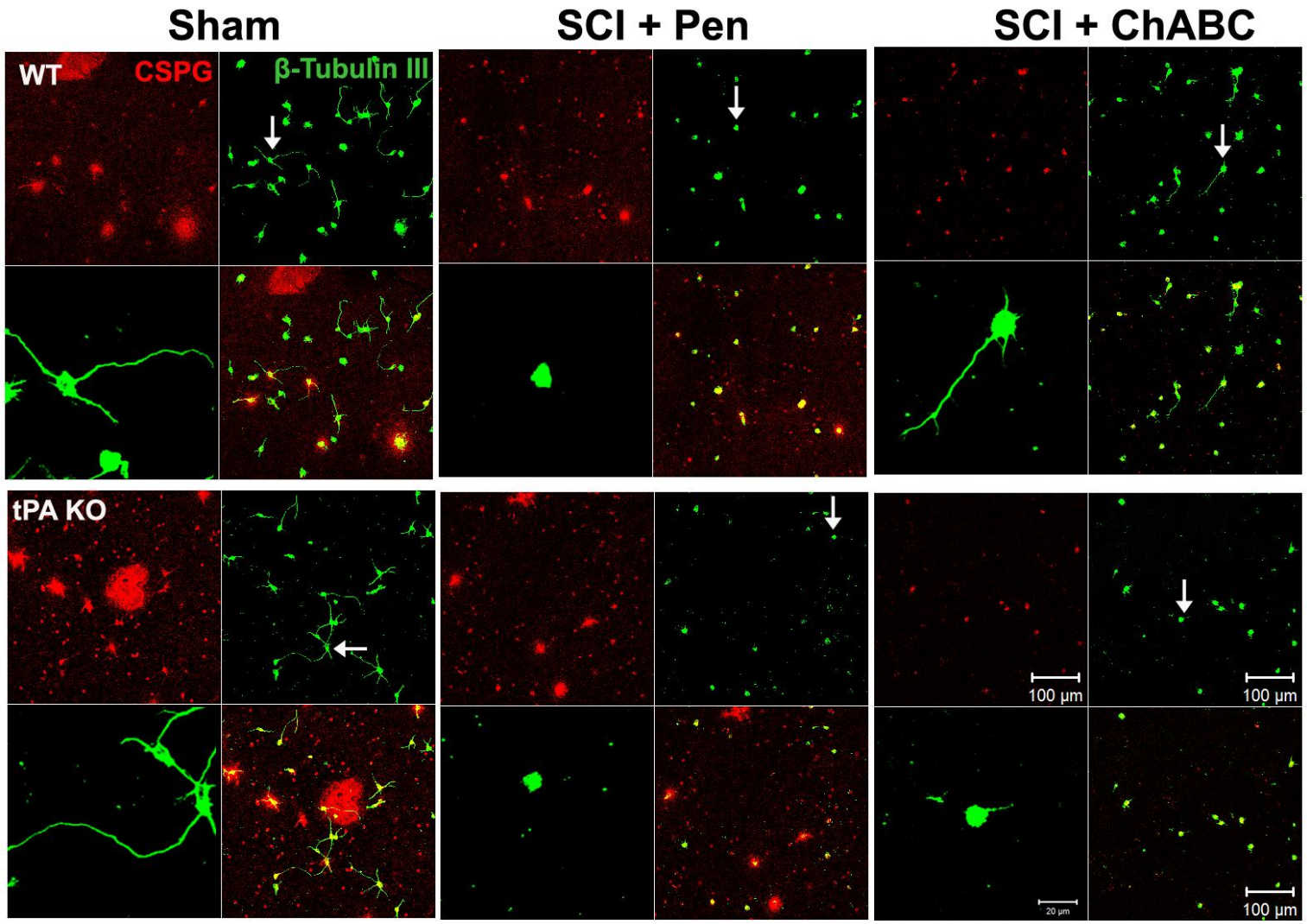
Sham
SCI + Pen
SCI + ChABC
WT
CSPG
β-Tubulin III
tPA KO
100 µm
100 µm
20 µm
100 µm

Figure 19: tPA/plasmin system allows for significant neurite outgrowth after ChABC cleavage of *ex vivo* glial scar. Spinal cord homogenates from sham or 14 day contusion injured mice were treated with Pen or ChABC (0.5U/ml) *in vitro* for 3 hours at 37°C. Embryonic day 15 WT and tPA KO cortical neurons were then plated on spinal cord homogenates of the same genotype. 2 days later, cultures were fixed with PFA and stained for intact CSPG (red; CS56; Sigma), and β-tubulin III (green; Tuj1; Covance). Scale bar = 100μm. Higher magnification image of a neuron in each group (indicated by an arrow in β-tubulin III staining) is provided in the lower left box of each image panel. Scale bar= 20μm. Images are representative of 3 biological replicates per group.

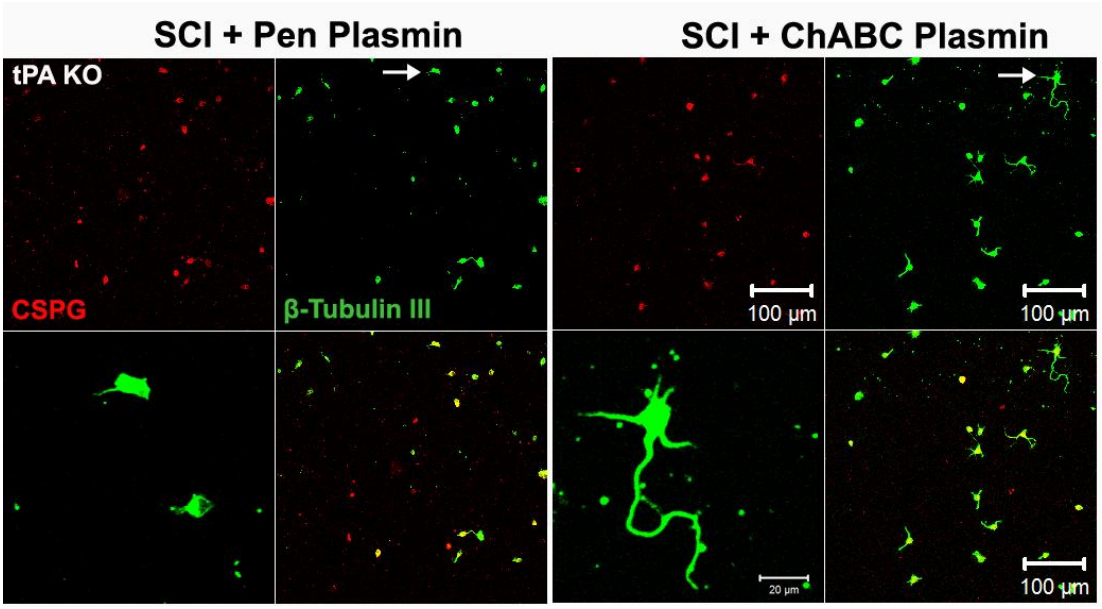

Figure 20: Plasmin can rescue attenuated neurite outgrowth in tPA KO cultures. Embyronic day 15 tPA KO cortical neurons were grown on contusion-injured tPA KO SCI homogenates previously co-treated with Pen and plasmin (0.06U/ml; List Labs) or ChABC and plasmin for 3hrs at 37°C. 2 days later, cultures were fixed with PFA and triple-stained for intact CSPG (red), β-tubulin III (green) and DAPI (blue). Scale bar = 100µm. Higher magnification image of a neuron in each group (indicated by an arrow in β-tubulin III staining) is provided in the lower left box of each image panel. Scale bar= 20µm. Images are representative of 3 biological replicates per group.

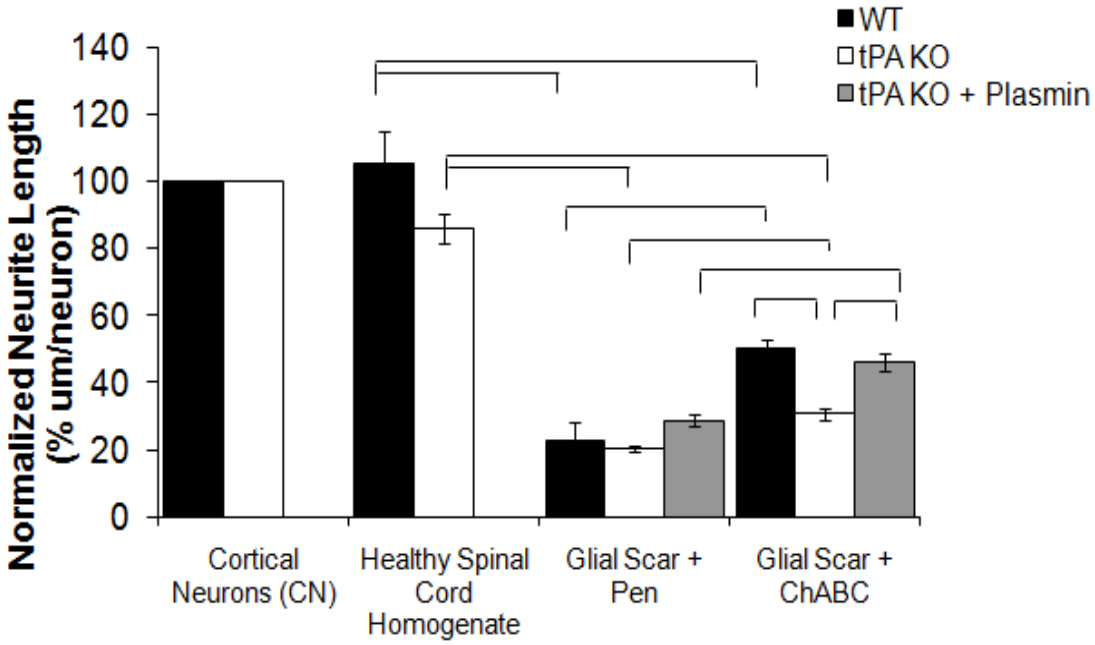

Figure 21: tPA/plasmin system act downstream of ChABC mediated neuronal plasticity. Quantification of WT and tPA KO cortical neurons grown on their genotypic equivalent *ex vivo* glial scar with *in vitro* ChABC or Pen and plasmin treatments. The Neurite Tracer plugin in ImageJ was used to calculate neurite length/neuron, and data normalized and plotted as a percentage of the cortical neuron only group of the same genotype (n=3). One Way ANOVA was used for comparisons. Significant ANOVA was followed by *post hoc* Holm Sidak test. Brackets indicate significant *post hoc* differences at a minimum of $p<0.05$.

tPA/plasmin pathway plays a role in ChABC-mediated sensory repair

To investigate the role of tPA/plasmin pathway after ChABC treatment *in vivo*, I first confirmed the technical feasibility of motor axon tracing. 10% biotinylated dextran amine (BDA) was bilaterally injected into the sensorimotor cortex of WT and tPA KO mice. Two weeks later, spinal cords from BDA-injected and non-injected mice were isolated and labeled with HRP-DAB reaction followed by silver-gold intensification. BDA labeled axons were visible in white matter regions of the spinal cord consistent with the known location of corticospinal tracts that control motor movements in rodents (Figure 22). WT and tPA KO SCI mice were treated with Pen or ChABC on day 14 and injected with BDA on day 16. Two weeks later, spinal cords were isolated and one mouse was randomly selected for a pilot quantification. All sections in the mouse spinal cord were stained with HRP-DAB followed by silver-gold reaction. Images were captured at the injury site, rostral and caudal regions in all the sections. Biological stacks for all the sections in each imaged region of the spinal cord were prepared. ImageJ with the plugin FeatureJ using Hessian filter was employed to quantify all the BDA-labeled axons in these regions as performed by others (Grider et al., 2006). A representative section of the tPA KO SCI and ChABC treated spinal cord indicates that while BDA axons approached the injured region, little to no axons entered and grew through the glial scar (Figure 23). Quantification of the motor axons in the spinal cord confirmed this lack of axonal regrowth (Figure 24). A review of literature revealed that a minimum of one week after treatment is necessary for stable axonal regrowth (Kerschensteiner et al., 2005; Sivasankaran et al., 2004; Zheng et al., 2003). Unfortunately, the contusion injured mice had a very high mortality rate beyond 28 days making this experimental timeline impractical for BDA-labeled axonal tracing.

Sensory anatomical tracing was, therefore, used as an alternate approach to investigate the role of tPA/plasmin pathway after ChABC treatment *in vivo.* As before, I first confirmed the technical feasibility of the sensory axon tracing. WT and tPA KO mice received a unilateral 1.5% CTB injection and spinal cords were isolated 4 days later. 20µm sagittal sections were, next, labeled with HRP-DAB and silver-gold reaction. CTB-labeled axons were visible in white matter region of the spinal cord consistent with the known location of sensory axon fibers in rodents (Figure 25). WT and tPA KO mice, then, underwent contusion injury followed by a single intraspinal injection of ChABC or Pen on day 14. CTB was injected on day 22 of injury and spinal cords isolated 4 days later. To optimize the co-labeling of CTB-labeled axons and spinal cord injury region, two different co-immunostaining reactions were tested. Both, the double immunofluorescent and histological-immunofluorescent co-stainings resulted in low-resolution and sub-optimal CTB labeling but clearly marked GFAP injured region (Figure 26). In contrast, the single CTB-HRP-DAB reaction and silver-gold intensification resolved the CTB-labeled axons well while both the gradation of DAB staining and dysmorphic spinal cord allowed for a demarcation of the injured region (Figure 27). As a result, single HRP-DAB immunostaining reaction was used for sensory axon tracing.

For sensory axon quantification, Neurolucida software was initially used to trace all the CTB-labeled axons in the injured region. However, the labor intensive and time-consuming nature of this quantification software led me to try a sequential random sampling approach for axon density measurements offered by the Stereoinvestigator program. A comparison of the two techniques revealed a similar trend of axon density

measurements, albeit lower error rate with Stereoinvestigator (Figure 28). Consequently, the Stereoinvestigator program was used for axon density quantification in all SCI groups. Since higher axon density was measured in the tPA KO SCI and Pen-treated mice compared to their WT counterparts (2.19e-3 vs 1.23e-3 $\mu m/\mu m^3$, Figure 28), data was normalized to the Pen-treated group of the corresponding genotype. A single high dose of plasmin was also co-administered with Pen or ChABC to WT SCI mice to determine if ChABC-mediated sensory recovery could be augmented, and to evaluate the therapeutic potential of engaging the tPA/plasmin mechanism. WT SCI mice showed a dose response curve with the WT SCI and ChABC treated group showing significantly higher axon recovery than the Pen group ($p<0.001$). In comparison, tPA KO ChABC mice showed much lower axon density ($p=0.029$), although slightly higher than the corresponding vehicle enzyme group ($p=0.024$). Co-treatment with Pen and plasmin resulted in improvement in sensory axon density over the Pen-treated group alone (163.6 vs 100.0 $\%\mu m/\mu m^3$), while co-administration of ChABC and plasmin yielded significantly higher axon density over Pen alone ($p<0.001$) and Pen-plasmin ($p=0.002$) groups, and a trend towards improvement over ChABC group (457.6 vs 392.4 $\%\mu m/\mu m^3$, Figure 29). Collectively, the sensory axon density data suggest that indeed, the tPA/plasmin system plays an important role in ChABC-mediated sensory axonal plasticity.

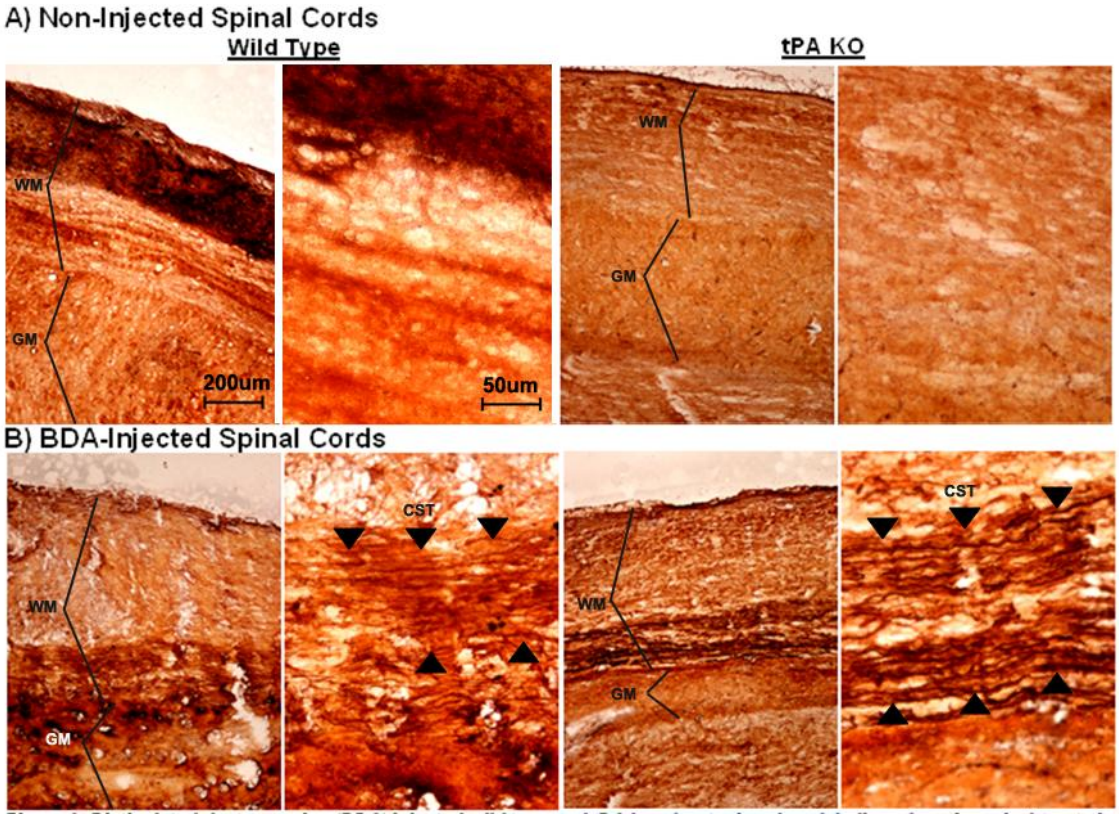

Figure 22: BDA injected WT and tPA KO mice show labeling of corticospinal tracts in white matter of intact spinal cords. A) Adult WT and tPA KO mice were perfused with 4% PFA and thoracic spinal cords isolated. 20µm sagittal sections were prepared and labeled with avidin and biotinylated HRP followed by DAB and enhanced with a silver-gold intensification reaction. B) WT and tPA KO mice received bilateral injections with 10% BDA in the sensorimotor cortex. Mice were perfused 14 days after injection and sections processed as above. WM and GM indicate white matter and gray matter regions in each spinal cord section while arrow heads and CST indicate corticospinal tracts axons in (B).

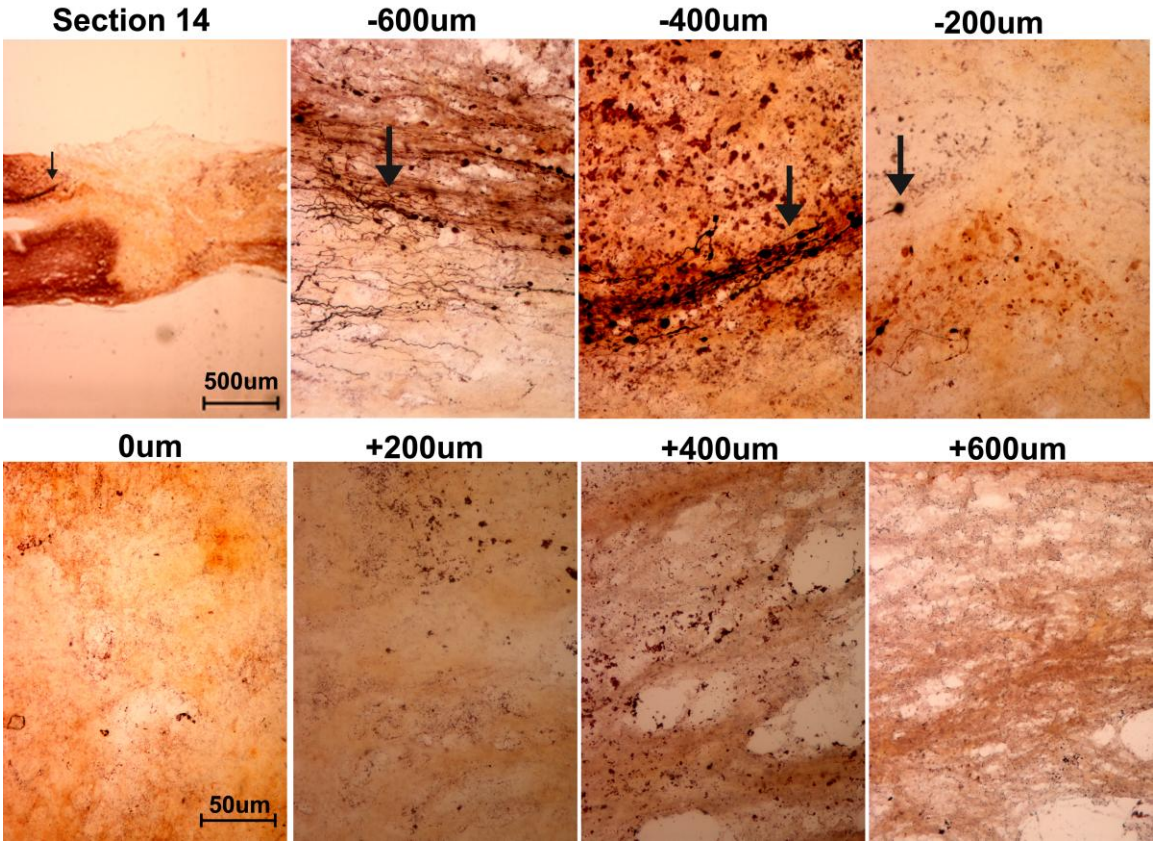

Figure 23: A tPA KO SCI mouse shows minimal motor axon density 2 days after ChABC treatment. A representative section of the tPA KO SCI mouse injected with 10% BDA 2 days after ChABC treatment. 2 weeks later, mouse was perfused with 4% PFA and 20µm sagittal sections were stained with HRP-DAB and silver-gold intensification reaction as previously outlined. Images were captured with Nikon E600 and Nis-Elements software at 200µm intervals with negative and positive signs denoting rostral and caudal to the injury region respectively. A low magnification of the same spinal cord section is shown in top left panel with dorsal side up and rostral side on the left of the image panel. Arrows point to corticospinal tract axons in each image.

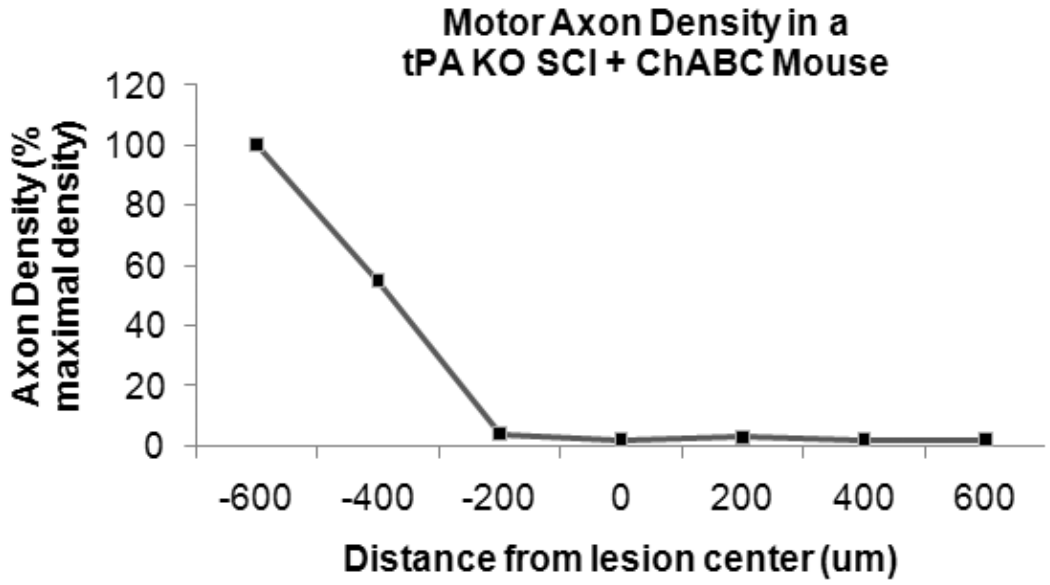

Figure 24: 2 days after ChABC treatment is not a good time point for motor axon density measurement. Quantification of motor axon density in a tPA KO SCI ChABC treated mouse injected 2 days later with BDA and imaged with Nikon E600 and Nis-Elements software at 200µm intervals. Hessian filter in ImageJ plugin FeatureJ was used to create binary traces of all the spinal cord sections. The total pixel intensity/area was then calculated for all the spinal cord sections in each region and data normalized to the region of maximal axon density.

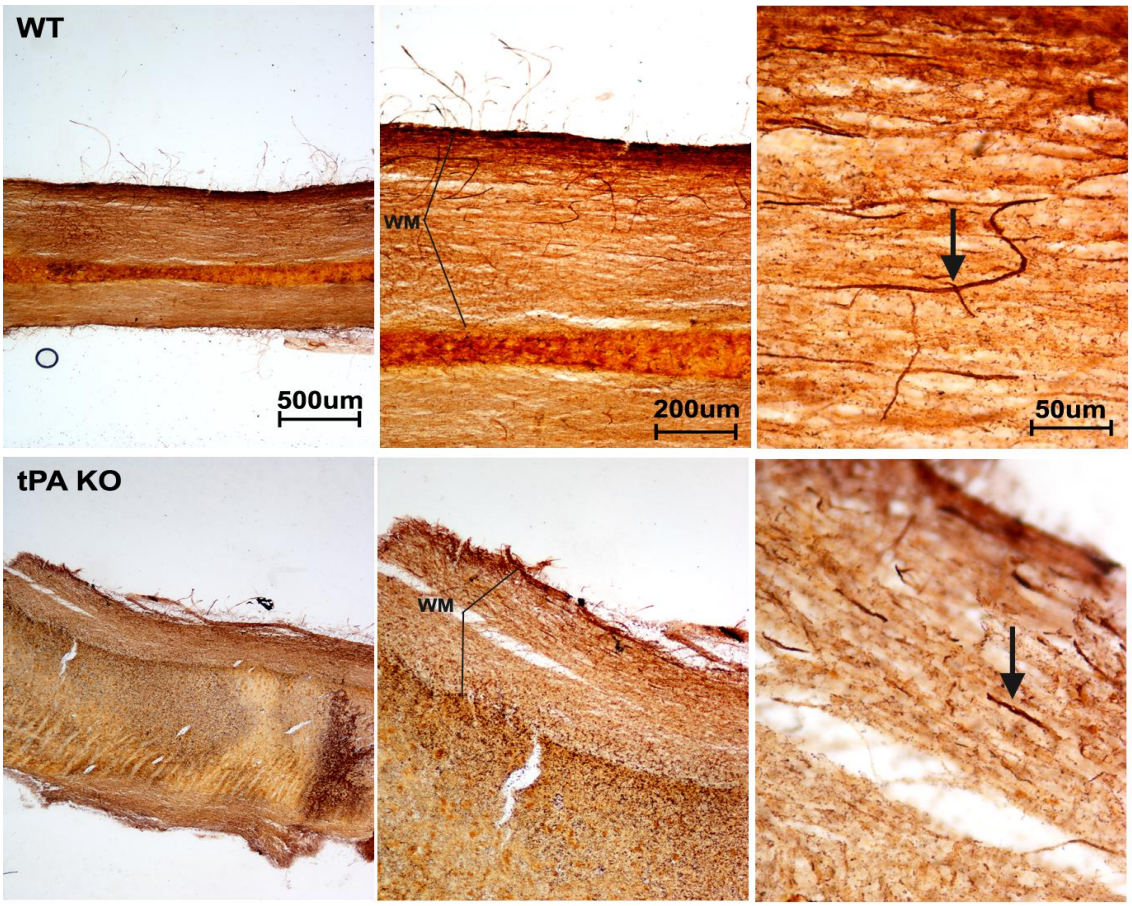

Figure 25: CTB injected WT and tPA KO mice show labeling of sensory axon fibers in white matter of intact spinal cords. Adult WT and tPA KO mice received 1.5% CTB injection into the right sciatic nerve. Spinal cords were isolated 4 days later and 20µm sagittal sections prepared and labeled with CTB-HRP followed by DAB and enhanced with a silver-gold intensification reaction. WM indicates the white matter region in each spinal cord section while arrows point to sensory tract axons in each section.

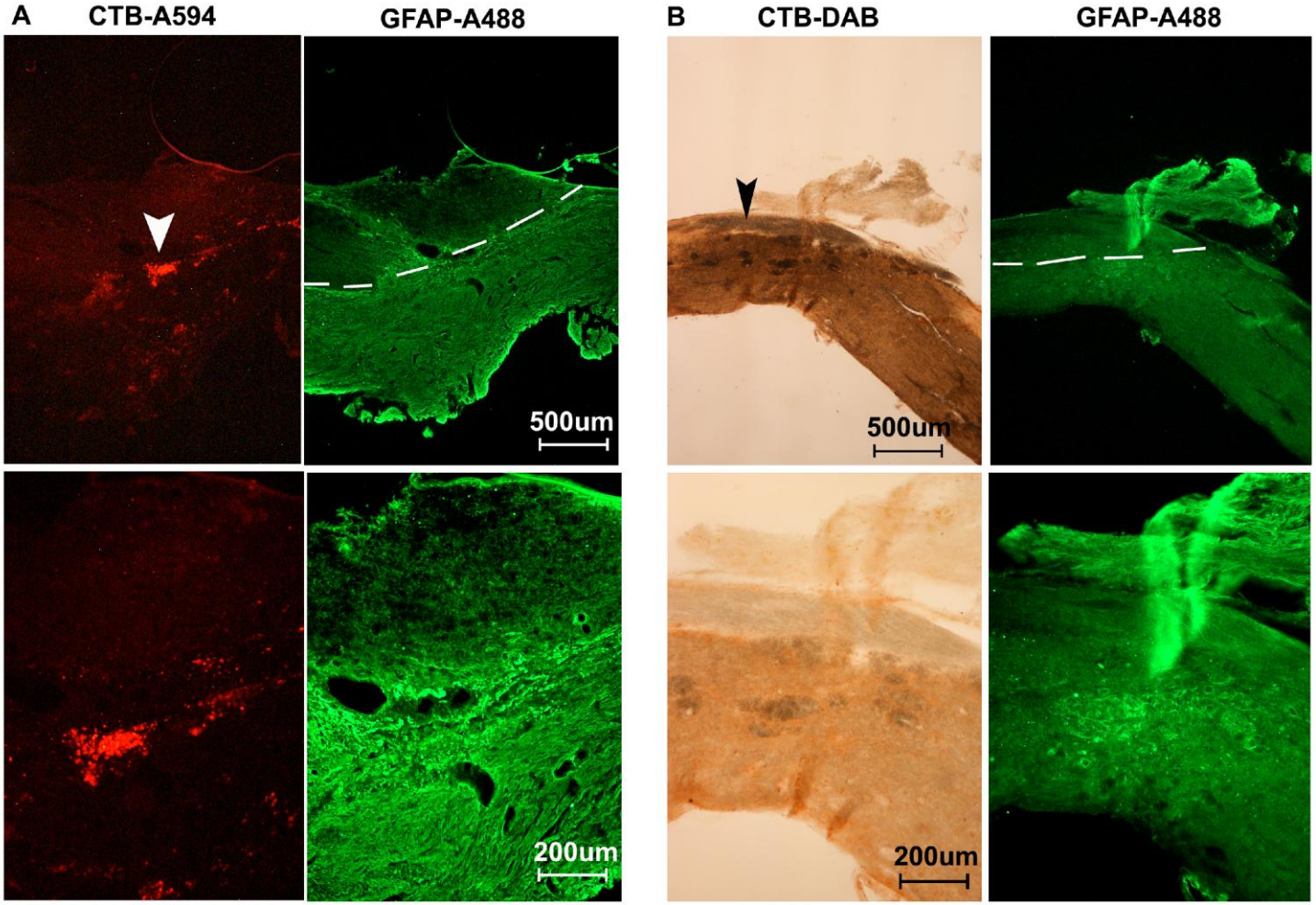
A
CTB-A594
GFAP-A488
500um
200um
B
CTB-DAB
GFAP-A488
500um
200um

Figure 26: SCI and CTB injected mice co-immunostained for sensory axons and glial scar. Two types of co-immunostaining reactions were performed. A) Double immunofluorescent staining of CTB-labeled sensory axons with Alexa-594 (white arrowhead) and GFAP-labeled glial scar with Alexa 488 (dashed line). B) Histological and immunofluorescent co-staining was performed with HRP-DAB staining of CTB-labeled sensory axons (black arrowhead) and Alexa 488 immunofluorescent staining of GFAP-labeled glial scar (dashed line). Images were captured on Nikon E600 microscope with Nis-Elements software. Lower panels show higher magnification images.

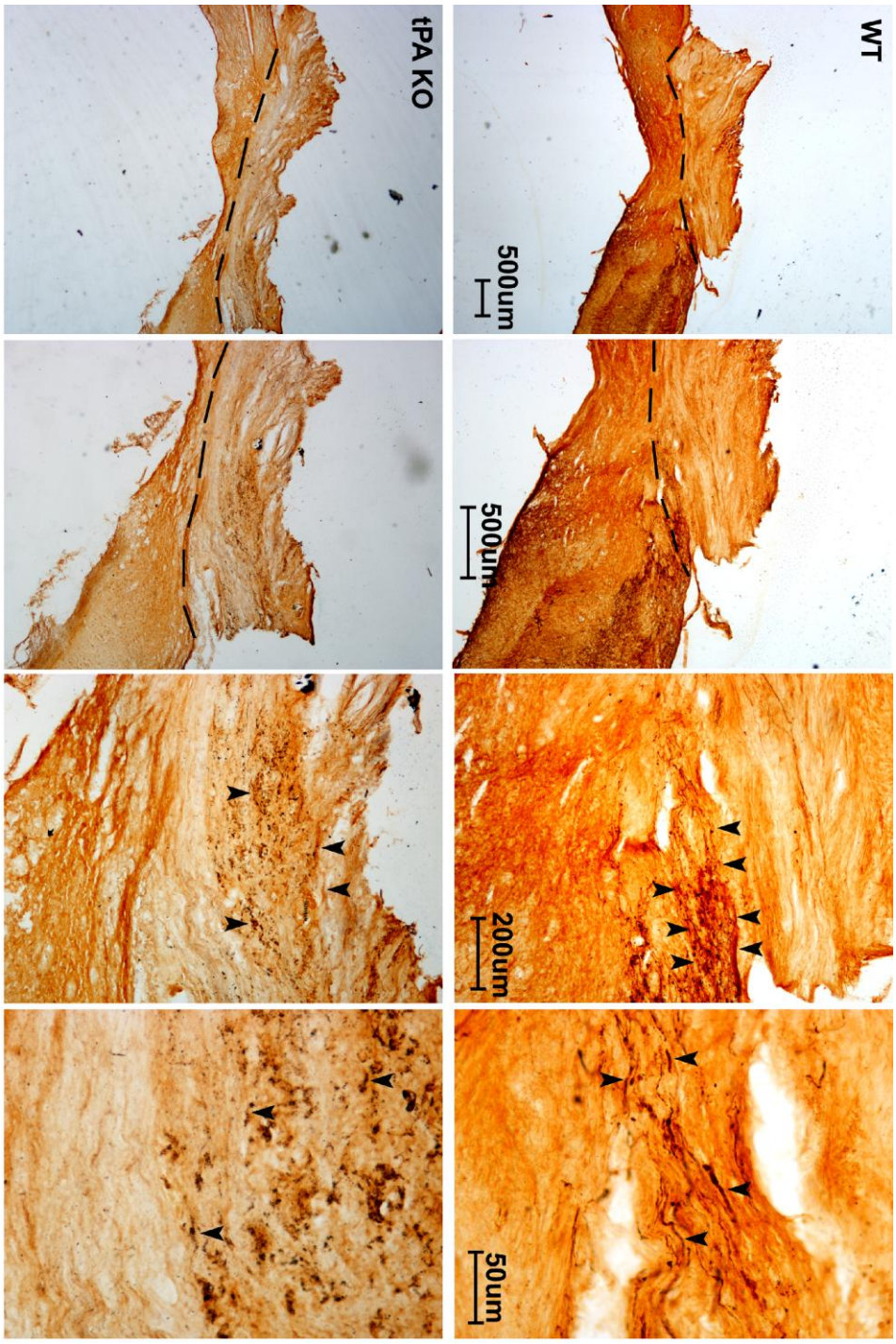
WT
tPA KO
500um
500um
200um
50um

Figure 27: HRP-DAB reaction allows for optimal sensory axon labeling and glial scar identification. WT and tPA KO SCI and ChABC treated mice were injected with 1.5% CTB on day 22 and spinal cord isolated 4 days later. 20µm sagittal spinal cord sections were stained with CTB-HRP followed by DAB and silver-gold intensification reaction. Images were captured on Nikon E600 microscope with Nis-Elements software and oriented with dorsal side up and rostral end on left. Injured region in each spinal cord section is indicated by dashed lines at low magnification images (first two columns) and CTB-labeled axons by arrowheads in the higher magnification images (second two columns).

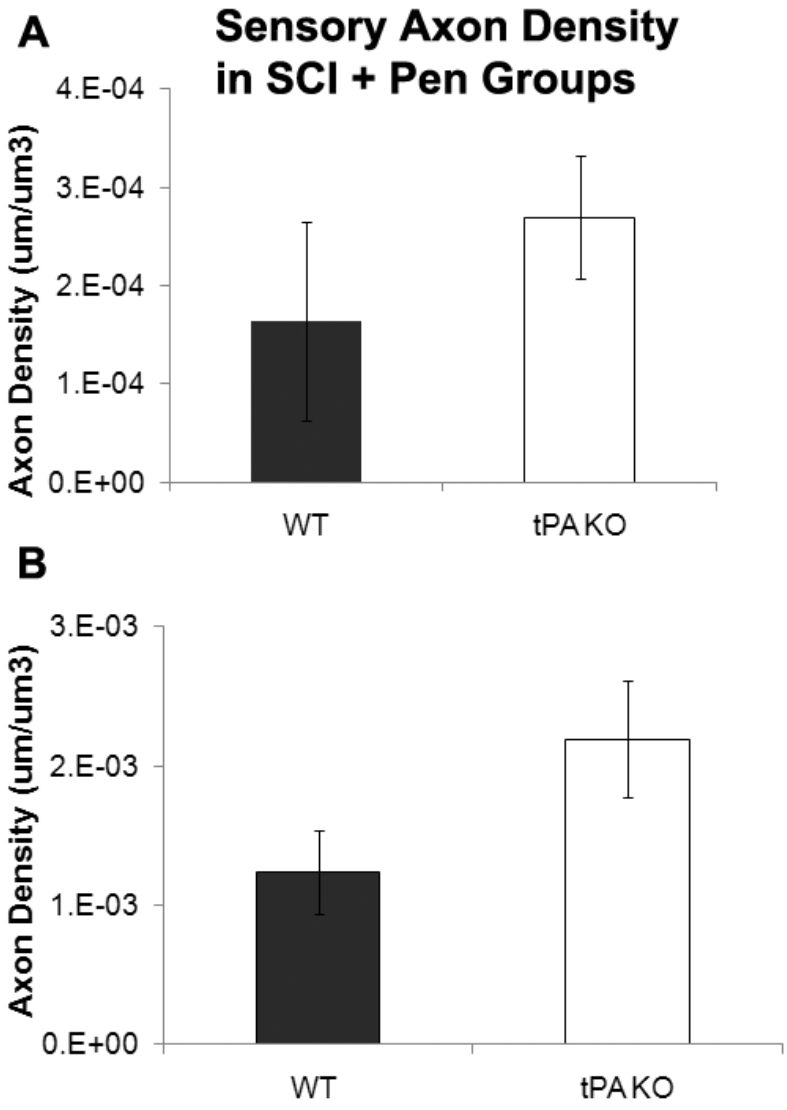
A
Sensory Axon Density in SCI + Pen Groups
Axon Density (um/um3)
4.E-04
3.E-04
2.E-04
1.E-04
0.E+00
WT
tPA KO
B
Axon Density (um/um3)
3.E-03
2.E-03
1.E-03
0.E+00
WT
tPA KO

Figure 28: In the absence of tPA, SCI mice show a trend towards modest sensory axon recovery. WT and tPA KO SCI and Pen treated mice underwent sensory axon tracing and quantification using two different softwares. A) Neurolucida software was used to trace all the CTB-labeled axons in the injured region and Neurolucida explorer used to calculate axon density of the traced axons in the injured region (n=2). B) Space Balls probe in Stereoinvestigator software was used to perform sequential random sampling of the injured region and mark the CTB-labeled axons that intersect the probe to provide a final axon density value per spinal cord (n=3). Both axon quantification approaches measured higher axon density in tPA KO SCI and Pen treated group compared to its respective WT group. Stereoinvestigator software was used to quantify sensory axon density in all other groups.

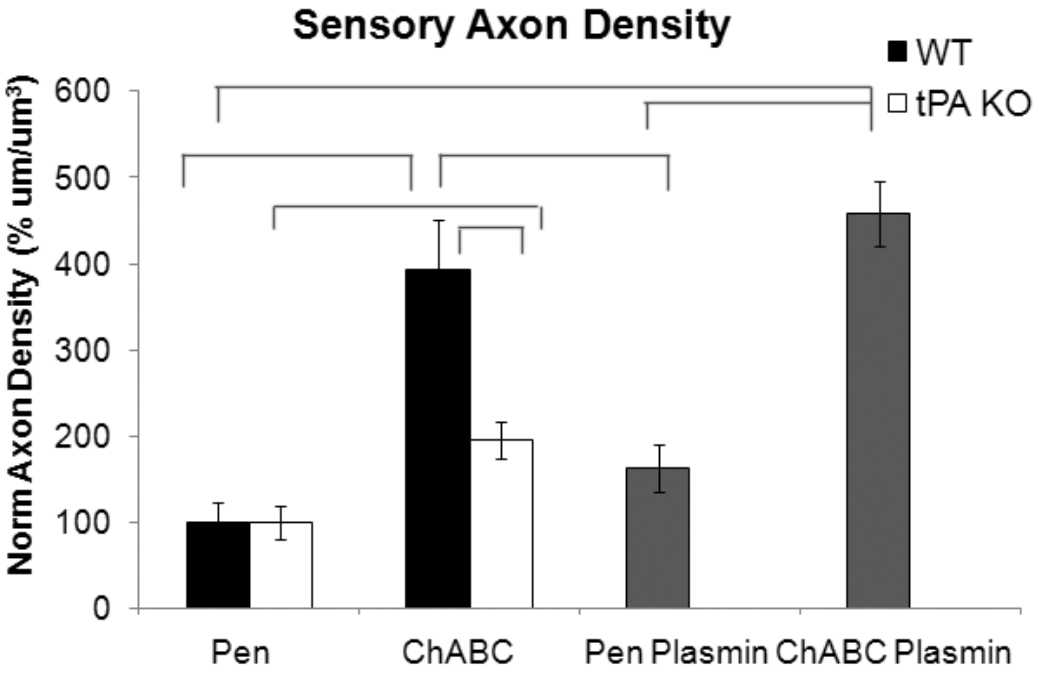

Figure 29: ChABC mediated sensory recovery is attenuated *in vivo* in the absence of tPA/plasmin system. Sensory axon density in all groups on day 21 after SCI showing higher sensory axon recovery in WT SCI ChABC mice and attenuated recovery in tPA KO ChABC treated group (n= 3-4). t-test was used to compare within each treatment and across tPA KO SCI group. One Way ANOVA was used to compare WT SCI mice. Significant ANOVA results were followed by *post hoc* Holm Sidak test. Brackets indicate significance due to t-test or *post hoc* analyses at a minimum of $p<0.05$.

Chapter IV- The tPA/plasmin system contributes to ChABC mediated motor recovery after SCI

Materials & Methods

Health measurements: Intact and injured mice's weight was routinely measured prior to every behavior experiment. Mice who lost more than 20% of their initial weight were eliminated from the experiment.

Motor Behavior:

Rotor Rod: Intact and injured WT and tPA KO mice were placed on a standard Rotarod (Med Associates, Inc., VT, USA) to assess motor performance at 7, 10, 16, 18, 21 and 28 days after SCI. The rod rotation accelerated over the course of the 5 min from 4 to 40 rotations per minutes (r.p.m.). Each mouse was given three trials to remain on the accelerating rod per day. Each trial was 5 min long or until the mouse fell off. The maximum speed and latency to fall was recorded automatically by the apparatus. The maximum speed each mouse remained on the rotor rod in the three trials per day was used for comparisons.

Open Field Activity: Intact and injured WT and tPA KO mice were placed in an empty rat cage (44cm x 21cm) situated inside an Opto-Varimex-Minor animal activity meter (Columbus Instruments). 15 x15 infrared beams running in the x-y coordinates and 2cm above the base of the machine recorded beam breaks associated with ambulatory activity (consecutive beam breaks) and total activity (all beam interruptions) during the 20 minute observation period. An observer manually recorded the animal's supported motor activity. Motor movements were defined as an animal using its upper and lower limbs to reach up the side of a cage and hold its body up (supported) or stand up on its lower

limbs without using any cage support (unsupported). Activity measurements were recorded on 7, 10, 18 and 21 days after contusion injury.

Statistics: All surgeries and measurements were performed with an observer blinded to the genotype of the mice. Two-Way Repeated Measures ANOVA was employed to analyze differences due to time and a second variable (genotype or treatment). In all other data sets, multiple group comparisons were made with One-Way ANOVA. Significant ANOVA was followed by *post hoc* Holm Sidak test in all cases. To compare the two genotypes within each treatment or time point, t-test was used. A minimum alpha value of 0.05 was accepted as statistically significant. Data are presented as mean $\pm$ SEM.

Results

tPA/plasmin pathway plays a role in ChABC-mediated motor repair

I used motor behavior to investigate the role of tPA/plasmin pathway after ChABC treatment *in vivo*. WT and tPA KO mice underwent contusion injury followed by a single intraspinal injection of ChABC or Pen on day 14. Pre-injection motor behaviors were determined on days 7 and 10, while post-injection behaviors were measured on days 16, 18, 21 and 28 for the pilot experiment and then only on days 18 and 21 for the remaining experiment. Since there were 6-8 groups in the behavior experiment with 3 different variables (genotype, treatment and time), 2-4 way group comparisons analyzing the effect of two variables while holding the third variable constant were performed.

To ensure that differences between groups were not due to changes in the animals' overall health, their weight was routinely measured prior to every behavior experiment. After normalizing to mean weight of intact mice of the respective genotype, no differences due to time or treatment were found across any of the 2-4 way group comparisons (Figure 30A, C & D). Significant difference, however, was measured between WT and tPA KO genotypes in the ChABC treated groups at all time points (Figure 30B & E) suggesting that tPA KO mice weigh slightly more than their respective WT group. At day 21, mice from both strains also retained 90-95% of their initial weight (Figure 30E) demonstrating that all the SCI mice in these behavior experiments remained healthy.

In the pilot behavior experiments, the motor coordination of intact and SCI mice was measured. WT and tPA KO intact mice showed no differences at all time points (Figure 31A). In contrast, tPA KO SCI and Pen-treated mice showed higher motor

balance than their genotypic WT group at all time points (Figure 31B). In the ChABC treated groups, no differences were measured due to genotype but significant differences due to time were found. ChABC treated SCI mice showed greater motor balance on days 18 compared to 7 and 10 days ($p=0.003$ and $p=0.004$ respectively) and on day 21 compared to day 7 ($p=0.004$) (Figure 30C). Differences due to treatment and time were then analyzed in two-way group comparisons holding genotype constant. WT SCI and ChABC treated mice showed significantly higher motor recovery at all post-injection timepoints compared to the same mice at pre-injection time points and WT SCI and Pen treated group at post-injection time points ($p<0.05$) (Figure 31D). tPA KO SCI mice, however, did not show any differences due to treatment or time (Figure 31E). Holding time constant, differences due to genotype and treatment were then compared on day 21 after injury. Since higher recovery was found in the tPA KO SCI and Pen- treated group compared to their genotypic equivalent WT controls, data were normalized to the Pen-treated groups. WT SCI and ChABC-treated mice showed higher motor balance compared to their genotypic equivalent Pen-treated group while tPA KO SCI and ChABC-treated mice showed attenuated activity compared to their genotypic equivalent tPA KO vehicle enzyme-treated group (Figure 31F). These data suggest that ChABC treatment can enhance the motor balance after SCI. Furthermore, these data propose that tPA play a dual role in motor recovery after SCI, one that is dependent on its interaction with CSPGs downstream of ChABC activity and the other is independent.

Total open field activity and ambulatory activity were automatically measured by the machine in all groups. Since the two behavior parameters showed the same pattern in all group comparisons, the analyses will be presented together. WT and tPA KO intact

mice exhibited the largest differences in open field and ambulatory activity across all time points with tPA KO mice showing significantly lower activity compared to the WT group ($p<0.05$) (Figures 32A & 33A). SCI and Pen treated mice showed a similar pattern of genotypic differences across all time points although with slightly greater variability ($p<0.05$) (Figures 32B & 33B). All other 2 or 4-way comparisons for genotype and time (Figures 32C & 33C) or treatment and time (Figures 32D, E & 33D, E) did not demonstrate any differences between the groups. Holding time constant, differences due to genotype and treatment were then compared on day 21 after injury. tPA KO intact and SCI+Pen treated groups showed significantly lower total activity compared to their respective WT groups ($p=0.003$ & $p=0.013$) (Figure 32F) while only tPA KO intact group showed significant difference compared to its respective control in ambulatory activity ($p<0.05$) (Figure 33F). Collectively, these data demonstrate that healthy and intact tPA KO mice show lower behavior activity in an open field cage system.

Supported motor activity was manually measured in all groups. WT and tPA KO intact mice exhibited similar levels of high motor activity at all time points (Figure 34A). Lower supported motor activity was seen on days 18 and 21 compared to day 7 due to habituation ($p<0.05$). All of the SCI groups demonstrated considerably lower levels of motor activity, confirming the effectiveness of the experimental SCI model (see y-axis Figures 34B-E). 2-way group comparisons between genotype and time were first analyzed. SCI and Pen-treated mice showed minimal motor recovery at pre-injection time points and some spontaneous improvement on day 21 compared to days 7 and 10 ($p=0.009$ & $p=0.010$ respectively) with tPA KO SCI group showing slightly better recovery compared to its equivalent WT SCI group (Figure 34B). SCI and ChABC

treated group also showed improvement over time with day 21 exhibiting the highest recovery compared to days 7 and 10 ($p=0.009$ & $p=0.010$ respectively). tPA KO SCI and ChABC treated mice showed slightly lower supported motor recovery when compared with its equivalent WT mice (Figure 34C). Although significant differences due to treatment were not seen, consistent trends were seen in group comparisons for treatment and time (Figure 34D). ChABC treated injured mice showed similar levels of motor activity to the Pen-treated group at pre-injection time points (D10: 1.5 ± 0.42 vs 1.75 ± 0.68 counts), but much higher levels of motor activity at post-injection time points. On day 21 they showed much better improvement than the Pen-treated group (10.0 ± 3.65 vs 2.25 ± 0.41 counts). A single high dose of plasmin was also co-administered with Pen or ChABC to WT SCI mice only to determine if ChABC-mediated motor recovery could be augmented and to evaluate the therapeutic potential of the tPA/plasmin mechanism. My data indicate that, compared to the same animals at earlier time points and to the ChABC-treated group at the same time point, the ChABC-plasmin co-treated mice show a trend towards significant motor recovery on day 21 suggesting that tPA/plasmin pathway could potentially enhance ChABC-mediated motor recovery. Since day 21 appears to be the critical time point when all groups showed some level of motor recovery, I also analyzed their behavior across all genotypes and treatments on day 21. Since the SCI and Pen treated mice showed some spontaneous recovery on day 21 with tPA KO group exhibiting slightly better recovery, the data were normalized to the Pen-treated group of the corresponding genotype. When compared across treatments, WT SCI mice showed a characteristic 'dose response' of motor recovery with the ChABC group displaying higher levels of motor recovery compared to Pen- and Pen-plasmin co-treated groups

(444.4 vs 100.0 vs 222.2), but lower than ChABC-plasmin co-treated groups (551.1 counts, Figure 34F). In contrast, the tPA KO ChABC mice displayed lower motor recovery response (255.0). Overall, the supported motor activity data suggest that the tPA/plasmin pathway plays an important role in ChABC-mediated motor recovery after SCI.

Unsupported motor activity was also manually measured in all groups. Since unsupported activity was only seen in the intact mice group and one WT SCI and ChABC treated mouse, data from all groups are presented together. tPA KO intact mice showed significantly lower unsupported activity at all time points compared to the equivalent WT group ($p<0.05$) (Figure 35A). Similarly, when compared across genotype and treatment on day 21, tPA KO intact mice also showed reduced unsupported activity compared to WT intact mice ($p=0.002$) (Figure 35B). These data consistently demonstrate that in the absence of tPA, mice exhibit lower unsupported motor activity in an open field cage system.

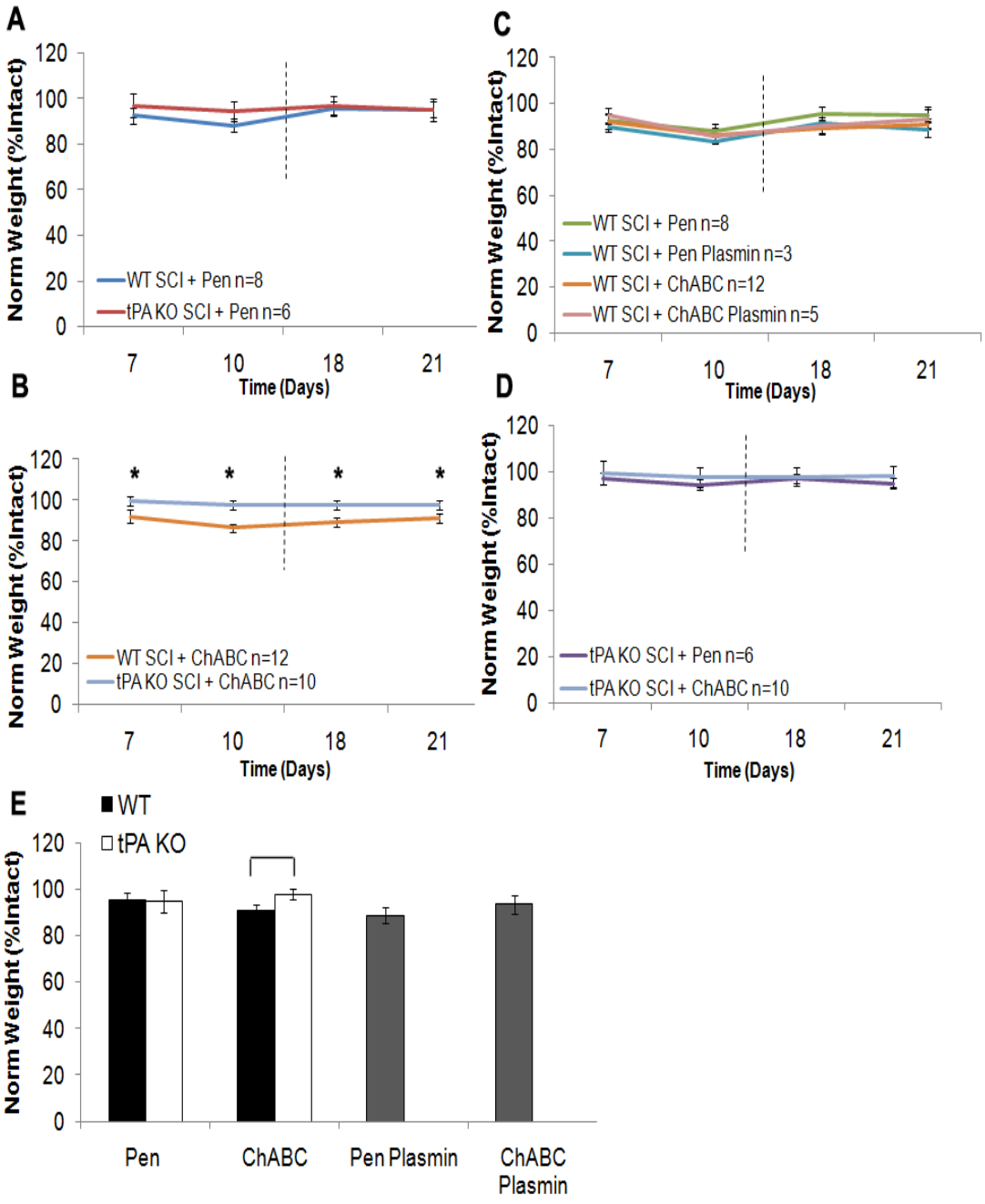
A
Norm Weight (%Intact)
120
100
80
60
40
20
0
WT SCI + Pen n=8
tPA KO SCI + Pen n=6
7
10
18
21
Time (Days)
C
Norm Weight (%Intact)
WT SCI + Pen n=8
WT SCI + Pen Plasmin n=3
WT SCI + ChABC n=12
WT SCI + ChABC Plasmin n=5
Time (Days)
B
Norm Weight (%Intact)
*
WT SCI + ChABC n=12
tPA KO SCI + ChABC n=10
Time (Days)
D
Norm Weight (%Intact)
tPA KO SCI + Pen n=6
tPA KO SCI + ChABC n=10
Time (Days)
E
WT
tPA KO
Norm Weight (%Intact)
Pen
ChABC
Pen Plasmin
ChABC Plasmin

Figure 30: Spinal cord injured mouse retained their weight throughout the experiment. WT and tPA KO mice underwent SCI and a single Pen or ChABC and plasmin injection on day 14. Mouse's weight was measured on designated days and data normalized to intact mouse's weight of the respective genotype. 2-way group comparisons are presented in graphs A-D with graphs A & B comparing differences due to genotype and time while graphs C-D illustrate differences due to treatment and time. 2-Way Repeated Measures ANOVA was used for multiple group comparisons. Significant ANOVA was followed by *post hoc* Holm Sidak test. Asterisks indicate significant differences at $p<0.001$. E) Weight differences due to genotype and treatment were compared on day 21. t-test was used to compare the two genotypes within each treatment. Brackets indicate significance at $p<0.05$.

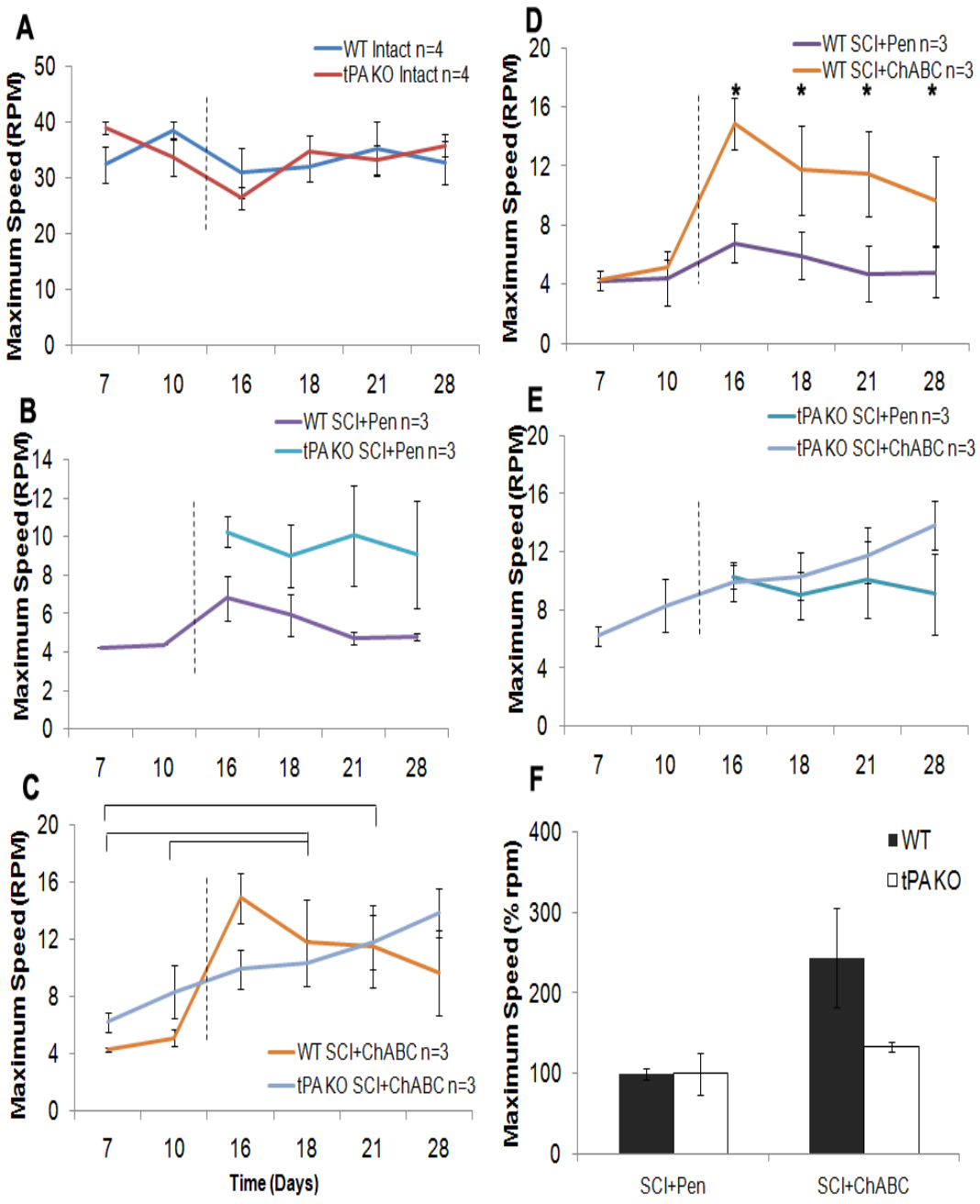
A
WT Intact n=4
tPA KO Intact n=4
Maximum Speed (RPM)
B
WT SCI+Pen n=3
tPA KO SCI+Pen n=3
Maximum Speed (RPM)
C
WT SCI+ChABC n=3
tPA KO SCI+ChABC n=3
Maximum Speed (RPM)
Time (Days)
D
WT SCI+Pen n=3
WT SCI+ChABC n=3
Maximum Speed (RPM)
E
tPA KO SCI+Pen n=3
tPA KO SCI+ChABC n=3
Maximum Speed (RPM)
F
WT
tPA KO
Maximum Speed (% rpm)
SCI+Pen
SCI+ChABC

Figure 31: ChABC enhances motor coordination in SCI mice.
WT and tPA KO mice underwent SCI and a single Pen or ChABC injection on day 14. An accelerating rotor rod was used to measure mice's motor coordination on designated days and the maximum speed the mice remained on the machine was recorded. 2-way group comparisons are presented in graphs A-E with graphs A-C comparing differences due to genotype and time while graphs D-E illustrate differences due to treatment and time. 2-Way Repeated Measures ANOVA was used for multiple group comparisons. Significant ANOVA was followed by *post hoc* Holm Sidak test. Brackets indicated significant difference between the specific time points at $p<0.01$ and asterisks indicate significant differences between the two groups at each time points at $p<0.001$. E) Motor coordination differences due to genotype and treatment were compared on day 21 (n=3).

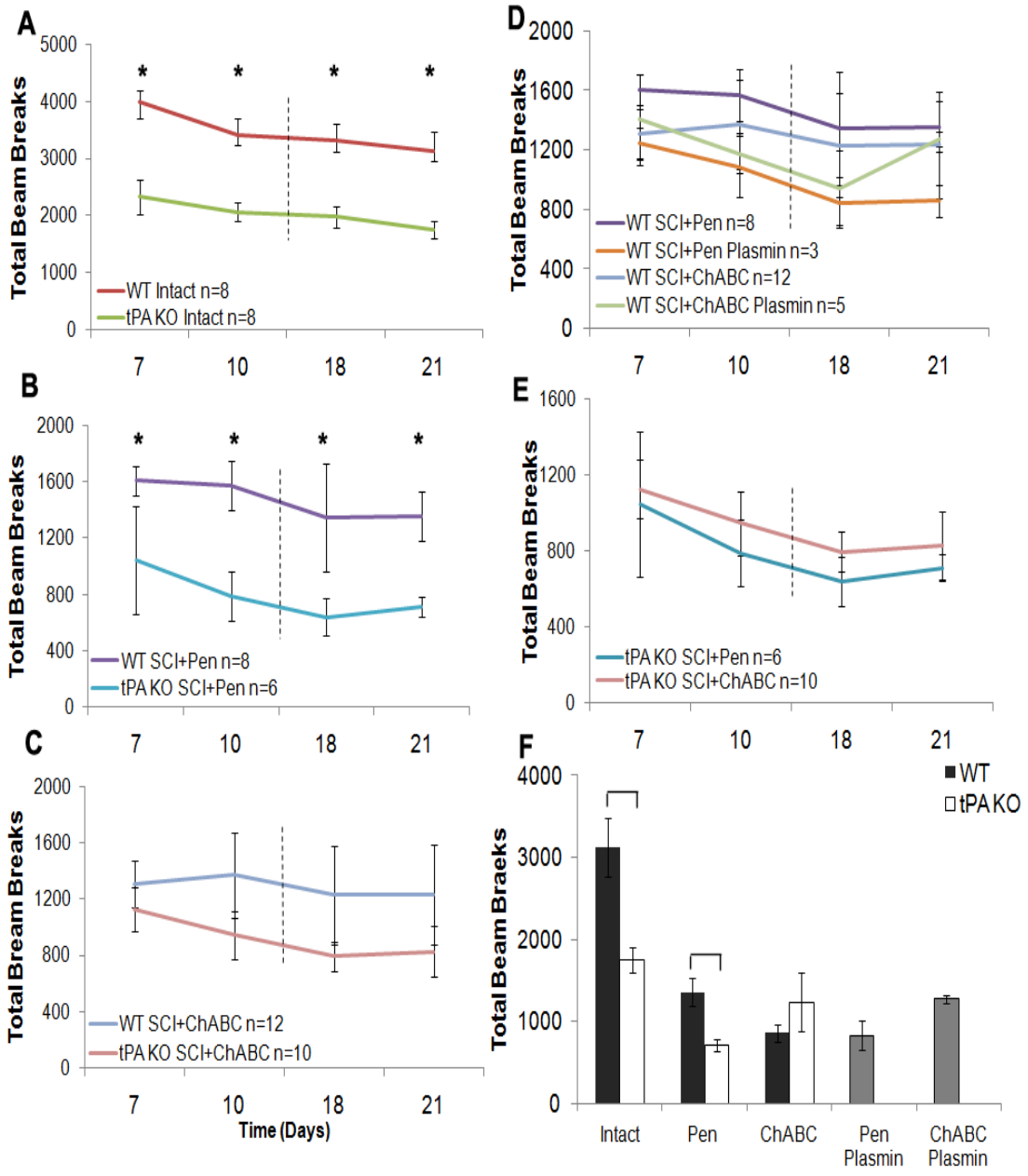
A
Total Beam Breaks
5000
4000
3000
2000
1000
0
*
*
*
*
WT Intact n=8
tPA KO Intact n=8
7
10
18
21
B
Total Beam Breaks
2000
1600
1200
800
400
0
*
*
*
*
WT SCI+Pen n=8
tPA KO SCI+Pen n=6
7
10
18
21
C
Total Beam Breaks
2000
1600
1200
800
400
0
WT SCI+ChABC n=12
tPA KO SCI+ChABC n=10
7
10
18
21
Time (Days)
D
Total Beam Breaks
2000
1600
1200
800
400
0
WT SCI+Pen n=8
WT SCI+Pen Plasmin n=3
WT SCI+ChABC n=12
WT SCI+ChABC Plasmin n=5
7
10
18
21
E
Total Beam Breaks
1600
1200
800
400
0
tPA KO SCI+Pen n=6
tPA KO SCI+ChABC n=10
7
10
18
21
F
Total Beam Braeks
4000
3000
2000
1000
0
WT
tPA KO
Intact
Pen
ChABC
Pen Plasmin
ChABC Plasmin

Figure 32: In the absence of tPA, mice show reduced total activity.
WT and tPA KO mice underwent SCI and a single Pen or ChABC injection on day 14. Mice were placed in an open field cage and total beam breaks in a 20 minute observation period was recorded by the machine on designated days. 2-way group comparisons are presented in graphs A-E with graphs A-C comparing differences due to genotype and time while graphs D-E illustrate differences due to treatment and time. 2-Way Repeated Measures ANOVA was used for multiple group comparisons. Significant ANOVA was followed by *post hoc* Holm Sidak test. Asterisks indicate significant differences between the two groups at each time points at $p<0.05$. E) Total activity differences due to genotype and treatment were compared on day 21. t-test was used to compare the two genotypes within each treatment. Brackets indicate significance at $p<0.001$.

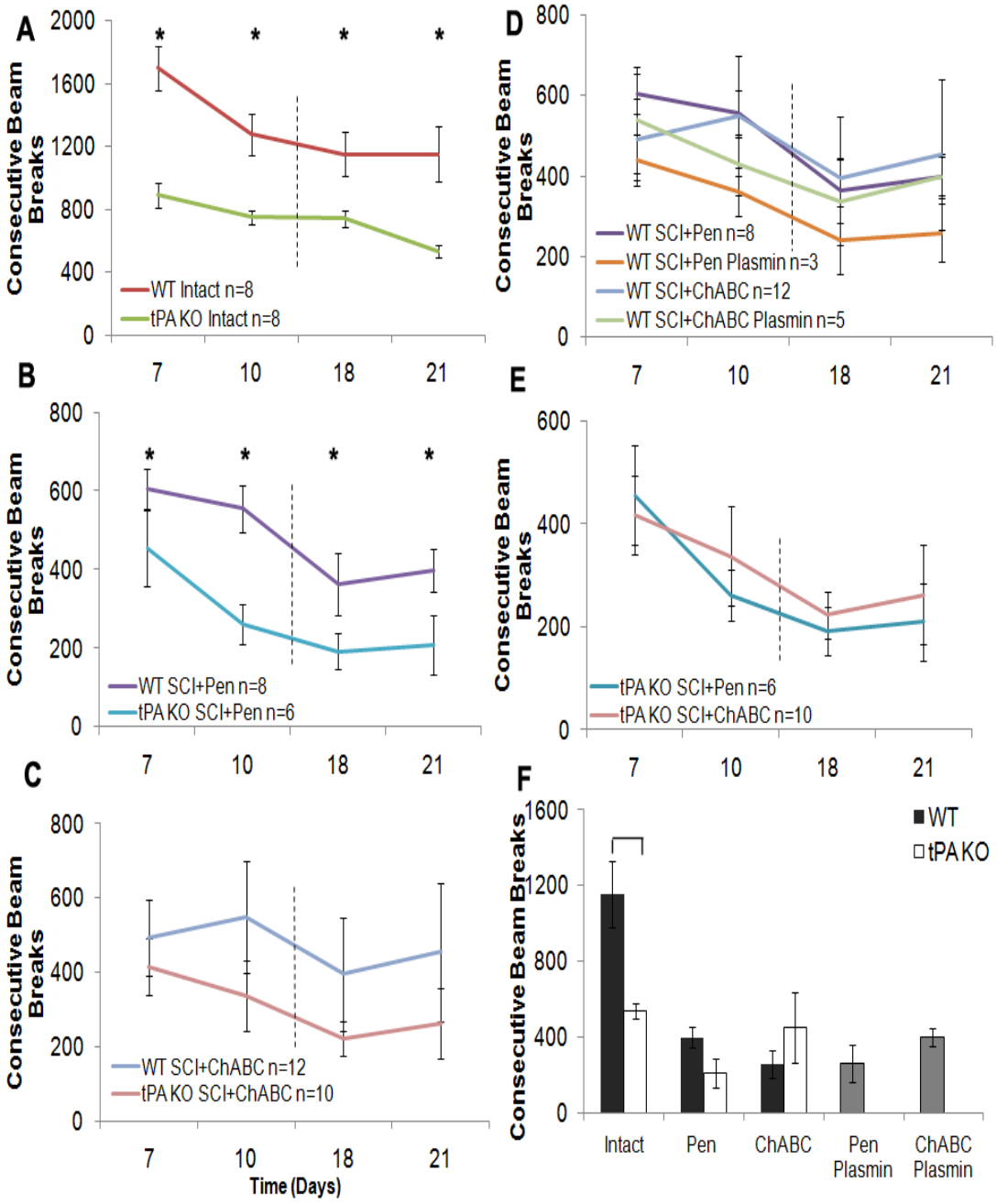
A
Consecutive Beam Breaks
2000
1600
1200
800
400
0
*
*
*
*
WT Intact n=8
tPA KO Intact n=8
7
10
18
21
B
Consecutive Beam Breaks
800
600
400
200
0
*
*
*
*
WT SCI+Pen n=8
tPA KO SCI+Pen n=6
7
10
18
21
C
Consecutive Beam Breaks
800
600
400
200
0
WT SCI+ChABC n=12
tPA KO SCI+ChABC n=10
7
10
18
21
Time (Days)
D
Consecutive Beam Breaks
800
600
400
200
0
WT SCI+Pen n=8
WT SCI+Pen Plasmin n=3
WT SCI+ChABC n=12
WT SCI+ChABC Plasmin n=5
7
10
18
21
E
Consecutive Beam Breaks
600
400
200
0
tPA KO SCI+Pen n=6
tPA KO SCI+ChABC n=10
7
10
18
21
F
Consecutive Beam Breaks
1600
1200
800
400
0
WT
tPA KO
Intact
Pen
ChABC
Pen Plasmin
ChABC Plasmin

Figure 33: In the absence of tPA, mice show reduced ambulatory activity.
WT and tPA KO mice underwent SCI and a single Pen or ChABC injection on day 14. Mice were placed in an open field cage and consecutive beam breaks in a 20 minute observation period was recorded by the machine on designated days. 2-way group comparisons are presented in graphs A-E with graphs A-C comparing differences due to genotype and time while graphs D-E illustrate differences due to treatment and time. 2-Way Repeated Measures ANOVA was used for multiple group comparisons. Significant ANOVA was followed by *post hoc* Holm Sidak test. Asterisks indicate significant differences between the two groups at each time points at $p<0.05$. E) Total activity differences due to genotype and treatment were compared on day 21. t-test was used to compare the two genotypes within each treatment. Brackets indicate significance at $p<0.01$.

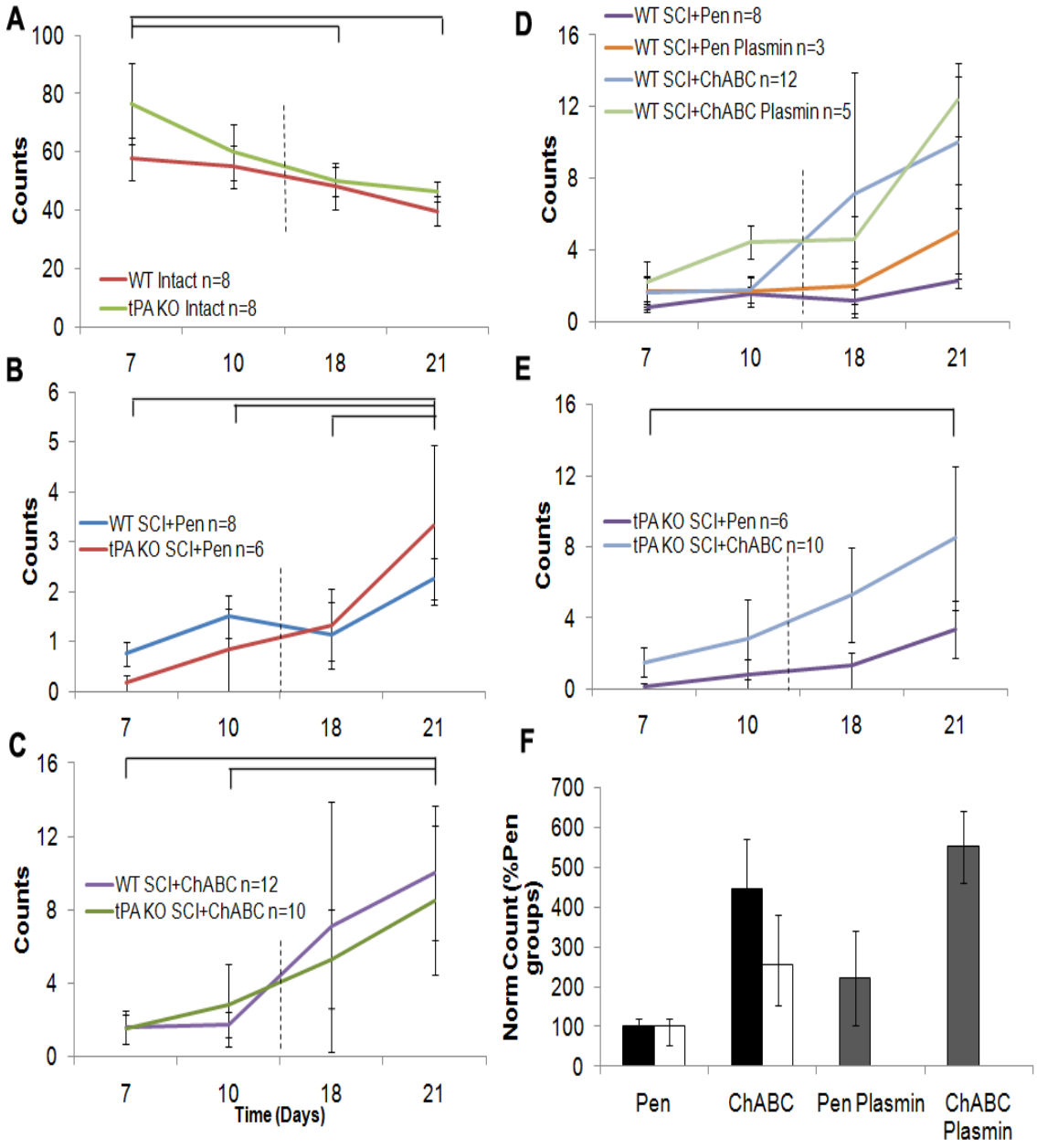
A
Counts
WT Intact n=8
tPA KO Intact n=8
B
Counts
WT SCI+Pen n=8
tPA KO SCI+Pen n=6
C
Counts
WT SCI+ChABC n=12
tPA KO SCI+ChABC n=10
Time (Days)
D
WT SCI+Pen n=8
WT SCI+Pen Plasmin n=3
WT SCI+ChABC n=12
WT SCI+ChABC Plasmin n=5
Counts
E
tPA KO SCI+Pen n=6
tPA KO SCI+ChABC n=10
Counts
F
Norm Count (%Pen groups)
Pen
ChABC
Pen Plasmin
ChABC Plasmin

Figure 34: In the absence of tPA/plasmin system, ChABC mediated motor recovery is attenuated. WT and tPA KO mice underwent SCI and a single Pen or ChABC and plasmin injection on day 14. Mice were placed in an open field cage and supported motor activity in a 20 minute observation period was manually recorded on designated days. 2-way group comparisons are presented in graphs A-E with graphs A-C comparing differences due to genotype and time while graphs D-E illustrate differences due to treatment and time. 2-Way Repeated Measures ANOVA was used for multiple group comparisons. Significant ANOVA was followed by *post hoc* Holm Sidak test. Brackets indicated significant difference between the specific time points at $p<0.05$. E) Supported motor activity differences due to genotype and treatment were compared on day 21.

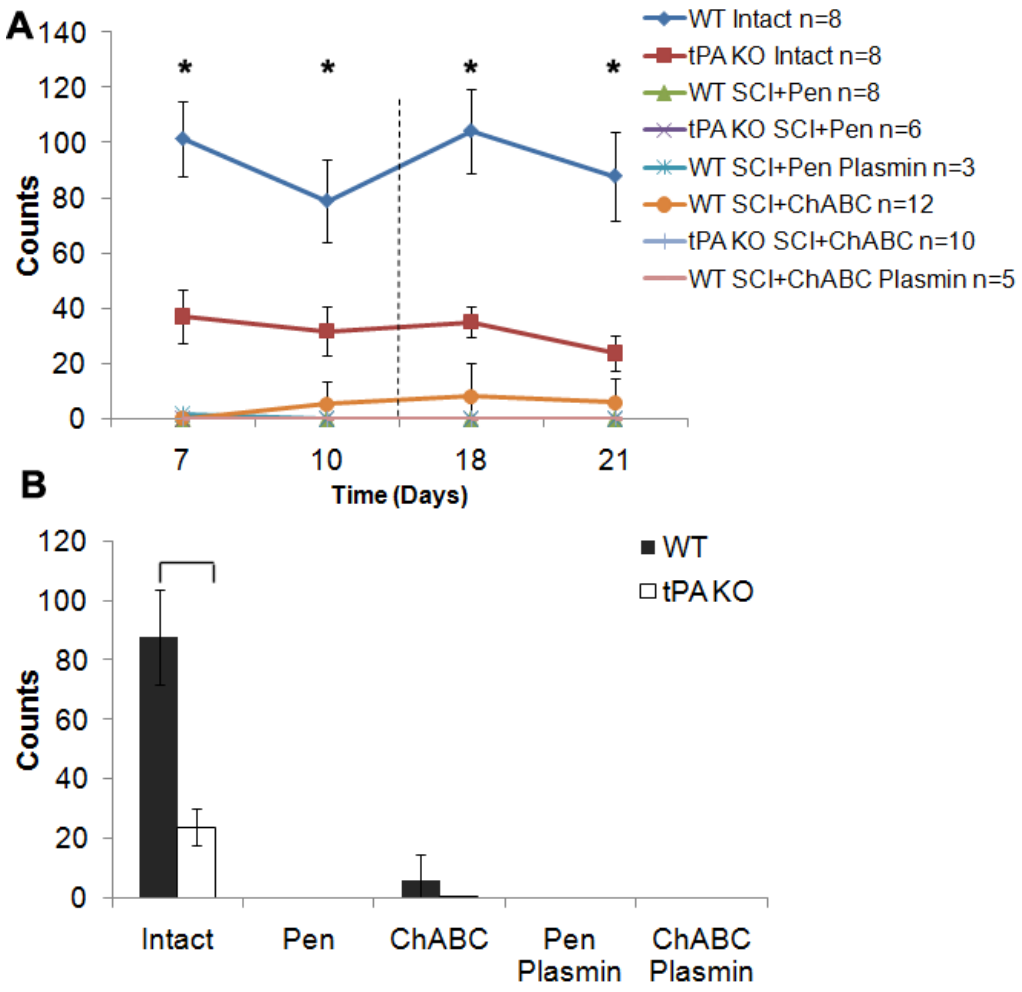
A
Counts
Time (Days)
WT Intact n=8
tPA KO Intact n=8
WT SCI+Pen n=8
tPA KO SCI+Pen n=6
WT SCI+Pen Plasmin n=3
WT SCI+ChABC n=12
tPA KO SCI+ChABC n=10
WT SCI+ChABC Plasmin n=5
B
Counts
WT
tPA KO
Intact
Pen
ChABC
Pen Plasmin
ChABC Plasmin

Figure 35: In the absence of tPA, mice demonstrate significantly lower unsupported motor activity. WT and tPA KO mice underwent SCI and a single Pen or ChABC injection on day 14. Mice were placed in an open field cage and unsupported motor activity in a 20 minute observation period was recorded by the machine on designated days. A) 2-way group comparisons are presented for all groups tested. 2-Way Repeated Measures ANOVA was used for multiple group comparisons. Significant ANOVA was followed by *post hoc* Holm Sidak test. Asterisks indicate significant differences between WT and tPA KO intact groups at each time points at $p<0.05$. B) Unsupported motor activity differences due to genotype and treatment were compared on day 21. t-test was used to compare the two genotypes within each treatment. Brackets indicate significance at $p<0.01$.

Chapter V- Discussion

After SCI occurs, CSPG molecules are upregulated in the glial scar region and inhibit axonal outgrowth. *In vitro* studies have demonstrated that both the GAG chains and core protein of CSPGs are inhibitory to neurite outgrowth (Dou and Levine, 1994; Laabs et al., 2007; Oohira et al., 1991; Wang et al., 2008). Due to limited molecular approaches, *in vivo* studies have primarily focused on the removal of GAG chains by ChABC (Bradbury et al., 2002; Moon et al., 2001). The role of the core CSPG protein in ChABC mediated axonal plasticity, however, has remained unclear.

Three CSPG molecules (NG2, phosphacan, and neurocan) were previously demonstrated by our lab to interact with the tPA/plasmin system and degrade CSPG proteins independent of ChABC function (Nolin et al., 2008; Wu et al., 2000). Tests on the NG2 protein *in vitro,* however, revealed that ChABC-mediated removal of GAG chains could enhance the interaction of tPA/plasminogen system and the local formation of more plasmin. This last finding led to the hypothesis that GAG chain elimination by ChABC may facilitate tPA/plasminogen binding to the core of CSPG molecules which then acts as a scaffold for the localized formation of more plasmin; plasmin, in turn, can target and degrade the core protein resulting in the clearance of CSPGs.

My results now propose that, indeed, the tPA/plasmin pathway plays a role in degrading certain CSPG molecules after ChABC cleavage of GAG chains. Although overall serine protease activity was upregulated as early as 4hrs after injury and remained elevated for up to 14days, specific plasminogen activator activity was slightly elevated at 7 days and significantly at 14 days after injury, closely paralleling the peak expression of most CSPG proteins. In the absence of tPA activity, degradation of NG2, and phosphacan proteins were attenuated after ChABC cleavage, while *in vitro* experiments

revealed that neurocan protein can be degraded by both the tPA and uPA proteases. The specific subtypes of CSPG protein degradation suggest that ChABC-facilitated tPA/plasmin binding and degradation may be specific to the structurally unique CSPG molecules, NG2 and phosphacan, but non-specific to the larger and structurally homologous family of lecticans, of which neurocan is a member. Clearance of these core CSPG proteins by the tPA/plasmin system is an important contributor to ChABC-mediated neurite outgrowth. WT cortical neurons grown on an *ex vivo* glial scar system extend significant neurite outgrowth after ChABC cleavage *in vitro* while the absence of tPA significantly attenuates this outgrowth response. Furthermore, the addition of plasmin to tPA KO SCI homogenates can rescue this attenuated cortical neuron outgrowth response after ChABC cleavage thereby fulfilling the necessary and sufficient clause for the tPA/plasmin mechanism.

My results also demonstrate for the first time that in the absence of the tPA/plasmin system, ChABC mediated functional repair can be attenuated. Functional repair was measured anatomically on sensory axons and behaviorally on motor recovery. WT SCI and ChABC treated mice showed high sensory axon regrowth compared to their genotypic equivalent vehicle enzyme group but significantly lower sensory recovery in tPA KO SCI and ChABC treated mice confirming that tPA/plasmin pathway plays a role in ChABC mediated sensory recovery after SCI. Although no significant differences were found with the motor behavior experiment due to high intra-group variability, consistent trends were seen throughout. WT SCI and ChABC treated mice showed a regain of motor balance compared to measurements at pre-injection time points and measurements in its genotypic equivalent vehicle enzyme group at post-injection time

points. In contrast, no significant differences were seen between the tPA KO SCI and Pen or ChABC treated mice. When normalized to the genotypic equivalent Pen-treated groups on day 21, tPA KO SCI mice show attenuated motor balance response compared to WT SCI mice after ChABC cleavage *in vivo*. Supported motor activity experiment provided similar trends with the WT SCI and ChABC treated mice showing higher motor recovery compared to itself at pre-injection time points and its genotypic equivalent vehicle enzyme group at post-injection time points. In contrast, no significant differences were seen between the tPA KO SCI and Pen or ChABC treated mice. When normalized to the genotypic equivalent Pen-treated groups on day 21, tPA KO SCI mice show attenuated supported motor activity response compared to WT SCI mice after ChABC cleavage *in vivo*. Collectively, the sensory axon and motor behavior experiments demonstrate that the tPA/plasmin system plays an important role in ChABC mediated functional recovery after SCI. I, therefore, propose that it is the cumulative clearance of GAG chains and core proteins by ChABC and tPA/plasmin system that results in enhanced axonal plasticity and improvements in sensory and motor behavior after SCI previously attributed only to GAG chain removal.

My results also suggest a role for uPA/plasmin system in SCI relevant to ChABC-mediated repair. uPA was found to be significantly upregulated after 14 days injury in tPA KO homogenates. The significant degradation of neurocan in tPA KO SCI and ChABC-treated group suggested degradation of the core protein by another protease, presumably uPA. uPA/plasmin interaction with pure neurocan after ChABC cleavage of GAG chains *in vitro* resulted in degradation of the core protein suggesting its potential role in binding and degrading the lectican family of CSPG proteins. Addition of ChABC

to tPA KO SCI homogenates also resulted in residual neurite outgrowth. The absence of tPA/plasmin system did not ablate the sensory axon regrowth in tPA KO SCI and ChABC-treated mice but rather allowed for residual repair that was significantly higher compared to its genotypic equivalent Pen group. Finally, in both the motor balance and supported motor activity experiments, the absence of tPA/plasmin system in tPA KO SCI and ChABC treated mice allowed for some motor behavior recovery that was higher than its genotypic equivalent Pen group. Therefore, similar to the tissue remodeling seen in the crossed phrenic phenomenon of respiratory function following SCI (Minor and Seeds, 2008; Seeds et al., 2009), I propose that both plasminogen activators are playing a role in ChABC-mediated axonal outgrowth and tissue remodeling after SCI.

To test the therapeutic potential of the tPA/plasmin pathway, plasmin was co-injected with ChABC into WT SCI mice. Some improvement in sensory and motor behavior were seen in these mice compared with recovery from the enzyme alone. Significant recovery, however, was not observed after the co-treatment of ChABC and plasmin, possibly due to the sufficient endogenous levels of tPA and uPA/plasminogen system present and saturating the CSPG core proteins immediately after the ChABC cleavage of GAG chains and generating plasmin. Since the zymogen plasminogen is expressed only in neurons in the rodent CNS tissue (Tsirka et al., 1997b), it may be rapidly depleted after SCI and limit the maximum axon outgrowth resulting from ChABC treatment. By not competing with the endogenous plasmin protease, a delayed treatment of plasmin after the enzyme injection *in vivo* may allow for more ChABC-mediated functional recovery through degradation of the residual CSPG core proteins. Indeed the optimal time for plasmin injection is critical, since the protease is rapidly inactivated by

its antagonist alpha$_2$-antiplasmin *in vivo* (Holmes et al., 1987; Meissauer et al., 1992). Therapeutically, however, my results propose that plasmin can be used to enhance ChABC-mediated repair and open a new opportunity for increasing the enzyme's treatment efficacy.

The WT SCI mice also showed modest improvement in sensory and motor recovery when plasmin was co-injected with the vehicle enzyme Pen *in vivo*. A previous study has shown that the endogenous plasminogen/plasmin pathway may play a role in degrading neurocan, brevican, phosphacan, and NG2 as they used the leucine rich proteoglycan decorin in a rat SCI model (Davies et al., 2006; Davies et al., 2004). Therefore, it is possible that plasmin alone can allow for some degradation of CSPG molecules after SCI. In fact, my lab previously demonstrated that plasmin can interact with NG2 molecules *in vitro* (Nolin et al., 2008), and that the cleavage of GAG chains by ChABC significantly enhances this interaction and allows for more NG2 breakdown. Consistent with these early findings, our *in vivo* immunohistochemistry quantification also showed that plasmin can minimally degrade both NG2 and phosphacan proteins after ChABC cleavage in tPA KO SCI mice but the protein degradation can be enhanced in the presence of tPA/plasmin system. The sensory and motor recovery results further extend this finding *in vivo* by showing some recovery due to plasmin and Pen treatments, but better recovery from ChABC and plasmin co-treatments, once again highlighting the regenerative potential of this combination approach.

It was recently shown that CSPG proteins inhibit neurite outgrowth after CNS injury by stimulating a specific receptor, PTPσ (Shen et al., 2009). Mice lacking this protein, in fact, exhibit corticospinal tract regeneration in both dorsal hemisection and

contusion injury models of spinal cord injury (Fry et al., 2009). Blocking the CSPG protein receptor on neurons can overcome the pharmacological inhibition against axonal outgrowth, but the upregulated CSPG molecules remain a spatial barrier in the injured region. Therefore, although blockade of PTPσ provides an important alternative therapy for axonal outgrowth, ChABC and its downstream targets, tPA/plasmin pathway are still necessary for CSPG clearance after SCI.

In contrast to the majority of SCI studies that have utilized continuous and prolonged infusion of ChABC and measured recovery in acute or subacute SCI models, I used a single high dose intraspinal injection of the enzyme to evaluate the therapeutic potential of this drug delivery mode in a chronic SCI model. Three other studies have evaluated *in vivo* repair after a single high dose injection of ChABC in rodent SCI models. One study found corticospinal axon regrowth after dorsal hemisection, but not contusion, with a high dose intraspinal ChABC injection in chronic SCI model (Iseda et al., 2008). A second study showed significant motor axon regrowth out of a peripheral nerve graft bridge after a unilateral dorsal quadrant lesion and concomitant intraspinal microinjection of the enzyme (Tom and Houle, 2008). The third study found significant sensory behavior and physiological afferent fiber recovery after unilateral cervical spared root injury model and concomitant high dose intraspinal injection (Cafferty et al., 2008). Building on these previous studies, my results suggest that a single high dose ChABC treatment can allow for both significant sensory axon and motor behavior recovery in a chronic SCI model. When compared with intact animals, the sensory and motor recovery in the SCI and ChABC or ChABC and plasmin co-treated animals may seem minimal. However, it is encouraging to note that only 10% of the original axons are necessary to

achieve a significant functional improvement in rodents (Barnett et al., 2000; Blight, 1983), although it is not yet fully established whether this is meaningful (directional and voluntary) functional improvement. In humans, a retention of approximately 8% axons fibers are necessary to maintain minimal motor function (plantar flexion)(Kakulas, 2004). My findings, in conjunction with others, indicate that a single high dose of the enzyme may be a viable and less invasive mode of enzyme delivery for therapeutic treatments. Furthermore, retaining enzyme efficacy in a chronic SCI model, as demonstrated here and in work by others, also significantly enhances the translational value of this enzymatic therapy.

Following contusion injury, the biochemical characterization also revealed an upregulation of overall serine protease activity. Since others and I have shown that plasminogen activators are chronically elevated, the presence and upregulation of other serine protease activities at acute and sub-acute time points after SCI require further studies. One such early study reported the upregulation of the neurotoxic serine protease prothrombin and its receptor protease-activated receptor gene family (PAR-1) beginning as early as 8 hours and reaching a maximal level at 24 hours in a rat contusion injury model (Citron et al., 2000). Furthermore, using gene array analyses of SCI tissue, they found that several serine proteases were activated by SCI underscoring the need for further characterization of serine protease activities at acute and sub-acute timepoints after injury.

Spontaneous recovery was seen in both the WT and tPA KO Pen-treated groups on day 21 (Figure 33B) indicating endogenous repair pathways are at work (Bareyre et al., 2004; Courtine et al., 2008). However, consistent with the known interaction of tPA and

myelin basic protein, my motor balance and supported motor activity results also demonstrate that in the absence of tPA, higher sensory and motor recovery occurred on day 21 after injury when the MBP expression is lowest (Abe et al., 2003; Veeravalli et al., 2009). My results, however, did not achieve statistical significance between the WT and tPA KO Pen-treated group in contrast to these studies. I believe this difference may have occurred for technical reasons: a large intragroup variability in the motor behavior experiment made it difficult to gain statistical power. Moreover, the quantification of both the white matter, myelin rich, and gray matter regions of the injured spinal cord in sensory axon measurements may have reduced the significant differences seen only in the white matter region.

Significantly reduced open field behavior activity was also seen in tPA KO intact mice consistent with the more extensive battery of exploratory behavior characterization previously reported by my lab. It was shown that reduced exploratory inhibition defined as impulsivity and higher anxiety in healthy tPA KO mice were accompanied with reduced levels of serotonin in several brains regions known for behavioral regulation (Pothakos et al., 2010). Indeed, significant differences were also seen in unsupported motor activity between the two genotypes. This can also be attributed to anxiety, because the tPA KO mice avoided the center of the open field cage where unsupported motor activity was generally performed, a classical behavior of anxious rodents.

Collectively, my results indicate that ChABC removal of the GAG chains enhances tPA/plasminogen's interaction with the core protein. The close proximity of tPA and plasminogen proteins results in formation of more plasmin which in turn can degrade the core CSPG proteins and allow for their clearance. Clearance of both the GAG chains

and core CSPG proteins *in vivo* allows for improvements in functional recovery. Based on my findings, I also propose that plasmin could be used therapeutically to enhance ChABC efficacy.

Chapter VI- Future Directions

Although a confirmation of tPA/plasmin's role in ChABC-mediated repair after SCI has been demonstrated in this project, only a proof of principle for the therapeutic efficacy of this pathway was presented. Therefore, it would be important to try a delayed treatment of plasmin after ChABC injection in WT SCI mice to test for the enhancement of functional repair mediated by the enzyme. Since ChABC activity lasts no more than 4 days after injection, it would be optimal to inject plasmin 5-7 days after the enzyme administration to test the efficacy of the dual therapy.

The role of uPA/plasmin system in ChABC-mediated functional repair would be another important area of investigation. My work revealed that uPA/plasmin system can degrade neurocan after ChABC cleavage *in vitro*. However, more *in vitro* tests need to be conducted for the interaction of uPA with the other lectican family of CSPG molecules such as brevican, verscian and aggrecan. As performed in this body of work, an *in vitro* confirmation can be followed by *in vivo* experiments on the role of uPA/plasmin in ChABC mediated sensory and motor repair. Alternatively, or in conjunction with this uPA hypothesis, it would be useful to test the effect of ablating both plasminogen activator activities on ChABC-mediated recovery. ChABC mediated repair is due not only to the cleavage of inhibitory GAG chains and core proteins, but the GAG chains themselves play neuroprotective and neurodegenerative roles in repair after SCI (Laabs et al., 2007; Rolls et al., 2006; Wang et al., 2008). Therefore, it is unlikely that removal of both plasminogen activators will result in complete ablation of enzyme-mediated recovery after SCI. However, the data will allow us to assess the extent to which ChABC-mediated repair can be attributed to plasminogen activators.

The neurite outgrowth assay used in this project employed a complex *ex vivo* glial scar to test the role of tPA/plasmin system in ChABC mediated repair. This assay can be optimized and the specific mechanism of ChABC mediated repair clarified in three specific ways. An *ex vivo* glial scar environment is composed of many other inhibitory molecules such as Nogo-A, myelin associated glycoproteins (MAG), oligodendrocyte-myelin glycoprotein (OMgp), Sema4D, and Ephrin B3 (Schwab et al., 2006). Neurite outgrowth response due to ChABC can be optimized in this complex assay environment by using blockers of myelin and axon guidance inhibitory molecules. Since NG2 protein is present as both a secreted ECM protein and surface receptor on OPC and macrophages, it would be important to determine to what extent the ECM NG2 protein degradation specifically contributes to ChABC mediated neurite outgrowth? Growing cortical neurons on OPCs and microglia/macrophages pre-treated with ChABC will measure neurite outgrowth due to cleavage of surface NG2 protein. Calculating the difference between neurite outgrowth on an *ex vivo* glial scar and neurite outgrowth on OPCs and macrophages will provide the final cortical neuron outgrowth due to ChABC mediated cleavage of NG2 ECM protein. Finally, the cortical neuron response measured in this dissertation did not distinguish between the specific types of neurite processes (axons or dendrites). To better understand the mechanism of ChABC mediated repair, it would also be worthwhile to determine the extent of dendritic and axonal outgrowth in the neurite assay resulting from ChABC treatment.

Although BDA-labeled motor axon tracing could not be performed due to the mice's high mortality beyond 30 days, an alternative dye called fluorescent-dextran amine can be used in the future to measure the role of tPA/plasmin in ChABC mediated motor

outgrowth. Dextran-amines only requires a 7 day incubation period and therefore, can be injected 21 days after injury and spinal cord isolated on day 28 post-SCI allowing for a measure of motor axons within the experimental timeline.

One could argue that the motor behavior experiments (motor coordination and supported motor activity) tested both the upper limb strength and lower limb recovery after SCI in rodents instead of a pure lower limb recovery. Although the behavioral assays include a measure of both regions, a review of literature reveals that after SCI, forelimb corticospinal neurons extend into the formally hindlimb cortex and cause enhanced forelimb function due to endogenous repair strategy (and potentially other therapeutic approaches such as ChABC)(Ghosh et al., 2010). Therefore, it is conceivable that both forelimb strength and hindlimb function were measured in these behavior experiments, since both are actively responding to SCI and therapy. Nevertheless, to tease out motor recovery occurring only in the lower limbs, a hanging wire test can be used to directly measure upper limb strength in SCI mice and the difference between the two types of recovery (lower and upper limbs motor recovery vs upper limbs motor recovery only) calculated to isolate a pure lower limbs recovery response.

To enhance the translational value of ChABC repair, a single intraspinal dose of the enzyme was performed in this work. It would, however, also be worthwhile to test the same hypothesis using a continuous drug delivery mode, such as osmotic pump of the ChABC enzyme and checking for attenuation of tPA activity in tPA KO mice. Therapeutically, one can also try a delayed continuous infusion of plasmin after ChABC injection in WT SCI mice to further augment the repair response. This delivery mode is especially important for plasmin since it has a short half-life *in vivo*.

Finally, ChABC-mediated regenerative repair is not only relevant in the context of SCI, but has also been shown in brain injury (Moon et al., 2001), retinal injury (Inatani et al., 2001; Pizzorusso et al., 2006) and the aging brain (Hafidi et al., 2004; Jenkins and Bachelard, 1988), where CSPG protein expressions are upregulated. Therefore, it would be important to test if the plasminogen activators are playing a role downstream of ChABC mediated repair in these different regions of the CNS. Ultimately, the questions that need to be answered by these experiments are: in addition to the cleavage of GAG chains, is the degradation of the core CSPG proteins important in all cases of ChABC mediated functional, meaningful repair and does the plasminogen activator/plasmin pathway universally degrade CSPG core proteins after ChABC cleavage of GAG chains in all regions of the CNS?

References

Abe, Y., Nakamura, H., Yoshino, O., Oya, T., and Kimura, T. (2003). Decreased neural damage after spinal cord injury in tPA-deficient mice. Journal of neurotrauma *20*, 43-57.

Akassoglou, K., Kombrinck, K.W., Degen, J.L., and Strickland, S. (2000). Tissue plasminogen activator-mediated fibrinolysis protects against axonal degeneration and demyelination after sciatic nerve injury. The Journal of cell biology *149*, 1157-1166.

Bareyre, F.M., Kerschensteiner, M., Raineteau, O., Mettenleiter, T.C., Weinmann, O., and Schwab, M.E. (2004). The injured spinal cord spontaneously forms a new intraspinal circuit in adult rats. Nature neuroscience *7*, 269-277.

Barnett, S.C., Alexander, C.L., Iwashita, Y., Gilson, J.M., Crowther, J., Clark, L., Dunn, L.T., Papanastassiou, V., Kennedy, P.G., and Franklin, R.J. (2000). Identification of a human olfactory ensheathing cell that can effect transplant-mediated remyelination of demyelinated CNS axons. Brain *123 (Pt 8)*, 1581-1588.

Barritt, A.W., Davies, M., Marchand, F., Hartley, R., Grist, J., Yip, P., McMahon, S.B., and Bradbury, E.J. (2006). Chondroitinase ABC promotes sprouting of intact and injured spinal systems after spinal cord injury. J Neurosci *26*, 10856-10867.

Blight, A.R. (1983). Cellular morphology of chronic spinal cord injury in the cat: analysis of myelinated axons by line-sampling. Neuroscience *10*, 521-543.

Bradbury, E.J., Moon, L.D., Popat, R.J., King, V.R., Bennett, G.S., Patel, P.N., Fawcett, J.W., and McMahon, S.B. (2002). Chondroitinase ABC promotes functional recovery after spinal cord injury. Nature *416*, 636-640.

Bush, T.G., Puvanachandra, N., Horner, C.H., Polito, A., Ostenfeld, T., Svendsen, C.N., Mucke, L., Johnson, M.H., and Sofroniew, M.V. (1999). Leukocyte infiltration, neuronal degeneration, and neurite outgrowth after ablation of scar-forming, reactive astrocytes in adult transgenic mice. Neuron *23*, 297-308.

Cafferty, W.B., Bradbury, E.J., Lidierth, M., Jones, M., Duffy, P.J., Pezet, S., and McMahon, S.B. (2008). Chondroitinase ABC-mediated plasticity of spinal sensory function. J Neurosci *28*, 11998-12009.

Cafferty, W.B., Yang, S.H., Duffy, P.J., Li, S., and Strittmatter, S.M. (2007). Functional axonal regeneration through astrocytic scar genetically modified to digest chondroitin sulfate proteoglycans. J Neurosci *27*, 2176-2185.

Caggiano, A.O., Zimber, M.P., Ganguly, A., Blight, A.R., and Gruskin, E.A. (2005). Chondroitinase ABCI improves locomotion and bladder function following contusion injury of the rat spinal cord. J Neurotrauma *22*, 226-239.

Carroll, P.M., Tsirka, S.E., Richards, W.G., Frohman, M.A., and Strickland, S. (1994). The mouse tissue plasminogen activator gene 5' flanking region directs appropriate expression in development and a seizure-enhanced response in the CNS. Development (Cambridge, England) *120*, 3173-3183.

Center, N.S.C.I.S. Facts & Figures at a Glance (Birmingham, Foundation for Spinal Cord Injury Prevention, Care & Cure).

Chen, Y., Vartiainen, N.E., Ying, W., Chan, P.H., Koistinaho, J., and Swanson, R.A. (2001). Astrocytes protect neurons from nitric oxide toxicity by a glutathione-dependent mechanism. J Neurochem *77*, 1601-1610.

Chen, Z.L., and Strickland, S. (1997). Neuronal death in the hippocampus is promoted by plasmin-catalyzed degradation of laminin. Cell *91*, 917-925.

Citron, B.A., Smirnova, I.V., Arnold, P.M., and Festoff, B.W. (2000). Upregulation of neurotoxic serine proteases, prothrombin, and protease-activated receptor 1 early after spinal cord injury. J Neurotrauma *17*, 1191-1203.

Collen, D. (1999). The plasminogen (fibrinolytic) system. Thrombosis and haemostasis *82*, 259-270.

Courtine, G., Song, B., Roy, R.R., Zhong, H., Herrmann, J.E., Ao, Y., Qi, J., Edgerton, V.R., and Sofroniew, M.V. (2008). Recovery of supraspinal control of stepping via indirect propriospinal relay connections after spinal cord injury. Nature medicine *14*, 69-74.

Crespo, D., Asher, R.A., Lin, R., Rhodes, K.E., and Fawcett, J.W. (2007). How does chondroitinase promote functional recovery in the damaged CNS? Exp Neurol *206*, 159-171.

Cui, W., Allen, N.D., Skynner, M., Gusterson, B., and Clark, A.J. (2001). Inducible ablation of astrocytes shows that these cells are required for neuronal survival in the adult brain. Glia *34*, 272-282.

Davies, J.E., Tang, X., Bournat, J.C., and Davies, S.J. (2006). Decorin promotes plasminogen/plasmin expression within acute spinal cord injuries and by adult microglia in vitro. J Neurotrauma *23*, 397-408.

Davies, J.E., Tang, X., Denning, J.W., Archibald, S.J., and Davies, S.J. (2004). Decorin suppresses neurocan, brevican, phosphacan and NG2 expression and promotes axon growth across adult rat spinal cord injuries. Eur J Neurosci *19*, 1226-1242.

Davies, S.J., Fitch, M.T., Memberg, S.P., Hall, A.K., Raisman, G., and Silver, J. (1997). Regeneration of adult axons in white matter tracts of the central nervous system. Nature *390*, 680-683.

Diapharma Chromogenic Substrates: Purified Proteins & Enzymes. Product Manual.

do Carmo Cunha, J., de Freitas Azevedo Levy, B., de Luca, B.A., de Andrade, M.S., Gomide, V.C., and Chadi, G. (2007). Responses of reactive astrocytes containing S100beta protein and fibroblast growth factor-2 in the border and in the adjacent preserved tissue after a contusion injury of the spinal cord in rats: implications for wound repair and neuroregeneration. Wound Repair Regen *15*, 134-146.

Dobbertin, A., Rhodes, K.E., Garwood, J., Properzi, F., Heck, N., Rogers, J.H., Fawcett, J.W., and Faissner, A. (2003). Regulation of RPTPbeta/phosphacan expression and glycosaminoglycan epitopes in injured brain and cytokine-treated glia. Mol Cell Neurosci *24*, 951-971.

Dou, C.L., and Levine, J.M. (1994). Inhibition of neurite growth by the NG2 chondroitin sulfate proteoglycan. J Neurosci *14*, 7616-7628.

Faulkner, J.R., Herrmann, J.E., Woo, M.J., Tansey, K.E., Doan, N.B., and Sofroniew, M.V. (2004). Reactive astrocytes protect tissue and preserve function after spinal cord injury. J Neurosci *24*, 2143-2155.

Fawcett, J.W., and Asher, R.A. (1999). The glial scar and central nervous system repair. Brain Res Bull *49*, 377-391.

Fouad, K., Klusman, I., and Schwab, M.E. (2004). Regenerating corticospinal fibers in the Marmoset (Callitrix jacchus) after spinal cord lesion and treatment with the anti-Nogo-A antibody IN-1. Eur J Neurosci *20*, 2479-2482.

Freund, P., Wannier, T., Schmidlin, E., Bloch, J., Mir, A., Schwab, M.E., and Rouiller, E.M. (2007). Anti-Nogo-A antibody treatment enhances sprouting of corticospinal axons rostral to a unilateral cervical spinal cord lesion in adult macaque monkey. J Comp Neurol *502*, 644-659.

Fry, E.J., Chagnon, M.J., Lopez-Vales, R., Tremblay, M.L., and David, S. Corticospinal tract regeneration after spinal cord injury in receptor protein tyrosine phosphatase sigma deficient mice. Glia *58*, 423-433.

Fry, E.J., Chagnon, M.J., Lopez-Vales, R., Tremblay, M.L., and David, S. (2009). Corticospinal tract regeneration after spinal cord injury in receptor protein tyrosine phosphatase sigma deficient mice. Glia *58*, 423-433.

Fulmer, T. (2009). Unblocking Axonal Regeneration. Science-Business Exchange *2*, 1588-1590.

Galtrey, C.M., and Fawcett, J.W. (2007). The role of chondroitin sulfate proteoglycans in regeneration and plasticity in the central nervous system. Brain research reviews *54*, 1-18.

Garcia-Alias, G., Lin, R., Akrimi, S.F., Story, D., Bradbury, E.J., and Fawcett, J.W. (2008). Therapeutic time window for the application of chondroitinase ABC after spinal cord injury. Exp Neurol *210*, 331-338.

Ghosh, A., Haiss, F., Sydekum, E., Schneider, R., Gullo, M., Wyss, M.T., Mueggler, T., Baltes, C., Rudin, M., Weber, B., *et al.* (2010). Rewiring of hindlimb corticospinal neurons after spinal cord injury. Nature neuroscience *13*, 97-104.

Grider, M.H., Chen, Q., and Shine, H.D. (2006). Semi-automated quantification of axonal densities in labeled CNS tissue. J Neurosci Methods *155*, 172-179.

Grimpe, B., and Silver, J. (2002). The extracellular matrix in axon regeneration. Prog Brain Res *137*, 333-349.

Hafidi, A., Grumet, M., and Sanes, D.H. (2004). In vitro analysis of mechanisms underlying age-dependent failure of axon regeneration. J Comp Neurol *470*, 80-92.

Holmes, W.E., Nelles, L., Lijnen, H.R., and Collen, D. (1987). Primary structure of human alpha 2-antiplasmin, a serine protease inhibitor (serpin). J Biol Chem *262*, 1659-1664.

Houle, J.D., Tom, V.J., Mayes, D., Wagoner, G., Phillips, N., and Silver, J. (2006). Combining an autologous peripheral nervous system "bridge" and matrix modification by chondroitinase allows robust, functional regeneration beyond a hemisection lesion of the adult rat spinal cord. J Neurosci *26*, 7405-7415.

Inatani, M., Honjo, M., Otori, Y., Oohira, A., Kido, N., Tano, Y., Honda, Y., and Tanihara, H. (2001). Inhibitory effects of neurocan and phosphacan on neurite outgrowth from retinal ganglion cells in culture. Invest Ophthalmol Vis Sci *42*, 1930-1938.

Iseda, T., Okuda, T., Kane-Goldsmith, N., Mathew, M., Ahmed, S., Chang, Y.W., Young, W., and Grumet, M. (2008). Single, high-dose intraspinal injection of chondroitinase reduces glycosaminoglycans in injured spinal cord and promotes corticospinal axonal regrowth after hemisection but not contusion. J Neurotrauma *25*, 334-349.

Jenkins, H.G., and Bachelard, H.S. (1988). Developmental and age-related changes in rat brain glycosaminoglycans. J Neurochem *51*, 1634-1640.

Jones, L.L., Margolis, R.U., and Tuszynski, M.H. (2003a). The chondroitin sulfate proteoglycans neurocan, brevican, phosphacan, and versican are differentially regulated following spinal cord injury. Experimental neurology *182*, 399-411.

Jones, L.L., Sajed, D., and Tuszynski, M.H. (2003b). Axonal regeneration through regions of chondroitin sulfate proteoglycan deposition after spinal cord injury: a balance of permissiveness and inhibition. J Neurosci *23*, 9276-9288.

Jones, L.L., Yamaguchi, Y., Stallcup, W.B., and Tuszynski, M.H. (2002). NG2 is a major chondroitin sulfate proteoglycan produced after spinal cord injury and is expressed by macrophages and oligodendrocyte progenitors. J Neurosci *22*, 2792-2803.

Kakulas, B.A. (2004). Neuropathology: the foundation for new treatments in spinal cord injury. Spinal Cord *42*, 549-563.

Kerschensteiner, M., Schwab, M.E., Lichtman, J.W., and Misgeld, T. (2005). In vivo imaging of axonal degeneration and regeneration in the injured spinal cord. Nature medicine *11*, 572-577.

Krystosek, A., and Seeds, N.W. (1981). Plasminogen activator release at the neuronal growth cone. Science (New York, NY *213*, 1532-1534.

Laabs, T.L., Wang, H., Katagiri, Y., McCann, T., Fawcett, J.W., and Geller, H.M. (2007). Inhibiting glycosaminoglycan chain polymerization decreases the inhibitory activity of astrocyte-derived chondroitin sulfate proteoglycans. J Neurosci *27*, 14494-14501.

Lee, R., Kermani, P., Teng, K.K., and Hempstead, B.L. (2001). Regulation of cell survival by secreted proneurotrophins. Science (New York, NY *294*, 1945-1948.

Li, J., Imitola, J., Snyder, E.Y., and Sidman, R.L. (2006). Neural stem cells rescue nervous purkinje neurons by restoring molecular homeostasis of tissue plasminogen activator and downstream targets. J Neurosci *26*, 7839-7848.

Medicine, N.L.o. (2008). Clinical Trials (United States National Institute of Health).

Meissauer, A., Kramer, M.D., Schirrmacher, V., and Brunner, G. (1992). Generation of cell surface-bound plasmin by cell-associated urokinase-type or secreted tissue-type plasminogen activator: a key event in melanoma cell invasiveness in vitro. Exp Cell Res *199*, 179-190.

Minor, K., Phillips, J., and Seeds, N.W. (2009). Tissue plasminogen activator promotes axonal outgrowth on CNS myelin after conditioned injury. J Neurochem *109*, 706-715.

Minor, K.H., and Seeds, N.W. (2008). Plasminogen activator induction facilitates recovery of respiratory function following spinal cord injury. Mol Cell Neurosci *37*, 143-152.

Moon, L.D., Asher, R.A., Rhodes, K.E., and Fawcett, J.W. (2001). Regeneration of CNS axons back to their target following treatment of adult rat brain with chondroitinase ABC. Nat Neurosci *4*, 465-466.

Morgenstern, D.A., Asher, R.A., and Fawcett, J.W. (2002). Chondroitin sulphate proteoglycans in the CNS injury response. Progress in brain research *137*, 313-332.

Nguyen, Q.T., Sanes, J.R., and Lichtman, J.W. (2002). Pre-existing pathways promote precise projection patterns. Nature neuroscience *5*, 861-867.

Nishiyama, A., Dahlin, K.J., Prince, J.T., Johnstone, S.R., and Stallcup, W.B. (1991). The primary structure of NG2, a novel membrane-spanning proteoglycan. The Journal of cell biology *114*, 359-371.

Nolin, W.B., Emmetsberger, J., Bukhari, N., Zhang, Y., Levine, J.M., and Tsirka, S.E. (2008). tPA-mediated generation of plasmin is catalyzed by the proteoglycan NG2. Glia *56*, 177-189.

Okada, S., Nakamura, M., Katoh, H., Miyao, T., Shimazaki, T., Ishii, K., Yamane, J., Yoshimura, A., Iwamoto, Y., Toyama, Y., *et al.* (2006). Conditional ablation of Stat3 or Socs3 discloses a dual role for reactive astrocytes after spinal cord injury. Nature medicine *12*, 829-834.

Onose, G., Anghelescu, A., Muresanu, D.F., Padure, L., Haras, M.A., Chendreanu, C.O., Onose, L.V., Mirea, A., Ciurea, A.V., El Masri, W.S., *et al.* (2009). A review of published reports on neuroprotection in spinal cord injury. Spinal Cord *47*, 716-726.

Oohira, A., Matsui, F., and Katoh-Semba, R. (1991). Inhibitory effects of brain chondroitin sulfate proteoglycans on neurite outgrowth from PC12D cells. J Neurosci *11*, 822-827.

Pang, P.T., Teng, H.K., Zaitsev, E., Woo, N.T., Sakata, K., Zhen, S., Teng, K.K., Yung, W.H., Hempstead, B.L., and Lu, B. (2004). Cleavage of proBDNF by tPA/plasmin is essential for long-term hippocampal plasticity. Science (New York, NY *306*, 487-491.

Pizzorusso, T., Medini, P., Landi, S., Baldini, S., Berardi, N., and Maffei, L. (2006). Structural and functional recovery from early monocular deprivation in adult rats. Proceedings of the National Academy of Sciences of the United States of America *103*, 8517-8522.

Pool, M., Thiemann, J., Bar-Or, A., and Fournier, A.E. (2008). NeuriteTracer: a novel ImageJ plugin for automated quantification of neurite outgrowth. J Neurosci Methods *168*, 134-139.

Pothakos, K., Robinson, J.K., Gravanis, I., Marsteller, D.A., Dewey, S.L., and Tsirka, S.E. (2010). Decreased serotonin levels associated with behavioral disinhibition in tissue plasminogen activator deficient (tPA-/-) mice. Brain Res *1326*, 135-142.

Reier, P.J., and Houle, J.D. (1988). The glial scar: its bearing on axonal elongation and transplantation approaches to CNS repair. Adv Neurol *47*, 87-138.

Renault-Mihara, F., Okada, S., Shibata, S., Nakamura, M., Toyama, Y., and Okano, H. (2008). Spinal cord injury: emerging beneficial role of reactive astrocytes' migration. Int J Biochem Cell Biol *40*, 1649-1653.

Rogove, A.D., and Tsirka, S.E. (1998). Neurotoxic responses by microglia elicited by excitotoxic injury in the mouse hippocampus. Curr Biol *8*, 19-25.

Roitbak, T., and Sykova, E. (1999). Diffusion barriers evoked in the rat cortex by reactive astrogliosis. Glia *28*, 40-48.

Rolls, A., Cahalon, L., Bakalash, S., Avidan, H., Lider, O., and Schwartz, M. (2006). A sulfated disaccharide derived from chondroitin sulfate proteoglycan protects against inflammation-associated neurodegeneration. FASEB J *20*, 547-549.

Rolls, A., Shechter, R., London, A., Segev, Y., Jacob-Hirsch, J., Amariglio, N., Rechavi, G., and Schwartz, M. (2008). Two faces of chondroitin sulfate proteoglycan in spinal cord repair: a role in microglia/macrophage activation. PLoS Med *5*, e171.

Rolls, A., Shechter, R., and Schwartz, M. (2009). The bright side of the glial scar in CNS repair. Nat Rev Neurosci *10*, 235-241.

Schreiber, D. (2009). Spinal Cord Injuries. In Emedicine.

Schwab, J.M., Brechtel, K., Mueller, C.A., Failli, V., Kaps, H.P., Tuli, S.K., and Schluesener, H.J. (2006). Experimental strategies to promote spinal cord regeneration--an integrative perspective. Progress in neurobiology *78*, 91-116.

Schwab, M.E., and Bartholdi, D. (1996). Degeneration and regeneration of axons in the lesioned spinal cord. Physiol Rev *76*, 319-370.

Schwartz, J.P., and Nishiyama, N. (1994). Neurotrophic factor gene expression in astrocytes during development and following injury. Brain Res Bull *35*, 403-407.

Seeds, N.W., Akison, L., and Minor, K. (2009). Role of plasminogen activator in spinal cord remodeling after spinal cord injury. Respir Physiol Neurobiol *169*, 141-149.

Seeds, N.W., Basham, M.E., and Ferguson, J.E. (2003). Absence of tissue plasminogen activator gene or activity impairs mouse cerebellar motor learning. J Neurosci *23*, 7368-7375.

Seeds, N.W., Basham, M.E., and Haffke, S.P. (1999). Neuronal migration is retarded in mice lacking the tissue plasminogen activator gene. Proceedings of the National Academy of Sciences of the United States of America *96*, 14118-14123.

Seeds, N.W., Williams, B.L., and Bickford, P.C. (1995). Tissue plasminogen activator induction in Purkinje neurons after cerebellar motor learning. Science (New York, NY *270*, 1992-1994.

Shen, Y., Tenney, A.P., Busch, S.A., Horn, K.P., Cuascut, F.X., Liu, K., He, Z., Silver, J., and Flanagan, J.G. (2009). PTPsigma is a receptor for chondroitin sulfate proteoglycan, an inhibitor of neural regeneration. Science *326*, 592-596.

Siao, C.J., and Tsirka, S.E. (2002). Tissue plasminogen activator mediates microglial activation via its finger domain through annexin II. J Neurosci *22*, 3352-3358.

Siconolfi, L.B., and Seeds, N.W. (2001). Mice lacking tPA, uPA, or plasminogen genes showed delayed functional recovery after sciatic nerve crush. J Neurosci *21*, 4348-4355.

Sivasankaran, R., Pei, J., Wang, K.C., Zhang, Y.P., Shields, C.B., Xu, X.M., and He, Z. (2004). PKC mediates inhibitory effects of myelin and chondroitin sulfate proteoglycans on axonal regeneration. Nature neuroscience *7*, 261-268.

Steinmetz, M.P., Horn, K.P., Tom, V.J., Miller, J.H., Busch, S.A., Nair, D., Silver, D.J., and Silver, J. (2005). Chronic enhancement of the intrinsic growth capacity of sensory neurons combined with the degradation of inhibitory proteoglycans allows functional regeneration of sensory axons through the dorsal root entry zone in the mammalian spinal cord. J Neurosci *25*, 8066-8076.

Stichel, C.C., Hermanns, S., Luhmann, H.J., Lausberg, F., Niermann, H., D'Urso, D., Servos, G., Hartwig, H.G., and Muller, H.W. (1999). Inhibition of collagen IV deposition promotes regeneration of injured CNS axons. Eur J Neurosci *11*, 632-646.

Sumi, Y., Dent, M.A., Owen, D.E., Seeley, P.J., and Morris, R.J. (1992). The expression of tissue and urokinase-type plasminogen activators in neural development suggests different modes of proteolytic involvement in neuronal growth. Development (Cambridge, England) *116*, 625-637.

Tan, A.M., Colletti, M., Rorai, A.T., Skene, J.H., and Levine, J.M. (2006). Antibodies against the NG2 proteoglycan promote the regeneration of sensory axons within the dorsal columns of the spinal cord. J Neurosci *26*, 4729-4739.

Tang, X., Davies, J.E., and Davies, S.J. (2003). Changes in distribution, cell associations, and protein expression levels of NG2, neurocan, phosphacan, brevican, versican V2, and tenascin-C during acute to chronic maturation of spinal cord scar tissue. Journal of neuroscience research *71*, 427-444.

Tarnawa, I., Bolcskei, H., and Kocsis, P. (2007). Blockers of voltage-gated sodium channels for the treatment of central nervous system diseases. Recent Pat CNS Drug Discov *2*, 57-78.

Tom, V.J., and Houle, J.D. (2008). Intraspinal microinjection of chondroitinase ABC following injury promotes axonal regeneration out of a peripheral nerve graft bridge. Experimental neurology *211*, 315-319.

Tsirka, S.E., Bugge, T.H., Degen, J.L., and Strickland, S. (1997a). Neuronal death in the central nervous system demonstrates a non-fibrin substrate for plasmin. Proceedings of the National Academy of Sciences of the United States of America *94*, 9779-9781.

Tsirka, S.E., Gualandris, A., Amaral, D.G., and Strickland, S. (1995). Excitotoxin-induced neuronal degeneration and seizure are mediated by tissue plasminogen activator. Nature *377*, 340-344.

Tsirka, S.E., Rogove, A.D., Bugge, T.H., Degen, J.L., and Strickland, S. (1997b). An extracellular proteolytic cascade promotes neuronal degeneration in the mouse hippocampus. J Neurosci *17*, 543-552.

Veeravalli, K.K., Dasari, V.R., Tsung, A.J., Dinh, D.H., Gujrati, M., Fassett, D., and Rao, J.S. (2009). Stem cells downregulate the elevated levels of tissue plasminogen activator in rats after spinal cord injury. Neurochem Res *34*, 1183-1194.

Vorisek, I., Hajek, M., Tintera, J., Nicolay, K., and Sykova, E. (2002). Water ADC, extracellular space volume, and tortuosity in the rat cortex after traumatic injury. Magn Reson Med *48*, 994-1003.

Vyas, A.A., Blixt, O., Paulson, J.C., and Schnaar, R.L. (2005). Potent glycan inhibitors of myelin-associated glycoprotein enhance axon outgrowth in vitro. J Biol Chem *280*, 16305-16310.

Wang, H., Katagiri, Y., McCann, T.E., Unsworth, E., Goldsmith, P., Yu, Z.X., Tan, F., Santiago, L., Mills, E.M., Wang, Y., *et al.* (2008). Chondroitin-4-sulfation negatively regulates axonal guidance and growth. J Cell Sci *121*, 3083-3091.

White, R.E., Yin, F.Q., and Jakeman, L.B. (2008). TGF-alpha increases astrocyte invasion and promotes axonal growth into the lesion following spinal cord injury in mice. Exp Neurol.

Wu, V.W., Nishiyama, N., and Schwartz, J.P. (1998). A culture model of reactive astrocytes: increased nerve growth factor synthesis and reexpression of cytokine responsiveness. J Neurochem *71*, 749-756.

Wu, Y.P., Siao, C.J., Lu, W., Sung, T.C., Frohman, M.A., Milev, P., Bugge, T.H., Degen, J.L., Levine, J.M., Margolis, R.U., *et al.* (2000). The tissue plasminogen activator (tPA)/plasmin extracellular proteolytic system regulates seizure-induced hippocampal mossy fiber outgrowth through a proteoglycan substrate. The Journal of cell biology *148*, 1295-1304.

Yick, L.W., Wu, W., So, K.F., Yip, H.K., and Shum, D.K. (2000). Chondroitinase ABC promotes axonal regeneration of Clarke's neurons after spinal cord injury. Neuroreport *11*, 1063-1067.

Young, W. (2008). Collaborative neurosciences and biological therapy of spinal cord injured people. In Summer School for the Biological Treatment of Chronic Spinal Cord Injury (Vienna, Austria).

Zhang, Y., Kanaho, Y., Frohman, M.A., and Tsirka, S.E. (2005). Phospholipase D1-promoted release of tissue plasminogen activator facilitates neurite outgrowth. J Neurosci *25*, 1797-1805.

Zheng, B., Ho, C., Li, S., Keirstead, H., Steward, O., and Tessier-Lavigne, M. (2003). Lack of enhanced spinal regeneration in Nogo-deficient mice. Neuron *38*, 213-224.

Zou, T., Ling, C., Xiao, Y., Tao, X., Ma, D., Chen, Z.L., Strickland, S., and Song, H. (2006). Exogenous tissue plasminogen activator enhances peripheral nerve regeneration and functional recovery after injury in mice. Journal of neuropathology and experimental neurology *65*, 78-86.